

Rather Exotic Types of Cyclic Peroxides: Heteroatom Dioxiranes

Nahed Sawwan and Alexander Greer*

Department of Chemistry, Graduate School and University Center and The City University of New York (CUNY), Brooklyn College, Brooklyn, New York 11210

Received November 6, 2006

Contents

1. Introduction	3247
2. Background	3247
3. Scope	3247
4. Heteroatom-Containing Dioxiranes	3248
4.1. Tetrahedral Dioxiranes	3248
4.1.1. Dioxaziridine, RNO_2	3248
4.1.2. Dioxasilirane, R_2SiO_2	3254
4.1.3. Dioxagermirane, Dioxastannirane, and Dioxastilbirane	3261
4.1.4. Cyclic Sulfur Dioxide, SO_2	3263
4.1.5. Cyclic Selenium Dioxide, SeO_2	3265
4.2. Trigonal Bipyramidal Dioxiranes	3265
4.2.1. Dioxaphosphirane, R_3PO_2	3265
4.2.2. Dioxathiirane, R_2SO_2	3270
4.2.3. Dioxaselenirane and Dioxatellurirane	3276
4.3. Cyclic and Ring-Opened Species	3276
4.4. Intermolecular Reactions	3280
4.5. Synthetic Prospectives	3280
5. Summary	3281
6. Acknowledgments	3282
7. References	3282

1. Introduction

This review discusses the heteroatom-containing dioxiranes in organic chemistry. Heteroatom-containing dioxiranes are three-membered ring peroxides with the form XO_2 , where X is R_3P , RN , R_2Si , R_2S , R_2Se , R_2Ge , R_2Sn , R_2Pb , R_2Te , S, or Se. The R group represents hydrogen, halogen, alkyl, or aryl substituents. In light of the remarkable success that R_2CO_2 dioxiranes have had in oxygen-transfer reactions in organic chemistry, a review of XO_2 dioxiranes is expected to encourage and uncover new possible oxidation reactions. The synthetic utility for chemical oxidations with XO_2 dioxiranes is presently untapped.

2. Background

XO_2 dioxiranes are intermediates in photochemical and thermal reactions. In some cases, XO_2 dioxiranes have been detected with low-temperature techniques (e.g., matrix isolation, NMR, X-ray crystallography). In other cases, evidence for the existence of XO_2 dioxiranes comes from indirect studies, such as chemical trapping data or unimolecular rearrangements of the dioxirane congeners to more stable products.

* To whom correspondence should be sent. Telephone: 718-951-5000 (ext 2830). Fax: 718-951-4607. E-mail: agreer@brooklyn.cuny.edu.

An approach to the generation of XO_2 dioxiranes is often based on the reaction of an oxidant with mono-, di-, or trivalent (neutral) centers, such as nitrenes, silylenes, phosphines, phosphites, phosphorane anions, phosphonium ion betaines, phosphine selenides, sulfides, selenides, and tellurides. Oxidants that have been used in the generation of these high-energy XO_2 dioxiranes include lowest excited singlet state oxygen ($^1\text{O}_2$), ground state triplet oxygen ($^3\text{O}_2$), ozone (O_3), superoxide ion ($\text{O}_2^{\bullet-}$), and hydrogen peroxide (H_2O_2).

Two general types of reactions give rise to XO_2 dioxiranes (Scheme 1). In the first case, XO_2 dioxiranes can arise from a “side-on” addition of the O_2 on the heteroatom center (e.g., reaction of Ph_3P with $^1\text{O}_2$). In the second case, XO_2 dioxiranes originate from cyclization of the acyclic XOO form, which arose from an initial “end-on” addition of O_2 (e.g., reaction of F_2Si with $^3\text{O}_2$). Methods that can generate XO_2 dioxiranes often do so in the presence of other reactive species, such as acyclic XOO or $^1\text{O}_2$.

The experimental requirements for producing XO_2 dioxiranes are not well defined, which leads to the question of how to develop this area. Our review of XO_2 dioxirane data in the solid-, solution-, and gas-phases will attempt to include substituent effects on the stability of XO_2 dioxiranes. The issues and challenges encountered in the synthesis of heteroatom-containing dioxiranes will be explored. Upon formation of XO_2 dioxiranes, subsequent intra- and intermolecular reactions take place. The analysis of structure and kinetics presented here can help guide thinking for the factors that underlie XO_2 dioxirane reactivity.

One aim of the review will be to consider the benefits of interplay between computational and experimental lines of evidence to help establish reactions that can generate XO_2 dioxiranes. Existing computational evidence will be summarized for XO_2 structures and their reactivities that are not yet characterized experimentally, such as in the cases where X equals R_2Ge , R_2Sn , R_2Te , S, and Se.

It should be noted that no comprehensive and critical coverage exists for cyclic XO_2 peroxide chemistry. Four previous reviews concerned with some aspects of XO_2 dioxiranes were published in 1995,¹ 1996,² 2000,³ and 2005.⁴ The metallodioxiranes, MO_2 (M = metal, e.g., Mo, etc.), will not be covered in this review. No comprehensive review exists for metallodioxiranes, MO_2 .⁵

3. Scope

This review will treat sequentially heteroatom-substituted dioxiranes possessing a tetrahedral and trigonal bipyramidal geometry. In section 4.1, tetrahedral “pyramidal” dioxiranes are discussed based upon the order of heteroatoms in the

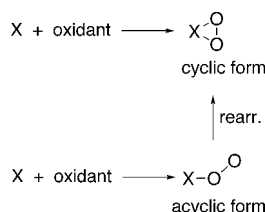


Nahed Sawwan was born in Gaza, Israel. After receiving her Pharmacy Assistant Diploma in 1991 and her B.S. degree in 1992 at the Islamic University in Gaza, she came to the United States. In 2000 she entered the Department of Chemistry at Long Island University—Brooklyn Campus, where she studied analogues of Kemp's triacid, leading to an M.S. degree in 2002. She is currently working toward her Ph.D. degree with A. Greer at Brooklyn College of the City University of New York, engaged in the synthesis and mechanistic studies of sulfur heterocyclic and dioxirane compounds. She enjoys activities with her children and family, such as hiking and climbing, and she is skilled in the sport of table tennis.



Alec Greer obtained his Ph.D. degree from the University of Wyoming under Edward L. Clennan. He was a postdoctoral fellow at University of California—Los Angeles with Christopher S. Foote, and then he moved to Brooklyn College of the City University of New York (CUNY) in 1999. His research interests are in physical organic chemistry, singlet oxygen and peroxide chemistry, as well as chemical evolution and natural products chemistry.

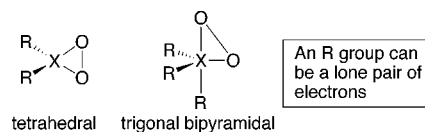
Scheme 1. Formation of XO_2 Dioxiranes



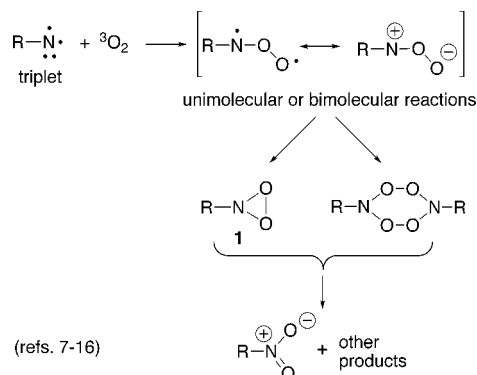
periodic table, with the exception of cyclic SO_2 and cyclic SeO_2 . In section 4.2, a similar approach will be used for the trigonal bipyramidal (TBP) dioxiranes. Each subsection will describe the structure, generation, and reactions involving the XO_2 dioxiranes, where data is available. The description of a particular XO_2 dioxirane will vary in length based upon whether investigations involved direct spectroscopic, indirect trapping, and/or computational techniques.

In section 4.3, the energetics of the interconversion between cyclic and ring-open XO_2 peroxides is discussed. A unimo-

Scheme 2. Types of XO_2 Dioxiranes



Scheme 3. Reaction of Nitrene with O_2



lecular reaction pathway is discussed in which XO_2 dioxiranes undergo an O—O bond homolysis to give the acyclic O—X—O isomer. In some cases XO_2 dioxiranes are thought to arise from the acyclic XOO form. Factors involved with intermolecular oxygen-transfer reactions of the XO_2 dioxiranes will be discussed in section 4.4. Lastly, the synthetic implications of XO_2 dioxiranes will be the topic of section 4.5.

We intend to compare R_2CO_2 dioxiranes with XO_2 dioxiranes. Some examples of R_2CO_2 dioxiranes will be mentioned but not explicitly covered. There is substantial literature on R_2CO_2 dioxiranes. We emphasize that R_2CO_2 dioxiranes are a topic of their own, which has been previously reviewed⁶ and is beyond the scope of this review. The restriction also applies to the carbonyl oxide/dioxirane pair. Carbon-based dioxiranes have proven to be highly useful in synthetic chemistry.

4. Heteroatom-Containing Dioxiranes

Heteroatom-containing dioxiranes, XO_2 , possess either tetrahedral or trigonal bipyramidal geometry (Scheme 2). A trigonal bipyramidal structure where both oxygens are equatorial, as opposed to one apical and one equatorial, has only been suggested in one case. Evidence for the existence of these three-membered-ring XO_2 peroxides, their possible rearrangements, and their oxygen-transfer reactions are outlined. Different levels of confidence exist in the assignment of XO_2 structures.

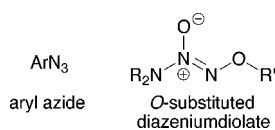
4.1. Tetrahedral Dioxiranes

Experimental evidence exists for tetrahedral XO_2 dioxiranes that take the form RNO_2 and R_2SiO_2 , but it is not available for R_2GeO_2 , R_2SnO_2 , R_2PbO_2 , SO_2 , and SeO_2 . The matrix isolation technique has played a key role in identifying RNO_2 and R_2SiO_2 dioxiranes. All of the tetrahedral XO_2 dioxiranes have been explored computationally except SeO_2 .

4.1.1. Dioxaziridine, RNO_2

4.1.1.1. Background Information. Dioxaziridine (azadioxirane, **1**, Scheme 3) has not been isolated as a pure compound but has been proposed as an unstable intermediate in glassy solutions (e.g., 2-methyltetrahydrofuran at 77 K)⁷

Scheme 4. Dioxaziridine Precursors



and in inert solvents (e.g., acetonitrile at 298 K).⁸ Dioxaziridines are not stable at room temperature. To date, ten studies have proposed the formation of dioxaziridine via nitrene–O₂ chemistry from aryl azide and O-substituted diazeniumdiolate photooxidations (Scheme 4).^{7–16} Tars also form in photooxidations of aryl azides.^{17–22} A non-nitrene route to dioxaziridine has not been suggested. The idea of dioxaziridine as an intermediate in azide–ozone chemistry has not been put forward.²³

Dioxaziridine may arise from the spin-allowed reaction of triplet nitrene with ³O₂, generated by cyclization of the initially formed nitroso oxide (Scheme 3). The reaction is analogous to the reaction of triplet carbenes with ³O₂. Owing to its ability to hydroxylate toluene,⁸ nitroso oxide has been described as possessing diradical character (RN[•]OO[•]) rather

than the zwitterionic character (RN⁺OO[−]); the latter is related to nucleophilic oxidants carbonyl oxides (R₂C⁺OO[−]) and persulfoxides (R₂S⁺OO[−]). However, there are differences of opinion as to the fate of the nitroso oxide. These differences may be reconciled based on nitroso oxide concentrations. High concentrations of nitroso oxide lead to dimerization to a six-membered-ring diperoxide, [1,2,4,5]-tetraoxa-3,6-diazinane, rather than intramolecular cyclization to the dioxaziridine. A compilation of the methods and reaction conditions proposed to generate dioxaziridine or tetraoxadiazinane is given in Table 1.

Matrix isolation has only been employed in one study to characterize structurally dioxaziridines.⁷ Dioxaziridines have been directly detected by UV–visible spectroscopy.⁷ Structural identification methods that use IR, EPR, luminescence, or NMR spectroscopy have not produced clear evidence for their detection. Dioxaziridines have so far not been trapped and are not capable of oxygen transfer to hydrocarbon molecules. This may be due to the powerful oxidation chemistry displayed by the precursor of the dioxaziridine, nitroso oxide.

Table 1. Generation of Dioxaziridines (RNO₂ Dioxirane) or Tetraoxadiazinane (Diperoxide)

Year	Structure	Evidence of Formation	T(K)	Method of Preparation ^a	Ref.	Comments
2004		Luminescence data	298	A	14, 15	
2002		Luminescence data	298	C	13	Dioxaziridine contained within a rubber polymer was proposed
2001		Kinetic and product study	298	D	10	Light source power suggested to influence dioxaziridine-to-tetraoxadiazinane contribution
2001		Luminescence data	293	A	16	
1999	1a - 1f	UV-Visible detection	77	A	7	Presumably formed by nitroso oxide isomerization
1996		¹⁸ O ₂ labeling	298	B	8	Dioxaziridine suggested to have a very short lifetime and convert rapidly to ArNO ₂ nitrobenzene
1991		¹⁸ O ₂ labeling	298	B	11	Suggestion of whether dioxaziridine was an intermediate or TS was not made
1987		¹⁸ O ₂ labeling	298	B	12	Unimolecular isomerization of PhNOO to nitrobenzene suggested to go via phenyldioxaziridine
1987		Product study	298	B	17	Product distribution varies based upon high- vs low power light source. Intractable tarry polymer product also formed
1971		Product study	77	A	9	Suggested assignment of dioxaziridine or tetraoxadiazinane is only tentative

^a A, matrix isolation of ArN₃ photooxidation; B, room-temperature solution-phase ArN₃ photooxidation; C, substrates adsorbed to natural rubber; D, room-temperature solution-phase diazeniumdiolate photooxidation.

Table 2. UV–visible Spectroscopic Data Obtained from Aryl Azide Photooxidations^a

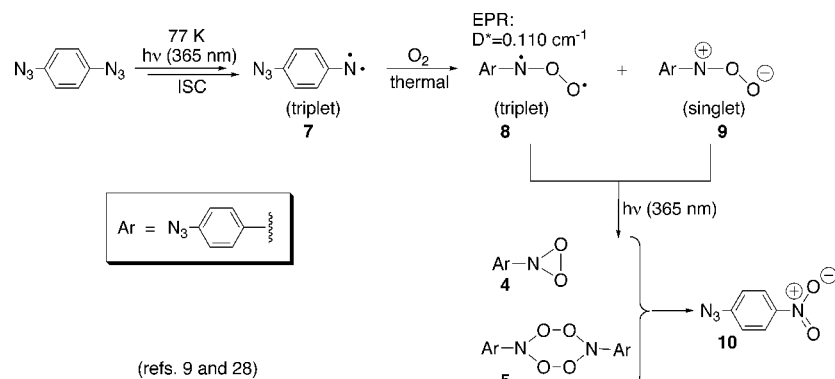
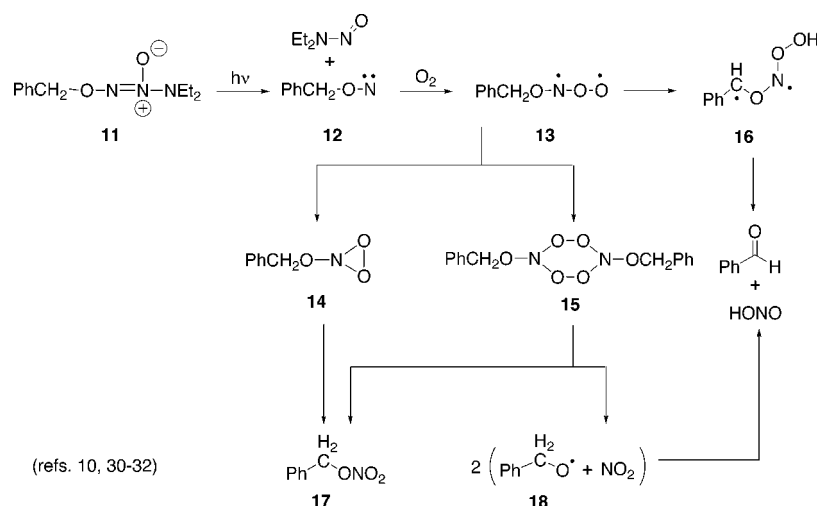
R	2 λ_{max} (nm)	1 λ_{max} (nm)	3 λ_{max} (nm)
	514	333, 348	373
	486	367	357, 374, 394
	703	414	477
	612	362	432
	541	-	389
	554	355, 371	379, 396, 425, 454

^a Matrix detection of nitroso oxides, dioxaziridines, and nitro compounds at 77 K. Adapted with permission from ref 7. Copyright 1999 American Chemical Society.

4.1.1.2. Low Temperature. UV–Visible Spectroscopy. We have only located one study that provided UV–visible spectroscopic evidence for the formation of dioxaziridines in the reaction of nitrenes with O₂ (Table 2). In 1999, the formation of 4-(dioxaziridinyl)stilbene (**1a**), 4-(dioxaziridinyl)-4'-nitrostilbene (**1b**), 4'-(dioxaziridinyl)-4-(dimethylami-

no)stilbene (**1c**), 4'-(dioxaziridinyl)-4-aminobiphenyl (**1d**), and 4-(dioxaziridinyl)-4'-(nitrene-substituted)stilbene (**1f**) was reported in rigid “glassy” 2-methyltetrahydrofuran (MTHF) at 77 K.^{7,24} UV or visible irradiation of various aryl azides in air-saturated MTHF solution produced the corresponding triplet nitrene precursors,²⁵ which can be detected by EPR and UV–visible spectroscopy.^{24,26,27} The reaction between the triplet nitrenes and O₂ is a thermal process and gives the corresponding nitroso oxides **2a–2e**, respectively, where **2f** arises from subsequent loss of N₂. Upon irradiation at 95 K, nitroso oxides **2a–2f** rearrange unimolecularly to dioxaziridines **1a–1f**. This process has a large barrier (computed value 45 kcal/mol).⁷ MTHF is a rigid medium at 77 K and thus bimolecular reactions leading to [1,2,4,5]-tetraoxa-3,6-diazinanes appear to be unlikely. The dioxaziridines **1a–1e** subsequently isomerize to give the corresponding nitro compounds (**3a–3e**).

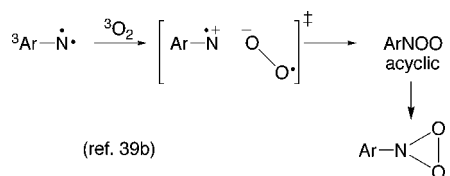
EPR Spectroscopy. In 1971, the intermediacy of dioxaziridine **4** or tetraoxadiazinane **5** was proposed in a photooxidation reaction with *p*-diazidobenzene (Scheme 5).^{9,28} The UV photolysis ($\lambda = 365$ nm) of *p*-diazidobenzene in O₂-saturated hydrocarbon solvents (3-methylpentane, methylcyclohexane, or ethanol) at 77 K produced the triplet mono-nitrene (**7**) in an early step.^{9,29} EPR, luminescence, and visible spectroscopy followed the course of the reaction. Interestingly, the thermal reaction between triplet nitrene and O₂ gave higher nitroso oxide concentrations in 3-methylpentane compared to methylcyclohexane glasses, likely due to enhanced O₂ solubility or diffusion in the 3-methylpentane matrix at 77 K. Compound **8** was suggested to possess triplet

Scheme 5. Photooxidation of *p*-Diazidobenzene**Scheme 6. Photooxidation of O-Substituted Diazeniumdiolate**

character (based on an observed triplet species with $D^* = 0.110 \text{ cm}^{-1}$ in the EPR spectrum, a signal only present in O_2 -containing samples), whereas **9** possessed singlet dipolar character (based on the observed diamagnetic yellow intermediate). On irradiation, the nitroso oxide(s) converted to the *p*-nitrophenyl azide product (**10**) via dioxaziridine or [1,2,4,5]-tetraoxa-3,6-diazinane intermediates. Only tentative evidence for dioxaziridine **4** was found, based on the possible interconversion of the nitroso oxide(s) to *p*-nitrophenyl azide **10**.

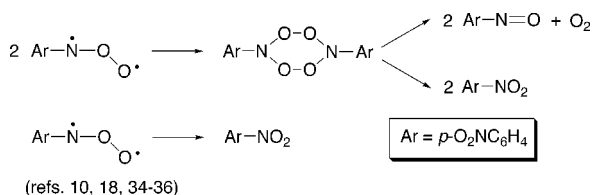
4.1.1.3. Room Temperature. Time-Resolved Infrared Study: Oxynitrene– O_2 Reaction. In 2001, a solution-phase O-substituted diazeniumdiolate (**11**) photooxidation reaction was conducted at room temperature.¹⁰ Laser light ($\lambda = 266 \text{ nm}$) was used to irradiate **11** in O_2 -saturated acetonitrile- d_3 , which led to an O-substituted nitrene (**12**) and $\text{Et}_2\text{NN}=\text{O}$ (Scheme 6).^{10,30–32} Time-resolved infrared (TRIR) spectroscopy was used and provided kinetic insight that dioxaziridine (**14**) and tetraoxadiazinane (**15**) are both present as transient intermediates in the reaction. A first-order pathway for the nitroso oxide **13** leads to dioxaziridine **14**, whereas a second-order pathway for **13** afforded tetraoxadiazinane **15**. The relative contributions of the uni- and bimolecular pathways depended on the initial concentration of nitroso oxide **13**. A higher concentration of **13** was achieved from the use of high laser power, which then favored the bimolecular reaction to give **15**. Low laser power resulted in low steady-state concentrations of **13**. This consequently favored the unimolecular conversion of nitroso oxide to dioxaziridine **14** or diradical **16**. Formation of benzyl nitrate (**17**) is proposed to take place via dioxaziridine and tetraoxadiazinane. Benzaldehyde and nitrous acid (HONO) are additional products, thought to arise from **13** to **16** or produced by fragmentation of **15** into $\cdot\text{NO}_2$ and benzyloxy radical **18** and subsequent coupling. Interestingly, oxynitrenes are known to react faster with $^3\text{O}_2$ compared to aryl nitrenes due to a possible electron transfer to form an ion pair, coupling to generate the nitrene oxide, which cyclizes to the dioxaziridine (Scheme 7).^{39b}

Scheme 7. Formation of an Ion Pair Transition State



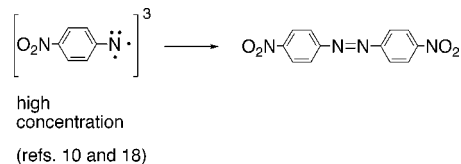
Laser Flash Photolysis: Aryl Nitrene– O_2 Reaction. In 1987, the photooxidation of *p*-nitrophenyl azide was reported in benzene and acetonitrile solution.¹⁷ The reaction of *p*-nitrophenyl nitrene reacted with O_2 afforded the corresponding nitroso oxide. Dimerization of the nitroso oxide was suggested to give [1,2,4,5]-tetraoxa-3,6-diazinane (Scheme 8).^{10,18,34–36} Cleavage of [1,2,4,5]-tetraoxa-3,6-diazinane yields $\text{ArN}=\text{O}$ and O_2 (in a spin-forbidden process giving $^3\text{O}_2$ or in a spin-allowed process giving $^1\text{O}_2$), or it can fragment to

Scheme 8. Reactions of Nitroso Oxides



give 2 equiv of ArNO_2 . ArNO_2 may also come directly from nitroso oxide ArNOO . $\text{ArN}=\text{O}$ reacts with triplet nitrene to give dinitroazobenzene [$\text{ArN}(\text{O})=\text{NAr}$], or nitrene dimerizes when its concentration is raised, as in the case of the high-power irradiation (Scheme 9). The observation that variation

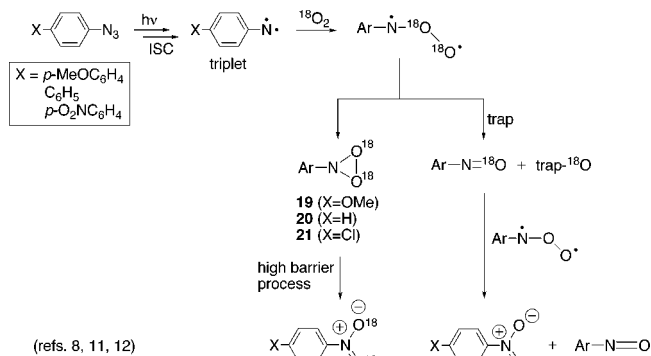
Scheme 9. Nitrene Dimerization



of the laser irradiation power leads to different product distributions constitutes an important discovery. One may anticipate that low-power irradiation conditions facilitate the unimolecular reaction of nitroso oxide **13** to dioxaziridine **14** (Scheme 6) by analogy with the *p*-nitrophenyl nitrene photooxidation reaction in dilute homogeneous solution (Scheme 8).¹⁰

^{18}O Isotope Labeling. ^{18}O labeling experiments carried out from 1987 to 1996 suggested that *p*-methoxyphenyl dioxaziridine (**19**), phenyl dioxaziridine (**20**), and *p*-nitrophenyl dioxaziridine (**21**) arise in the photooxidation of *p*-methylphenyl azide, phenyl azide, and *p*-nitrophenyl azide, respectively (Scheme 10).^{8,11,12} The ^{18}O -tracer experiments

Scheme 10. ^{18}O -Labeling Study in Aryl Azide Photooxidations



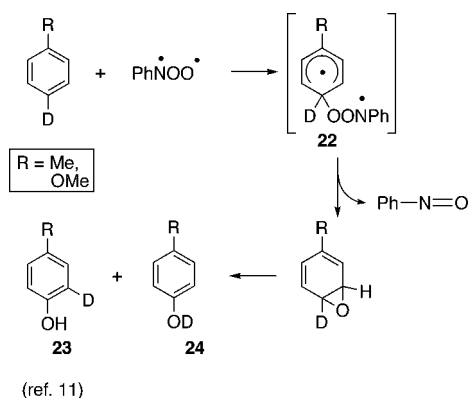
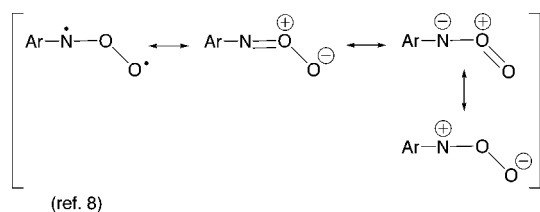
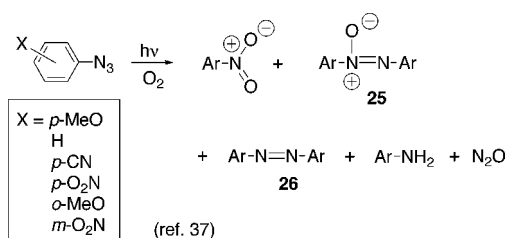
were conducted in acetonitrile solvent at $20 \text{ }^\circ\text{C}$ ($\lambda > 350 \text{ nm}$) by using a mixture of $^{18}\text{O}_2$ and $^{16}\text{O}_2$ gas. GC/MS determined the content of ^{18}O and ^{16}O within the products. Indirect evidence pointed to a dioxaziridine intermediate, since retention of two ^{18}O atoms in the nitro product originated from one $^{18}\text{O}_2$ molecule. A unimolecular cyclization of the two oxygen atom labels in the nitro product (Table 3). Scrambling would have indicated that the oxygen atoms come from different O_2 molecules. Table 3 also shows that the unimolecular rearrangement of nitroso oxide to dioxaziridine is competitive with oxygen transfer (trapping) from the nitroso oxide to $\text{PhN}=\text{O}$, Ph_2S , Ph_2SO , and benzene. The work identified the electrophilic character in the phenyl nitroso oxide (PhN^+OO^-). PhN^+OO^- is capable of hydroxylating toluene-4-*d* and anisole-4-*d* via an NIH shift to give the products 4-methylphenol-*d* (**23**; $\text{R} = \text{Me}$), 4-methoxyphenol-*d* (**23**; $\text{R} = \text{OMe}$), 4-methylphenyl-2-*d*-ol (**24**; $\text{R} = \text{Me}$), and 4-methoxyphenyl-2-*d*-ol (**24**; $\text{R} = \text{OMe}$) (Scheme 11).

According to computations, a large energy barrier separates the nitroso oxide and dioxaziridine ($\sim 45 \text{ kcal/mol}$) (section

Table 3. ^{18}O -Tracer Study in the Photooxidation of Aryl Azides^a

ArN ₃	additive	conv (%)	yield (%) of ArNO ₂	mass data of ArNO ₂ : M/(M+2)/(M+4)	retention/scrambling ^b
				100/0.6/8.4	100:0 (calculated)
				100/16.8/0.7	0:100 (calculated)
<i>p</i> -MeOC ₆ H ₄	Ph ₂ S	85	14	100/10.8/3.3	35:65
<i>p</i> -MeOC ₆ H ₄	Ph ₂ SO	94	25	>100/55.7/7.5	16:84
C ₆ H ₅		41	28	100/10.7/4.0	41:59
<i>p</i> -O ₂ NC ₆ H ₄	Ph ₂ SO	90	30	100/14.0/2.1	19:81

^a Irradiation of ArN₃ ($\lambda = 350$ nm) in acetonitrile under oxygen ($^{32}\text{O}_2/^{34}\text{O}_2/^{16}\text{O}_2 = 100:0.6:8.4$). Adapted with permission from ref. 8. Copyright 1996 by the Royal Society of Chemistry. ^b Retention means the formation of PhNO₂ from one molecule of oxygen. Scrambling means that the two oxygen atoms in ArNO₂ are derived from two different oxygen molecules.

Scheme 11. Oxygen Transfer from Phenyl Nitroso Oxide to Toluene-4-*d* and Methoxybenzene-4-*d***Scheme 12.** Resonance Forms of Nitroso Oxide**Scheme 13.** Photooxidations of Aryl Azides

4.1.1.5). Thus, it is likely that a photochemical interconversion is necessary to overcome the high barrier,⁷ although some authors argue that a greater diradical character (versus the zwitterion resonance form) will enable cyclization of the RNOO intermediate (Scheme 12).^{8,11,12}

Sensitized Reaction. In 1983, a photooxidation reaction of aryl azides was conducted in acetonitrile, acetone, and benzene solvents at 30 °C (Scheme 13).³⁷ While dioxaziridine and tetraoxadiazinane were not suggested as intermediates in the reaction, this study is worth mentioning. This appears to be the only example of triplet sensitization in connection with the addition of oxygen during the photolysis of organic

azides. A medium-pressure mercury lamp was used as the light source. When the triplet sensitizers acetone or acetophenone were added, an increased yield of nitrobenzene product resulted. Addition of a triplet quencher (piperylene) led to negligible yields of nitrobenzene product; however, addition of singlet oxygen sensitizers, Rose Bengal or methylene blue, had no effect on the product yields, which suggested that $^1\text{O}_2$ is not playing a role in the photooxidation. The presence of amine additives influenced the product distribution, in that primary or secondary amines increase production of tar while tertiary amines lower it.³⁸ Such effects with added amines have also been observed by others.^{18,38–40}

4.1.1.4. Miscellaneous. In 2002, it was suggested that formation of dioxaziridine takes place in 4,4'-diazobiphenyl-containing rubber polymer samples which had been applied to a glass surface and dried before photolysis.¹³ The photooxidation reaction has been proposed to proceed via a nitrene and then subsequently to dioxaziridine N₃C₆H₄–C₆H₄NO₂, where the dioxaziridine was suggested to luminesce at $\lambda_{\text{max}} = 456, 457, 461, 462,$ and 470 nm. Unfortunately, these rubber polymer experiments provide only tentative evidence for the presence of dioxaziridine, since the intermediate(s) responsible for the luminescence has(ve) not been detected. Other experiments have proposed the formation of dioxaziridines from photooxidations of phenylazide and 4,4'-diazodiphenyl in acetonitrile or ethanol solutions at room temperature.^{14–16} It should be mentioned that reactions of molecular oxygen with imidogen (NH) have been studied in combustion processes. The addition of NH ($^3\Sigma^-$) and O₂ ($^3\Sigma_g^-$) is predicted to give imine peroxide, HNOO. Imidogen is generated in the laboratory, for example, by photolysis of hydrazoic acid, where NH ($^1\Delta$) is generated.^{40,41} As yet, there are no experimental data that suggest the formation of unsubstituted dioxaziridine HNO₂ in the imidogen–O₂ reactions, although other HNO_x species have been observed.

4.1.1.5. Calculations. Structure. Computational results for the dioxaziridine are addressed in this section. HNO₂ and PhNO₂ dioxiranes are minima at the G2(MP2), B3LYP/6-31G(d), MP2/6-31G(d), and multiconfigurational MC-SCF/6-31G(d) levels and have been used to explain the experimental data on the nitrene–O₂ reactions.^{7,42–50}

Calculated bond distances and a bond angle are shown in Table 4. Dioxaziridine HNO₂ and PhNO₂ bond distances for O–O range from a high of 1.487 Å to a low of 1.404 Å. The sensitivity of the dioxaziridine geometry to the identity of the substituent R has not been examined in detail. Dioxaziridine HNO₂ and PhNO₂ bear a resemblance to each other independent of the computational method used. For example, at the B3LYP/6-31G* level, the O–O bond distance is 0.002 Å shorter and the N–O bond 0.002 Å shorter in the HNO₂ dioxirane than in the PhNO₂ dioxirane. However, the reported literature value for O–O is 1.404 Å at the MP2/6-31G(d) level and 1.487 Å at the MP2/6-31G(d,p) level. This represents a large difference in the predicted O–O bond distance, which has not been explained. The bond distances for the computed N–O range from a high of 1.451 Å to a low of 1.373 Å. The O–N–O bond angle ranges from a high of 61.8° to a low of 59.2°, with the exception of the MCSCF/6-31G(d) value of 68.3°. A sample computed structure for the unsubstituted dioxaziridine is given in Figure 1.

Dioxaziridines HNO₂ and PhNO₂ have C_s symmetry and negatively charged oxygen atoms. The atomic charges, as predicted by Mulliken, indicate negative charge density at

Table 4. Calculated Energies and Geometries of the Dioxaziridines

Year	Structure	State	Energy ^a	Method and Basis Set	O-O ^b	N-O ^b	O-N-O ^c	Ref.	Comments
1999		S ₀	-205.5670	B3LYP/6-31G(d)	1.461	1.431	61.4	7	Both N-O bond distances are equal in length
1999		S ₀	-436.6261	B3LYP/6-31G(d)	1.463	1.443	60.9	7	
1998		S ₀	-205.32839	G2(MP2)	—	1.449	61.8	46	
1997		S ₀	-205.07655	MP2/6-31G(d,p)	1.487	1.451	59.2	45	
1997		S ₀	—	MP2/6-311G (2df,2p)	1.464	1.435	61.4	45	
1992		S ₀	—	MCSCF/6-31G(d,p) 6-electron-6-orbital	—	1.374	68.3	43	Geometries also optimized for singlet and triplet acyclic HNOO
1989		S ₀	—	MP2/6-31G(d)	1.404	1.373	61.5	44	Basis set dependence on HNOO dihedral angle also reported
1987		S ₀	—	HF/4-31G(d)	1.405	1.374	61.5	47	Structure for dithiaziridine (HNS ₂) also reported

^a Energies in atomic units. ^b Bond distances in angstroms. ^c Bond angles in degrees.

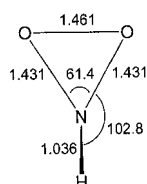


Figure 1. B3LYP/6-31G(d) computed structure of the unsubstituted dioxaziridine from ref 7. Bond lengths in angstroms; bond angles in degrees.

the oxygen atoms (−0.202) and positive ones on the hydrogen (+0.341) and nitrogen atoms (+0.063) (Table 5). Other properties that have been calculated for dioxaziridine HNO₂ include dipole moment (Table 6), energies of the HOMO and LUMO (Table 7), and vibrational frequencies (Table 8).

Energetics. Saddle points connecting the nitroso oxide and dioxaziridine have been located in four studies (Table 9). The cyclization barrier for MeO–NOO to MeONO₂ dioxirane is 21.6 kcal/mol at the B3LYP/6-311+G(d,p)//B3LYP/6-31G(d) level,^{39b} that for PhNOO to PhNO₂ dioxirane is 40.9 kcal/mol at the B3LYP/6-31G(d) level, and that for HNOO to HNO₂ dioxirane is 43.8 kcal/mol at the MCSCF level.⁴³ The barrier is lower at the MP4/6-31G(d,p)//HF/6-31G(d) level, 12 kcal/mol.⁴⁹

Dioxaziridine is apparently isoenergetic with the nitroso oxide in the gas phase. The interconversion of *trans* nitroso

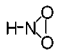
oxide HNOO to dioxaziridine HNO₂ has been calculated to be endothermic by 4.2 kcal/mol (MCSCF) and 4 kcal/mol [MP4/6-31G(d,p)//HF/6-31G(d)] and exothermic by −3.1 kcal/mol [MP2/6-31G(d,p)]. It should be worthwhile to compute the energetics and barrier for conversion of nitroso oxide to the six-membered diperoxide, [1,2,4,5]-tetraoxa-3,6-diazinane. Calculated structures on model systems provide evidence for the formation of dioxaziridine, but they have not been scrutinized against the dimerization pathway thus far.

The activation energies for the interconversion of dioxaziridine to the corresponding nitro compound are 33.2 kcal/mol [MeONO₂, B3LYP/6-311+G(d,p)//B3LYP/6-31G(d)], 14.2 kcal/mol [HNO₂, B3LYP/6-31G(d)], and 18.8 kcal/mol [PhNO₂, B3LYP/6-31G(d)] (Table 9). However, a discrepancy exists since there is a reported value of 2 kcal/mol for HNO₂ [MP2/6-31G(d)]. The exothermicity of the reaction is −70.2 kcal/mol [MeONO₂, B3LYP/6-311+G(d,p)//B3LYP/6-31G(d)], −74.0 kcal/mol [HNO₂, B3LYP/6-31G(d)], −80.7 kcal/mol [PhNO₂, B3LYP/6-31G(d)], −66 kcal/mol (PhNO₂), −64 kcal/mol (PhNO₂, MCSCF), −77.7 kcal/mol [HNO₂, MP2/6-31G(d,p)], −76 kcal/mol [HNO₂, MP4/6-31G(d,p)//HF/6-31G(d)]. For calculated energetics, isomerization and fragmentation are provided in Table 9. This includes conversion of dioxaziridine HNO₂ to acyclic HOON. The reaction of NH (³Σ[−]) and O₂ (³Σ_g[−]) to give acyclic HNOO has been investigated by SCF and MRD-CI calculations with the

Table 5. Calculated Charge Densities of the Unsubstituted Dioxaziridine

Year	Structure	Mulliken Charge				Method and Basis Set	Ref.	Comment
		H	N	O	O			
1997		0.341	0.063	-0.202	-0.202	MP2/6-31G(d,p)	45	A Mulliken gross population was calculated, where q = d _{xx} + d _{yy} + d _{zz} + d _{xy} + d _{yz} + d _{xz}
1987		—	0.094	0.090	0.090	HF/6-31G(d,p)	47	

Table 6. Calculated Dipole Moment of the Unsubstituted Dioxaziridine^a

Year	Structure	μ (Debyes)	Method and Basis Set
1989		2.22	MP2/6-31G(d)

^a Adapted with permission from ref 44. Copyright Wiley.

6-31G(d,p) basis set.^{43,49,50} The reaction between NH (¹ Δ) + O₂ (¹ Δ_g) has been suggested to give dioxaziridine HNO₂ in a concerted addition process, where acyclic HNOO does not intercede. The reaction of HNO₂ dioxirane to ¹HNO + O(³P) is predicted to be endothermic by 7.0 kcal/mol from MCSCF calculations.⁴³ The activation energies for nitroso oxide or dioxaziridine to release an oxygen atom intramolecularly have not been computed to date. Formation of the dioxaziridine by the isomerization of peroxyxynitrite has not been proposed (Scheme 14), presumably due to the high instability expected; however, the isomerization of peroxyxynitrite to nitrate is known.^{23e}

In conclusion, dioxaziridines do not arise as a primary species from a side-on attack of ³O₂ with electron-deficient triplet nitrene. Instead, these nitrene reactions with O₂ produce nitroso oxide, which subsequently may cyclize to dioxaziridine. Persistent isolable dioxaziridines have so far not been prepared. The generation of dioxaziridine as a transient intermediate has been achieved; however, other reactive species are also present, such as azide excited states, nitrenes, nitroso oxides, and tetraoxadiazinanes. To avoid the formation of such reactive intermediates in nitrene chemistry presents a challenge for the clean production of dioxaziridines.

4.1.2. Dioxasilirane, R₂SiO₂

4.1.2.1. Background Information. Dioxasilirane (also known as siladioxirane or dioxasilacyclopropane, **27**) has not yet been isolated as a pure compound due to its instability.

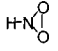
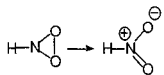
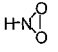
Dioxasilirane can be formed in a reaction of singlet or triplet silylene (silanediyl, R₂Si) with ³O₂. Silylenes generated from azo-, fluoro-, chloro-, methyl-, and methoxy-containing silanes in argon matrices have served as precursors to dioxasiliranes (Scheme 15).^{51–58} Studies also suggest the intermediacy of dioxasilirane from solution-phase, SiO₂-surface, and combustion experiments.^{59–74} A compilation of reaction conditions thought to give rise to dioxasiliranes is given in Table 10.

To date, three studies provide direct spectroscopic evidence for the formation of dioxasilirane intermediates. Surprisingly little indirect evidence has been collected to support the existence of dioxasiliranes. On reaction of silylene with O₂, silanone *O*-oxide (**28**) is thought to form initially and then rapidly interconvert to the dioxasilirane **27**, given the low barrier separating **27** and **28**. Silanone *O*-oxide is the congener of carbonyl oxide, but its oxygen transfer or other chemical reactivity is unknown, so that clarification about the importance of diradical character (R₂Si[•]OO[•]) and zwitterionic character (R₂Si⁺OO⁻) is not available. Bimolecular reactions of **27** or **28** are unknown in matrix and solution phases. 3,3,6,6-Tetrasubstituted-[1,2,4,5]-tetraoxa-3,6-disilane and silanone [RSi(O)R] are not proposed as products formed in silylene–O₂ reactions; however, dioxasilirane can rearrange unimolecularly to a silaester [RSi(O)OR].

A large body of literature is available for silylenes, but only a fraction of it focuses on silylene–O₂ chemistry. The literature on silylenes under oxygen-free conditions will not be covered here.

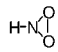
4.1.2.2. Low Temperature. Infrared Spectroscopy. We have located three studies that provide IR spectroscopic evidence for dioxasilirane.^{51–58} In 2000, the synthesis of methylphenyldioxasilirane (MePhSiO₂, **31**) in an oxygen-doped argon matrix at 10 K was reported (Scheme 16).⁵¹ UV irradiation ($\lambda > 305$ nm) of phenylsilyldiazomethane (**29**) in the argon matrix produces methylphenylsilylene via a 2-silapropene intermediate (**30**). Thermal annealing of the argon matrix to 30–45 K led to the reaction of silylene with

Table 7. Calculated HOMO and LUMO Energies of the Unsubstituted Dioxaziridine^a

Year	Structure	HOMO(au)	LUMO(au)	Method and Basis Set	Ref.	Comments
1999		-0.49245	0.20580	HF/6-31G(d)	7	An orbital diagram for the conversion of the following is also given: 
1989		-0.49111	0.21799	MP2/6-31G(d)	44	HOMO and LUMO values also reported for TS for NH inversion process

^a Both N–O bond distances are equal in length.

Table 8. Calculated Vibrational Frequencies of the Unsubstituted Dioxaziridine

Year	Structure	Symmetry	a'	a''	a ^a	a ^b	a'	a ^b	Method and Basis Set	Ref.
1997		Scaled Harmonic Vibrational Frequencies (cm ⁻¹)							MP2/6-31G(d,p)	45
		Scaled Freq.	748	761	1035	1140	1344	3177		
		Unscaled Freq.	801	814	1107	1219	1437	3398		
		IR intensity	0.3	2.9	0.5	39.3	34.8	2.6		

^a Cyclic breathing vibration. ^b Exo N–H stretching vibration.

Table 9. Calculated Relative Energies of Species on the Dioxaziridine Reaction Surface^a

Year	A	B	$\Delta E_{A \rightarrow B}$	Method and Basis Set	Ref.	Comments
2006		 (Ring closing)	21.6 ^b	B3LYP/6-311+G(d,p)// B3LYP/6-31G(d)	39b	Energies are given as $\Delta G(298K)$. Calculations were also performed at the CBS-QB3 level.
			8.6			
		 (Ring opening)	33.2 ^b			
			-70.2			
	³ PhN + PhNOO	2 PhN=O	-79.5			
	³ PhN +	2 PhN=O	-93.5			
2002		 (Ring closure)	40.9 ^b	B3LYP/6-31G(d)	13	Singlet-triplet gap for acyclic PhNOO is 19.0 kcal/mol with the CASSCF/6-31G(d) method
1999		 (Ring opening)	14.2 ^b	B3LYP/6-31G(d)	7	Zero-point energy (ZPE) correction included
		 (Ring opening)	18.8 ^b			
			-74.0			
			-80.7			
	PhNO ₂	PhNO ₂ perpendicular Ph group	3.5			Energy represents the barrier to forcing the phenyl ring to be perpendicular to the dioxaziridine ring
1998	 + 2 NH ₂ OH + HOOH	2 NH ₂ OOH + HON(H)OH	-28.0	G2 (MP2)	46	Atomization energies were also reported
	 + 2NH ₃ + 2HO ₂	2 NH ₂ OH + HOOH	11.8			
1997			-74.7	MP4 SDTQ//MP2/ 6-31G(d,p)	45	ZPE corrected values also available
		 (trans)	-82.0			
		 (cis)	-83.2			
1996			-66		8	Computational method used was not mentioned

Table 9 (Continued)

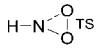
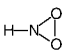
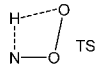
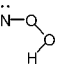
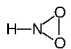
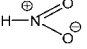
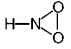
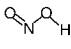
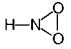
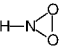
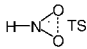
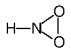
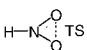
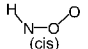
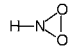
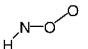
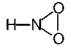
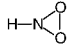
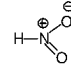
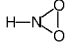
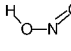
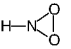
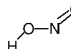
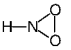
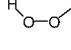
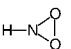
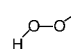
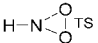
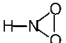
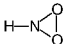
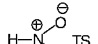
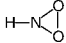
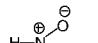
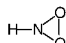
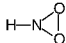
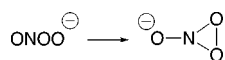
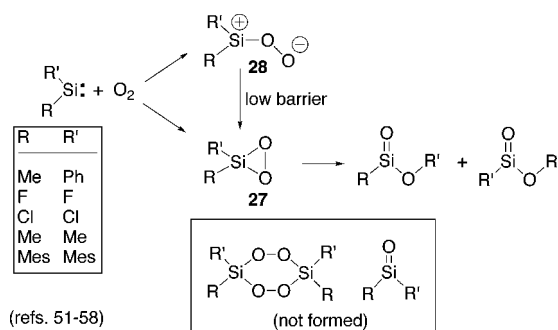
Year	A	B	$\Delta E_{A \rightarrow B}$	Method and Basis Set	Ref.	Comments
1992	H-NOO	 (Ring closure)	43.8 ^b	6-electron/6-orbital MCSCF	43	A multiconfigurational SCF procedure was used and the transition state calculated with CI (full)
	H-NOO		4.2			
1992	H-NOO	 TS	17.2 ^b	6-electron/6-orbital MCSCF	43	Favors route from HNOO to NOOH and then cleavage to NO+OH rather than less stable route of HNOO to cyclic HNO ₂
	H-NOO		-35.7			
			-64.0			
			-81.6			
		HNO + O(³ P)	7.0			
1989		 (Ring opening)	60.7	MP2/6-31G(d)	44	Values from the SCF method, the MP3 method and 6-31G, 6-31G+R. F., and 6-31G+(d) basis set were also reported. Inversion barrier of dioxaziridine is greater than 1H-azirine (46.3), oxaziridine(41.5), 1H-diazirine (34.7), and aziridene (19.9) at the MP2/6-31G(d) level. MP2/6-31G(d) inversion barrier reported on rotation about the HNOO dihedral angle.
		 (Ring opening)	56.8	MP2/6-31+G(d)		
1987	 (cis)		-1.3	MP2/6-31G(d,p)	47	Values also reported at the levels RHF/4-31G, RHF/4-31G(d), RHF/6-31G(d), and MP2/6-31G(d,p)
	 (trans)		-3.1			
			-77.7			
		 (cis)	-83.8			
		 (trans)	-82.4			
		 (cis)	-9.8			
		 (trans)	-18.0			

Table 9 (Continued)

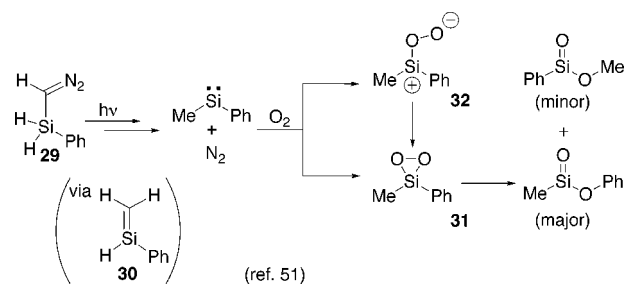
Year	A	B	$\Delta E_{A \rightarrow B}$	Method and Basis Set	Ref.	Comments
1984	HNOO	 TS (Ring closure)	12 ^b	MP4/6-31G(d,p)//HF/6-31G(d)	49	ZPE correction included. Bond additivity-type corrections also included giving sufficient electron correlation contribution. Energy values are taken from a Figure in the original manuscript and are subject to errors of ± 3 kcal/mol.
	HNOO		4			
		 TS (Ring opening)	2 ^b			
			-76			
	¹ NH + ¹ O ₂		-20			Path does not proceed through the HNOO species
		HONO	-81			

^a Energies in kcal/mol. ^b Transition state energies in kcal/mol.

Scheme 14. Cyclization of Peroxynitrite

Scheme 15. Reaction of Silylene with O₂

O₂, giving dioxasilirane **31**. IR spectroscopy detected both silylene and dioxasilirane intermediates. Dioxasilirane **31**

Scheme 16. Reaction of Silylene with O₂

displays a strong Si—O stretching mode at 1002 cm⁻¹ (1005 cm⁻¹ predicted) and a weak O—O stretching mode at 577 cm⁻¹ (608 cm⁻¹ predicted) (Table 11). The predictions were made on the basis of B3LYP/6-311++G(2d,p) calculations. ¹⁸O₂ labeling confirms the assignment of methylphenyldioxasilirane, in which the Si—O stretching vibration is red-shifted by 25.3 cm⁻¹ (28 cm⁻¹ predicted) and the O—O stretching vibration by 23.5 cm⁻¹ (21 cm⁻¹ predicted). The DFT

Table 10. Generation of Dioxasiliranes (R¹R²SiO₂) or Silanone O-Oxides (R¹R²SiOO)

year	R ¹	R ²	evidence of formation	T (K)	method of generation ^a	ref	comments
2000	Me	Ph	IR spectroscopy	30–40	A	51	direct evidence for dioxasilirane obtained
1996	H	H	product analysis		B	74	dioxasilirane proposed among other reactive intermediates
1990	F	F	IR spectroscopy	10	C	52	direct evidence for dioxasilirane obtained
1990	Cl	Cl	IR spectroscopy	10	C	52	direct evidence for dioxasilirane obtained
1989	Me	Me	IR spectroscopy	35–42	D	53, 54	direct evidence for dioxasilirane obtained
1988	Mes	Mes	IR spectroscopy	16	E	82	silanone O-oxide suggested as the intermediate rather than dioxasilirane
1988–2004			UV–vis and IR spectroscopy	700	F	63–73	conclusion for surface-bound silylene contradicts that of previous researchers
1987	Me	Ph	product analysis	298	G	59	tentative indirect evidence for the existence of dimesityldioxasilirane

^a A, matrix isolation from phenylsilyldiazomethane photooxidation; B, laser photolysis of a SiH₄/O₂/CCl₄ mixture; C, matrix isolation from X₃SiX₃ (X = F, Cl) pyrolysis and subsequent photooxidation; D, matrix isolation from diazidodimethylsilane photolysis and pyrolysis of 1,2-dimethoxytetramethyldisilane; E, matrix isolation from reaction of dimesitylsilylene with O₂; F, silica-gel reaction; G, solution-phase reaction of methylphenylsilylene with O₂.

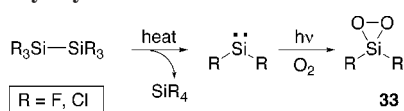
Table 11. IR Data for Matrix-Isolated Methylphenyldioxasilirane, MePhSiO₂

argon, 10 K			B3LYP/6-311++G(d,p)				assignment
$\tilde{\nu}$, cm ⁻¹	<i>I</i> ^a	$\tilde{\nu}_i/\tilde{\nu}^b$	$\tilde{\nu}$, cm ⁻¹	<i>I</i> ^a	$\tilde{\nu}_i/\tilde{\nu}^b$	sym	
3086.3	2	1.000	3191	11	1.000	A'	C–H str
3075.2	1		3183	13	1.000	A'	C–H str
3071.6	3	1.000	3175	5	1.000	A'	C–H str
3058.7	2	1.000	3156	3	1.000	A'	C–H str
3024.7	1		3122	1	1.000	A'	CH ₃ str
3015.1	3	1.000	3099	2	1.000	A''	CH ₃ str
1596.8	17	1.000	1629	10	1.000	A'	ring str
1435.0	30	1.000	1461	13	1.000	A'	skel ring, in pl C–H
1432.5	2	1.000	1456	3	1.000	A'	HCH bend
1429.5	7	1.000	1455	6	1.000	A''	HCH bend
1336.9	3	1.000	1357	4	1.000	A'	skel ring, in pl C–H
1307.5	5	1.000	1311	10	1.000	A'	HCH bend, ring str
1260.3	10	0.998	1301	20	1.000	A'	HCH bend
1218.0	4		1211	2	1.000	A'	in pl C–H bend
1135.6	92	0.999	1139	97	0.999	A'	skel ring, in pl C–H
1033.7	4	0.999	1049	1	0.999	A'	skel ring, in pl C–H
1013.1	1		1013	3	1.000	A'	ring breathing
1002.1	81	0.975	1005	100	0.972	A'	SiO str
998.2	28						
792.7	100	0.999	820	72	0.998	A'	CH ₃ rock
783.4	4	0.994	800	15	0.998	A''	CH ₃ twist
777.0	4						
737.5	29	0.999	750	40	1.000	A''	C–H wag
729.9	17	1.004	747	38	0.996	A'	SiC str, CH ₃ def
717.6	3	0.952	731	3	0.956	A''	SiC def, CH ₃ def
694.5	39	1.000	710	31	1.000	A''	C–H wag
678.8	8	0.991	695	8	0.986	A'	
576.7	28	0.959	608	25	0.965	A'	O ₂ str, CH ₃ def
456.3	11	0.999	466	9	1.000	A''	C–H wag

^aRelative intensity based on the strongest peak. ^bRatio of the frequencies of the ¹⁸O versus ¹⁶O isotopomers. ^cThe assignment of experimental and calculated IR absorption is based on peak positions and peak intensities and is only tentative for the weak absorptions. Ref 51.

calculations reveal a barrier of about 1 kcal/mol for the cyclization of the silanone *O*-oxide **32** to dioxasilirane **31**. The silanone *O*-oxide **32** is not observed experimentally, probably because of a rapid interconversion to the dioxasilirane. Since silanone *O*-oxide **32** exists in a very shallow minimum and may not be chemically relevant, the generation of dioxasilirane **31** via MePhSi and O₂ is conceivable as a direct addition. Dioxasilirane **31** is photolabile and with 420-nm light interconverts to the silaester, MeSi(O)OPh via a [1,2]-phenyl migration or to PhSi(O)OMe via a [1,2]-methyl migration.

In 1990, the pyrolysis of hexafluorodisilane and hexachlorodisilane was reported (Scheme 17).^{52,55,56} The loss of SiF₄

Scheme 17. Pyrolysis of Hexahalodisilane

(refs. 52, 55, 56)

and SiCl₄ takes place in an argon or argon–oxygen matrix, in which difluorosilylene and dichlorosilylene were subsequently trapped at 10 K. UV–visible photolysis of matrix-isolated difluorosilylene and dichlorosilylene in an O₂-containing matrix at 45 K yielded difluorodioxasilirane (**33**, R = F) and dichlorodioxasilirane (**33**, R = Cl). Isotopic labeling with ¹⁶O₂/¹⁶O¹⁸O/¹⁸O₂ mixtures and HF/6-31G(d) calculations aided in the analysis of the IR spectra and in assigning the dioxasilirane structures (Table 12). ¹⁸O-isotopic

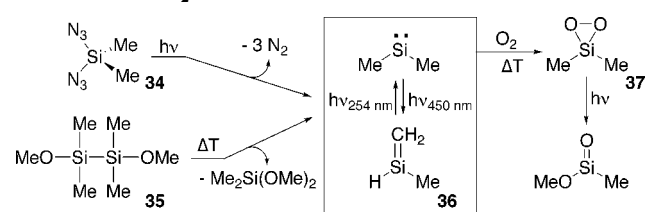
Table 12. IR Spectroscopic Data of F₂SiO₂ and Cl₂SiO₂ Dioxiranes, Matrix-Isolated in O₂ at 10 K and ab initio Data of F₂SiO₂ Dioxirane Calculated at the HF/6-31G(d) Level^a

matrix				6-31G(d)				assignment ^f
$\tilde{\nu}^b$	<i>I</i> ^c	$\Delta\tilde{\nu}_1^d$	$\Delta\tilde{\nu}_2^e$	$\tilde{\nu}^b$	<i>I</i> ^c	$\Delta\tilde{\nu}_1^d$	$\Delta\tilde{\nu}_2^e$	
1155.2								
1153.5								
1152.0	1.00	-9.6	-19.3	1120.0	1.00	-12.7	-25.9	$\delta(\text{Si–F})$
1150.8								
1013.7	0.86	-0.5	-3.7	967.0	0.87	-0.1	-0.1	$\delta(\text{Si–F})$
862.7	0.02	<i>g</i>	-32.4	800.0	0.12	-9.0	-26.2	$\delta(\text{Si–O})$
				615.0	0.08	-13.7	-28.1	$\delta(\text{O–O})$
1054.4	1.00	-14.5	-30.9					$\delta(\text{Si–O})$
649.9	0.71	0.0	0.0					$\delta(\text{Si–O})$
647	0.63	0.0	0.0					$\delta(\text{Si–Cl})$
576.1	0.30	-11.1	21.1					$\delta(\text{O–O})$

^aReferences 52, 55, and 56. ^bWavelength in cm⁻¹. ^cRelative intensity. ^dIsotopic shift if one ¹⁶O atom is replaced by ¹⁸O. ^eIsotopic shift if two ¹⁶O atoms are replaced by ¹⁸O. ^fApproximate description on the basis of observed isotopic shifts and the calculated mode vectors. ^gThis weak peak of the O–O isotopomer could not be observed.

labeling reveals the equivalence of the oxygen atoms in C_{2v}-symmetric dioxasilirane **33**. When one ¹⁶O atom in **33** (R = F) is replaced with ¹⁸O, the strong band at 1153 cm⁻¹ (four peaks) shifts to a lower frequency (by 9.6 cm⁻¹). Replacement of both oxygens by ¹⁸O results in a shift to lower frequency by 19.3 cm⁻¹. A photolysis reaction was required to generate the dioxasiliranes **33** (R = F, Cl). Thermal reactions (up to 45 K) between O₂ and difluorosilylene and dichlorosilylene did not yield the corresponding dioxasiliranes. The dioxasilirane stability depends on substituent effects. Dioxasiliranes **33** (R = F, Cl) are stable to UV irradiation, unlike methylphenyldioxasilirane **31** and dimethyldioxasilirane **37**. The stronger Si–F and Si–Cl versus Si–C bonds play a role so that the [1,2]-fluoro or -chloro (rearranged) products, namely fluorine fluorosilanoate [FSi(O)OF] and chlorine chlorosilanoate [ClSi(O)OCl], are not easily formed.

In 1989, a matrix isolation study^{53,54} demonstrated that dimethyldioxasilirane **37** forms in the 254-nm photolysis of diazidodimethylsilane [Me₂Si(N₃)₂, **34**] in O₂-doped argon at 10 K or by pyrolysis (700 °C) of 1,2-dimethoxytetramethyldisilane (**35**), followed by O₂ trapping in an argon matrix (Scheme 18).^{55,56} A photochemical equilibrium exists

Scheme 18. Generation of Silylene and a Subsequent Reaction with O₂

(refs. 53, 54)

between 2-silapropene (**36**) and dimethylsilylene (Me₂Si),^{75–80} in which dimethylsilylene is subsequently trapped by O₂.⁸¹ IR spectroscopy revealed the splitting of an 1021 cm⁻¹ absorption with ¹⁸O labeling, which when coupled with the propensity of the intermediate to rearrange to methoxymethylsilanone [MeSi(O)OMe] led to the assignment of the intermediate as dimethyldioxasilirane **37**. The strong Si–O stretching mode at 1013 cm⁻¹ and the weak O–O stretching mode at 554 cm⁻¹ for dimethyldioxasilirane **37** are consistent

with similar assignments made for methylphenyldioxasilirane **31** of 1002 and 577 cm^{-1} .⁵¹ Dioxasilirane **37** is photochemically unstable and with 436 nm light rearranges to the corresponding silaester. MP2/6-31G(d) and HF/6-31G(d) calculations aided in the interpretation of the experimental IR data (Table 13). There is no evidence for the dimethylsilanone *O*-oxide intermediate.

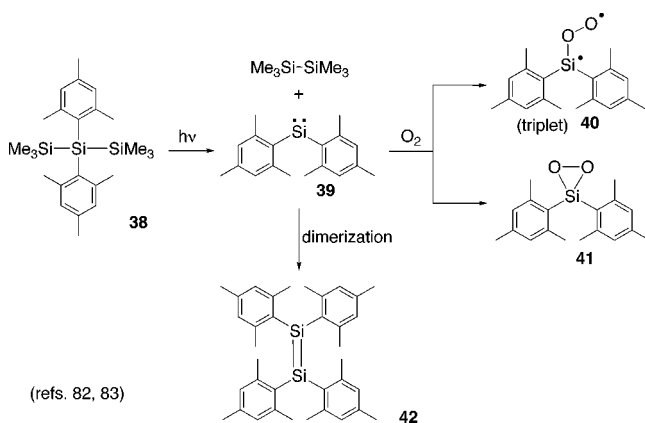
Table 13. IR Spectroscopic Data of Dimethyldioxasilirane (37), Matrix-Isolated in Ar at 10 K ($\bar{\nu}$ [cm^{-1}], $\Delta\bar{\nu}$ Isotopic Shift)^a

frequencies ($\bar{\nu}$)		$\Delta\bar{\nu}$	$[\text{O}_2]$ - 37		assignment ^c
$[\text{O}_2]$ - 37	$[\text{O}_2]$ - 37 ^b		$[\text{O}_2]$ - 37	$[\text{O}_2]$ - 37	
1431.4 (w)	1430.9 (w)	-0.5	1430.4 (w)	-1.0	$\delta_{\text{as}}(\text{CH}_3)$
1260.3 (m)	1260.0 (m)	0.0	1258.8 (m)	-1.5	$\delta_{\text{s}}(\text{CH}_3)$
1021.1 (s)	1009.6 (s)	-11.5	997.0 (s)	-24.1	$\bar{\nu}_{\text{as}}(\text{Si}-\text{O})$
1012.9 (w)	1005.2 (m)	-7.7	988.8 (w)	-24.1	<i>d</i>
1005.7 (w)	993.2 (w)	-12.5	981.1 (w)	-24.6	$\bar{\nu}_{\text{as}}(\text{Si}-\text{O})$ ^d
820.1 (m)	814.8 (m)	-5.3	810.4 (m)	-9.7	
820.1 (m)	814.8 (m)	-5.3	809.5 (m)	-10.6	$\delta(\text{CH}_3)$ ^e
809.5 (m)	814.8 (m)	-5.3	800.8 (w)	-8.7	$\delta(\text{CH}_3)$ ^e
554.4 (w)			530.8 (w)	-23.6	$\bar{\nu}(\text{O}-\text{O})$

^a References 53 and 54. ^b Due to the presence of three isotopomers in the spectra, not all bands could be assigned. ^c Approximate description on the basis of observed isotopic shifts and by comparison with ab initio calculations. ^d The assignment of the weak bands at 1012.9 and 1005.7 is not definite. ^e Rocking mode.

In one study, the formation of a silanone *O*-oxide was suggested instead of dioxasilirane. In 1988, the reaction of di-2,4,6-trimethylphenylsilylene (dimesitylsilylene, **39**) was conducted in a cryogenic solid-oxygen matrix at 16 K (Scheme 19).⁸² An analysis of the products by IR spectroscopy

Scheme 19. Irradiation of 2,2-Bis(2,4,6-trimethylphenyl)hexamethyltrisilane

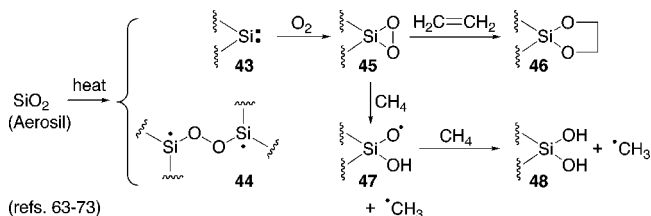


concluded that a triplet state silanone *O*-oxide **40** was present and not the dioxasilirane **41** based on data from isotopic mixtures of oxygen gas ($^{18}\text{O}_2$ and $^{16}\text{O}_2$) and HF/6-31G(d) computations. Dimerization of dimesitylsilylene **39** to form stable tetramesityldisilene **42** can take place in the absence of O_2 .⁸³ This example for the intermediacy of silanone *O*-oxide stands in contrast to other reports of O_2 with silylenes (MePhSi , F_2Si , Cl_2Si , and Me_2Si), which point to a facile interconversion to the dioxasilirane.^{51-54,61,62}

4.1.2.3. Room Temperature. Silylene- O_2 Reaction. While some work has been performed on the silylene- O_2 reaction in low-temperature argon matrices, little is known about the involvement of dioxasilirane in solution or at room temperature.⁵⁹⁻⁶² In 1987, laser photolysis ($\lambda = 266$ nm) of $(\text{Me}_3\text{Si})_2\text{SiMePh}$ was conducted in air-saturated cyclohexane solutions at 298 K. This reaction yielded methylphenylsilylene, which subsequently reacted with O_2 .^{59,61,62} Only a tentative suggestion was made for formation of the silanone *O*-oxide **32** or dioxasilirane **31** intermediates;^{3,61,62,84} thus, there is some uncertainty as to whether the dioxasilirane had been generated in cyclohexane solution.

4.1.2.4. Miscellaneous. In work that has spanned the period from 1988 to 2004,⁶³⁻⁷³ a surface-bound dioxasilirane [$(\text{Si}-\text{O})_2\text{SiO}_2$, **45**] was suggested in the reaction of O_2 with silylene **43**, generated by vacuum pyrolysis of methoxylated silica (Scheme 20). Experiments were conducted on hetero-

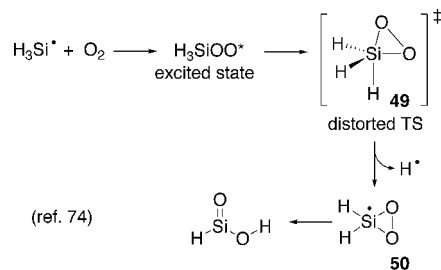
Scheme 20. A Possible Surface-Bound Dioxasilirane



geneous samples (aerosil SiO_2), in which defects in the aerosil were thought to give rise to silylene **43** in SiO_2 . Previous EPR work came to a different conclusion about the identity of the silicon intermediate in SiO_2 pyrolysis reactions and suggested formation of diradical **44** rather than silylene **43**.⁸⁵⁻⁸⁸ UV-visible and IR spectroscopy cannot easily identify reactive species (e.g., silylene **43**, $\text{R}_2\text{Si}\cdot\text{OOSi}\cdot\text{R}_2$ diradical **44**, and dioxasilirane **45**) on silicon surfaces, and there are difficulties in establishing the structure of intermediate(s) formed in the reaction. The surface-bound dioxasilirane **45** was suggested to react with ethylene to give **46** and not oxirane. A series of radical reactions were also proposed, such as the formation of **47** and **48**, in addition to reactions of dioxasilirane **45** with H_2 , D_2 , carbon monoxide, and ethane. In 2006, evidence suggested that dehydroxylation of either silica or hydroxylated silicon forms defects that lead to silylene and dioxasilirane at temperatures ranging from 100 to 400 $^\circ\text{C}$.⁵⁸

In 1996, a laser photolysis of silane (SiH_4)-oxygen (O_2) mixtures was reported.⁷⁴ The combustion reaction conditions generated silyl radical $\text{H}_3\text{Si}\cdot$, which reacted with O_2 to give an excited acyclic H_3SiOO species. It was proposed that acyclic H_3SiOO cyclized to the unsubstituted dioxasilirane H_2SiO_2 radical (**50**), which then rearranged to silaformic acid [$\text{H}_2\text{Si}(\text{=O})\text{OH}$] (Scheme 21). MP2(full)/6-31G(d)

Scheme 21. Possible Reaction of the SiH_3 Radical with O_2



and G2(MP2) calculations predicted dioxasilirane **50** to be a minimum on the potential energy surface, in which TS structure **49** involved the loss of a hydrogen atom. Silanoic acid is not the only product in the reaction, since silicon oxide (SiO) is also a final product that arises by high computed barriers (e.g., 67.6 kcal/mol), made possible by the combustion conditions.

Table 14. Calculated Geometries of Dioxasilranes

Year	Structure	State	Method and Basis Set	O-O ^a	Si-O ^a	Si-O-O ^b	O-Si-O ^b	Ref.	Comments
2006		S ₀	B3LYP/6-31G(d)	1.614	1.650, 1.666	—	—	58	
2005		S ₀	MP2(Full)/6-31G(d)	1.628	1.672	—	58.3	58	Computed data also reported at the MCSCF (FORS) level with the 6-31G(d) basis set
2000		S ₀	B3LYP/6-311++G(d,p)	1.584	1.672	61.7	56.5	51	Both Si-O bond distances are equal in length
1999		S ₀	B3LYP/TZ2P	1.571	1.678	—	—	90	Computed data also reported at the B3LYP level with DZP and DZP-ECP basis sets
1996		S ₀	SCF/6-31G(d,p)	—	1.632	—	55.6	91	
1993		S ₀	MP2/6-31G(d)	1.628	1.672	—	—	93	
1989		S ₀	MP2/6-31G(d)	1.628	1.672	60.9	—	92	
1989		S ₀	GVB/6-31G(d)	1.81	1.66	57.0	—	92	CASSCF calculation also carried out with 6 electrons distributed in 6 active orbitals

^a Bond distances in angstroms. ^b Bond angles in degrees.

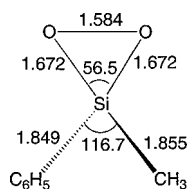


Figure 2. B3LYP/6-311++G(d,p) computed structure of the methylphenyldioxasilirane from ref 51. Bond lengths in angstroms; bond angles in degrees.

There is one recent report in the literature which suggests the formation of unsubstituted dioxasilirane H₂SiO₂ in a dihydrogensilylene-O₂ reaction. In 2006, the gas-phase reaction of silylene, SiH₂ (generated from the photolysis of phenylsilane), and O₂ was carried out at 297–600 K.⁵⁷ G3 calculations pointed to the formation of H₂SiOO followed by cyclization to the dioxasilirane H₂SiO₂.

4.1.2.5. Calculations. Structure. Dioxasilirane structures optimize to minima at various levels of theory.^{51,57,89–92} Calculated bond distances and bond angles are shown in Table 14. Dioxasilirane ((HO)₃CO)₂SiO₂, MePhSiO₂, and H₂SiO₂ bear a resemblance to each other regardless of the computational method used. Dioxasilirane bond distances for O–O range from a high of 1.81 Å to a low of 1.571 Å. Bond distances for Si–O range from a high of 1.678 Å to a low of 1.632 Å. A sample computed structure for methylphenyldioxasilirane is given in Figure 2. Computed data for the Si–O–O and O–Si–O bond angles are also given in Table 14. The strain energy has been calculated for dioxasilirane H₂SiO₂ (Table 15). Bach estimated strain energies by using the CBS-Q method, along with cyclopropane and a six-membered ring Si-, O-, and C-containing heterocycle reference compound.⁸⁹ Calculated atomic charges are in Table 16, and the vibrational frequencies and infrared intensities are in Table 17. Dioxasilirane H₂SiO₂ possesses negative charge density on the oxygen atoms.

Energetics. Saddle points which connect silanone *O*-oxide and dioxasilirane have been located in four studies in the gas phase (Table 18).^{51,57,90–92} The cyclization barrier for silanone *O*-oxide MePhSiOO to dioxasilirane MePhSiO₂ is 0.8 kcal/mol at the B3LYP/6-311++G(d,p) level.⁵¹ The barrier for converting acyclic Me₂SiOO to dioxasilirane Me₂SiO₂ is 6.5 kcal/mol at the HF/6-31G(d) level^{53,54} and that for acyclic H₂SiOO to dioxasilirane H₂SiO₂ is 6.5 and 2.2 kcal/mol at the HF/6-31G(d) and GVB/6-31G(d) levels.⁹² Silanone *O*-oxide is predicted to be higher in energy than dioxasilirane. The conversion of singlet acyclic MePhSiOO to dioxasilirane MePhSiO₂ is calculated to be exothermic by –49.6 kcal/mol at the B3LYP/6-311++G(d,p) level.⁵¹ Subsequent conversion of dioxasilirane MePhSiO₂ to silaester [PhSi(O)OMe] is calculated to be exothermic by –59.3 kcal/mol. The conversion of singlet acyclic Me₂SiOO to dioxasilirane Me₂SiO₂ is calculated to be exothermic by –63.8 kcal/mol at the HF/6-31G(d) level, and the subsequent conversion from dioxasilirane Me₂SiO₂ to MeSi(O)OMe is exothermic by –63.8 kcal/mol.^{53,54}

The computational work predicts a facile conversion of singlet silanone *O*-oxide to dioxasilirane in an exothermic low-barrier process. In all cases, the dioxasilirane is calculated to be more stable than silanone *O*-oxide. A suggestion has also been made that this highly exothermic isomerization process could lead to vibrationally “hot” dioxasiliranes with excess energy.⁹² The silanone *O*-oxide to dioxasilirane barrier height is much lower compared to that of the carbon analogue H₂C⁺OO[–] to dioxirane H₂CO₂ (23 kcal/mol barrier at various levels of theory).^{3,53–58} The relative energies for other bimolecular and isomerization reactions are listed in Table 18.^{51,53,54,57,74,82,89,90,92–95}

In conclusion, section 4.1.2 provides evidence that is compelling for the direct detection of dioxasiliranes from matrix isolation experiments of the reaction of silylene with O₂. The generation of dioxasilirane has been achieved in the

Table 15. Calculated Properties of the Dioxasilirane Ring^a

Year	Structure	Estimated Strain Energy	Method and Basis Set	Ref.	Comments
2006		36.0	CBS-Q	89	Calculated from a 6-membered ring reference compound and a combination reaction of cyclopropane and dioxasilirane. In the same study, the strain energy for H ₂ CO ₂ dioxirane was calculated to be 16-17 kcal/mol.
1996		34.1	MP2/6-31G(d,p)	91	Calculated from $\text{H}_2\text{Si} \begin{array}{c} \diagup \text{O} \\ \diagdown \text{O} \end{array} \longrightarrow \text{H}_2\text{Si} + \text{O} + \text{O}$
		44.9	SCF/6-31G(d,p)		
		27.7	MP2/6-31G(d,p)		Calculated from $\text{H}_2\text{Si} \begin{array}{c} \diagup \text{O} \\ \diagdown \text{O} \end{array} + 3\text{H}_2 \longrightarrow \text{H}_4\text{Si} + 2\text{H}_2\text{O}$
		26.6	SCF/6-31G(d,p)		

^a Energies in kilocalories per mole.Table 16. Calculated Properties of the Dioxasilirane Ring^a

Year	Structure	Natural Atomic Charge			Natural Bond Order			Method	Comments
		Si	O	H	Si-O	O-O	Si-H		
1999		1.82	-0.56	-0.34	0.42	1.00	0.66	B3LYP/DZP	
		1.60	-0.57	-0.23	0.41	1.00	0.76	B3LYP/DZP-ECP	ECP = effective core potential

^a Reference 90.Table 17. Harmonic Vibrational Frequencies ($\tilde{\nu}$) and Infrared Intensities of the Dioxasilirane H₂SiO₂^a

MP2/6-31G(d)		GVB/6-31G(d)		assignment	
$\tilde{\nu}$, cm ⁻¹	I ^b	$\tilde{\nu}$, cm ⁻¹	I ^b		
490	0	526	0	a ₂	SiH ₂ twist
613	21	284	10	a ₁	OSiO bend
734	97	755	126	b ₁	SiH ₂ rock
792	11	822	1	b ₂	OSiO a-str ^c
871	141	923	192	b ₂	SiH ₂ bend
976	2	956	40	a ₁	OSiO a-str ^c
1083	174	1123	206	a ₁	SiH ₂ bend
2377	79	2464	106	a ₁	SiH ₂ a-str
2393	168	2464	228	b ₁	SiH ₂ a-str

^a Reference 92. ^b Infrared intensities. ^c Strongly coupled with the bending of SiH₂.

absence of other reactive species such as silylenes and silanone O-oxides; however, formation of a stable isolable dioxasilirane has not yet been achieved.

4.1.3. Dioxagermirane, Dioxastannirane, and Dioxastilbirane

A photooxidation reaction of germanium has been conducted with deposited germanium chalcogenides with sulfur, selenium, and tellurium onto thin films, but peroxides were not suggested as intermediates.⁹⁶ Spectroscopic detection has been achieved for the heavy carbenes,⁹⁷⁻¹⁰¹ germylenes, and stannylenes (e.g., H₂Ge, Me₂Ge, and Me₂Sn), but there are no experimental reports of the corresponding dioxiranes. Dioxagermirane (**51**), dioxastannirane (**52**), and dioxastilbi-

rane (**53**) have been examined with computational methods but have not been investigated experimentally (Scheme 22).^{90,102}

Structure. In 1999, a computational study examined H₂GeO₂ (**51**), H₂SnO₂ (**52**), and H₂SbO₂ (**53**) at the B3LYP and CCSD(T) levels with various basis sets and an effective core potential (ECP) treatment.^{90,102} These heteroatom-substituted dioxiranes optimize to minima on the potential energy surface (PES). Calculated bond distances are shown in Table 19. The B3LYP/TZ2P-ECP computed dioxirane structures show decreasing O–O bond distances in the order Ge > Sn > Pb with bond lengths of 1.566 Å (H₂GeO₂), 1.561 Å (H₂SnO₂), and 1.555 Å (H₂PbO₂). The O–O bond distances show a similar trend at the B3LYP/DZP-ECP level. The O–O bond distance decreases by increments of 0.005 and 0.006 Å in the series of H₂GeO₂, H₂SnO₂, and H₂SbO₂ dioxiranes. Other bond distances include Ge–O (1.778 Å), Sn–O (1.931 Å), and Pb–O (1.992 Å) at the B3LYP/TZ2P-ECP level. The natural atomic charges indicate a negative density at the oxygen and hydrogen atoms and a positive charge density on Ge, Sn, and Pb (Table 20). Natural bond order data are also presented in Table 20.

Energetics. Calculated energetics are provided in Table 21, in which data compare the higher homologue dioxiranes (cyclic H₂YO₂) with dihydroxycarbenes (HOYOH) and formic acid congeners [HY(=O)OH] (Y = Ge, Sn, and Pb). According to B3LYP/TZ2P-ECP calculations, the conversion of H₂GeO₂ dioxirane to HGe(=O)OH is exothermic by –76.9 kcal/mol. Similar exothermicities are calculated for

Table 18. Calculated Relative Energies for Intramolecular and Intermolecular Reactions of Dioxasilirane^a

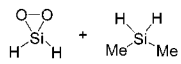
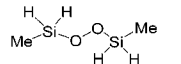
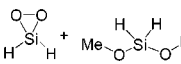
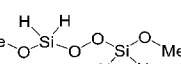
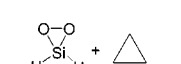
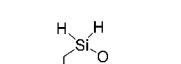
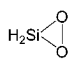
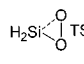
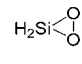
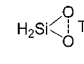
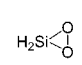
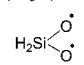
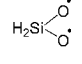
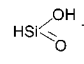
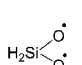
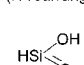
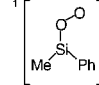
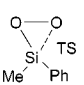
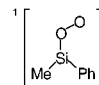
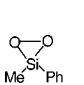
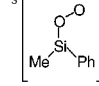
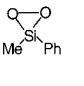
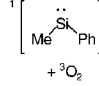
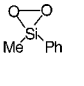
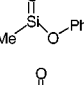
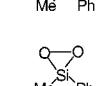
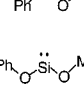
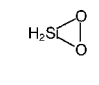
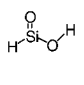


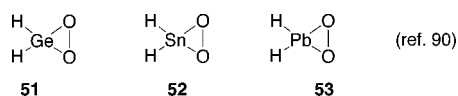
Year	A	B	$\Delta E_{A \rightarrow B}$	Method and Basis Set	Ref.	Comments
2006			-35.5	CBS-Q	89	These represent homodesmotic reactions
			-36.0			
			-31.2			
2005	H ₂ SiOO		-64.5	G3	57	Computed values vary widely depending on the theoretical method. Values also reported at the MCSCF level. Use of the Cc-pVTZ basis set also reported
	H ₂ SiOO		4.5 ^b	G3		
		(ring closure)				
			14.4 ^b	MRMP2/6-31G(d)		
		(ring opening)				
			8.8	MRMP2/6-31G(d)		
			1.4 ^b	MRMP2/6-31G(d)		
		(H-rearrange)				
			-85.9	MRMP2/6-31G(d)		
2000	¹ 		0.8 ^b	B3LYP/6-311++G(d,p)	51	
		(ring closure)				
	¹ 		-49.6	B3LYP/6-311++G(d,p)		
	³ 		-57.8	B3LYP/6-311++G(d,p)		
	¹ 		-77.4	B3LYP/6-311++G(d,p)		
	+ ³ O ₂		-61.7	B3LYP/6-311++G(d,p)		
			-59.3	B3LYP/6-311++G(d,p)		
		-49.1	B3LYP/6-311++G(d,p)			
1999			-81.1	B3LYP/DZP	90	Calculations also performed at other levels of theory levels such as B3LYP/DZP-ECP, BLYP/ DZP, B3LYP/TZ2P, B3LYP/TZ2P-ECP, BLYP/DZ2P, BLYP/ TZ2P-ECP CCSD/TZ2P//BLYP/TZ2P, BLYP/DZ2P, BLYP/ TZ2P-ECP CCSD/TZ2P//BLYP/TZ2P, CCSD/TZ2P-ECP//BLYP/TZ2P-ECP, CCSD(T)/TZ2P-ECP//BLYP/TZ2P-ECP

Table 18 (Continued)

Year	A	B	$\Delta E_{A \rightarrow B}$	Method and Basis Set	Ref.	Comments
			-80.1	CCSD(T)/TZ2P-ECP//BLYP/TZ2P-ECP		
			-88.6	B3LYP/DZP		
			-88.0	CCSD(T)/TZ2P-ECP//BLYP/TZ2P-ECP		
			20.9	B3LYP/DZP		
			24.6	CCSD(T)/TZ2P-ECP//BLYP/TZ2P-ECP		
1996			6.4 ^b	CASSCF(6/6)/6-31G(d)	74	6 electrons in 6 orbitals
			-8.3	CASSCF(6/6)/6-31G(d)		Predictions of the SiH ₃ + O ₂ reaction to give SiH ₃ OO and then cyclization to H ₂ SiO ₂ atom
	—		-28.1	G2	93, 94	Calculated heat of formation at 298 K
1989			6.5 ^b	HF/6-31G(d)	53, 54	
			-63.8	HF/6-31G(d)		
1989	H ₂ SiOO		6.5 ^b	MP2/6-31G(d)	92	Single point values also calculated at various levels: MP3, MP4, CI with the 6-31G(2d,p) basis set
	H ₂ SiOO		2.2 ^b	GVB/6-31G(d)		Single point energies also calculated with GVB/6-31G(2d,p) and CASSCF/6-31G(d)
	H ₂ SiOO		-63.8	MP2/6-31G(d)		
	H ₂ SiOO		-62.1	GVB/6-31G(d)		
1988			-61.5	MP4SDTQ/6-31G(d)// HF/6-31G(d)	82	
	¹ H ₂ Si + ³ O ₂		-84.2	MP4SDTQ/6-31G(d)// HF/6-31G(d)		

^a Energies in kilocalories per mole. ^b Transition state energies.

Scheme 22. Dioxagermirane, Dioxastannirane, and Dioxastilbirane



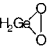
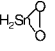
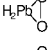
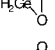
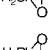
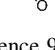
dioxastannirane (−70.6 kcal/mol) and dioxastilbirane (−71.8 kcal/mol) in their conversion to the corresponding formic acid congeners. H₂YO₂ dioxiranes vary in their Y–O bond strengths, namely 77.4 kcal/mol for Y = Ge, 63.6 kcal/mol for Y = Sn, and 34.0 kcal/mol for Y = Pb). The heteroatom-substituted dioxiranes are less stable for the heavier members of group 14. For example, the H₂PbO₂ dioxirane is 149.4 kcal/mol less stable than the corresponding dihydroxy species

(plumbous hydroxide) according to B3LYP/TZ2P-ECP calculations. This instability correlates with a decrease in Y–O bond dissociation energies.

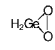
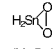
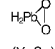
4.1.4. Cyclic Sulfur Dioxide, SO₂

The literature of the sulfur dioxide structure is enormous. Studies that have considered SO₂ structural isomers span a period of 50 years.^{103–110} A variety of experimental methods have been used, but none have provided evidence for cyclic SO₂. Experimental methods have included, for example, flash photolysis of SO₂, gaseous CS₂–oxygen mixtures in explosions, and flash-initiated explosions of H₂S, CS₂, and COS. In 1996, an infrared absorption study of SO₂ in an argon

Table 19. Calculated Geometries of Dioxagermirane, Dioxastannirane, and Dioxastilbirane^a

Year	Structure	State	Method of Basis Set	O-O ^b	Y-O ^b
1999		S ₀	B3LYP/TZ2P-ECP	1.566	1.778 (Y=Ge)
		S ₀		1.561	1.931 (Y=Sn)
		S ₀		1.555	1.992 (Y=Pb)
		S ₀	B3LYP/DZP-ECP	1.555	1.785 (Y=Ge)
		S ₀		1.550	1.936 (Y=Sn)
		S ₀		1.544	2.001 (Y=Pb)

^a Reference 90. ^b Bond distances in angstroms.**Table 20. Calculated Structural Properties of Dioxagermirane, Dioxastannirane, and Dioxastilbirane^a**

Year	Structure	Natural Atomic Charge			Natural Bond Order			Method and Basis Set
		Y	O	H	Y-O	O-O	Y-H	
1999	 (Y=Ge)	1.42	-0.5	-0.16	0.45	1.00	0.82	B3LYP/DZP
		1.57	-0.6	-0.22	0.42	1.00	0.77	B3LYP/DZP-ECP
	 (Y=Sn)	1.88	-0.6	-0.32	0.37	1.00	0.67	B3LYP/DZP-ECP
	 (Y=Sn)	1.54	-0.6	-0.21	0.42	1.00	0.76	B3LYP/DZP-ECP

^a Reference 90.

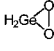
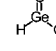
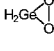
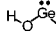
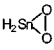
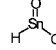
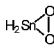
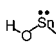
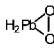
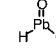
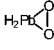
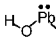
matrix was conducted using 193-nm light from an ArF eximer laser.¹¹¹ From ¹⁸O-labeling experiments, along with the analysis of IR intensities and B3LYP/cc-pVTZ calculations, it was concluded that the acyclic SOO was present, but not cyclic SO₂.¹¹¹ In 2006, cyclic SO₂ was suggested to

form in a two-photon irradiation (248 nm) of acyclic SO₂ in a MTHF or ethanol matrix at 11 K, based on the temperature-dependent shift of the SO₂ λ_{max}.¹¹² There is uncertainty in the spectral assignment of the cyclic SO₂ structure due to the strong absorption of acyclic SO₂.

Structure. Given the absence of experimental data on cyclic SO₂, computational approaches have been used. Cyclic SO₂ optimizes to a minimum at many levels of theory, such as B3LYP/cc-pVTZ, BP86/cc-pVTZ, CCSD(T)/TZ2P(f), SCF/DZP, MRCI/cc-pVTZ, and GVB.^{111,113–118} Calculated bond distances and a bond angle are shown in Table 22. The O₁–O₂ bond distances range from a high of 1.504 Å to a low of 1.479 Å,^{111,113,114} the S–O bond distances range from 1.705 to 1.686 Å, and the O–S–O bond angle ranges from 52.7° to 51.9°. Calculated vibrational frequencies, IR intensities, and excitation energies for cyclic SO₂ are shown in Table 23.

Energetics. According to gas-phase CCSD(T)/TZ2P(f), B3LYP/cc-pVTZ, and BP86/cc-pVTZ calculations, cyclic SO₂ is 1–18 kcal/mol more stable than acyclic SOO. Cyclic SO₂ is highly unstable; the exothermicity on the ring opening to acyclic OSO is about 99–111 kcal/mol according to the above computed methods (Table 24).^{111,114} The barrier to breaking the O–O bond of cyclic SO₂ is predicted to be 15.6 kcal/mol, based on MCSCF calculations.¹¹⁷ The computed energetics and barrier for conversion of SO₂ to the six-membered ring diperoxide have not been determined, although DFT studies have focused on other combinations of dimers, trimers, and oligomers of sulfur oxides.^{119–121} A series of calculations have been performed on the ground state PES of SO₂.^{122–129} The activation energies for SOO or cyclic SO₂ to release an O-atom intermolecularly have not been computed to date. Additional work in this area is needed, such as the success found in the computed and still theoretical complexes [S₃W(NO)₃]³⁺, [O₃M(NO)₃]³⁺ (M = Cr, Mo, W, Fe, Ru, Os), and [S₃W(NO)₂(CO)]²⁺ containing cyclic O₃ and S₃.^{123,130}

Table 21. Calculated Energies for Rearrangements of Dioxagermirane, Dioxastannirane, and Dioxastilbirane^a

Year	A	B	ΔE _{A→B}	Method and Basis Set	Ref.	Comments
1999			-72.3	B3LYP/DZP-ECP	90	Calculations also performed at different levels of theory including single point calculations at the CCSD(T)/TZP-ECP level
			-76.9	B3LYP/TZ2P-ECP		
			-106.9	B3LYP/DZP-ECP		
			-109.7	B3LYP/TZ2P-ECP		
			-67.2	B3LYP/DZP-ECP		
			-70.6	B3LYP/TZ2P-ECP		
			-122.2	B3LYP/DZP-ECP		
			-125.9	B3LYP/TZ2P-ECP		
			-68.0	B3LYP/DZP-ECP		
			-71.8	B3LYP/TZ2P-ECP		
			-144.8	B3LYP/DZP-ECP		
			-149.4	B3LYP/TZ2P-ECP		

^a Energies in kilocalories per mole.

Table 22. Calculated Geometries of Cyclic SO₂

Year	Structure	State	Method and Basis Set	O-O ^a	S-O ^a	O-S-O ^b	Ref.
1997		S ₀	CCSD(T)/TZ2P(f)	1.500	1.690	52.7	113, 114
1996		S ₀	B3LYP/cc-pVTZ	1.479	1.686	51.9	111
		S ₀	BP86/cc-pVTZ	1.504	1.705	51.9	111

^a Bond distances in angstroms. ^b Bond angles in degrees.

Table 23. Calculated Values of Cyclic SO₂

(a) Vibrational Frequencies and IR Intensities					
year	$\tilde{\nu}_1$ (A ₁) ^a	$\tilde{\nu}_2$ (A ₁) ^a	$\tilde{\nu}_3$ (B ₂) ^a	method and basis set	ref
1996	1009 (13.3) ^b	682 (3.9) ^b	739 (9.8) ^b	B3LYP/cc-pVTZ	111
	970 (11.0) ^b	662 (4.0) ^b	721 (8.8) ^b	BP86/cc-pVTZ	
(b) Excitation Energies					
	state	energy (eV) MRCI	oscillator strength	energy (eV) MRCI + Q	ref
2005 ^c	1 ¹ A ₁	4.511		4.465	118
	1 ³ A ₂	6.081	0	5.985	
	1 ¹ A ₂	6.752	0	6.660	
	1 ³ B ₁	7.715	0	7.647	
	1 ¹ B ₁	8.078	0.00124	8.033	
	2 ³ B ₁	8.887	0	8.738	
	2 ³ A ₂	9.170	0	8.85	
	1 ³ B ₂	9.930	0	9.824	

^a Symmetries of vibrational modes are listed in parentheses. ^b IR intensities are listed in parentheses. ^c Cyclic SO₂ was computed for C_{2v} symmetry.

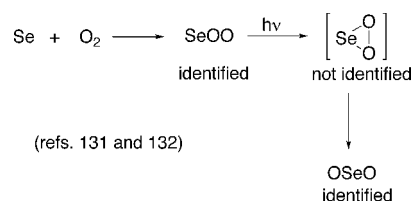
Table 24. Calculated Energies for the Rearrangements of Acyclic and Cyclic SO₂^a

Year	A	B	$\Delta E_{A \rightarrow B}$	Method and Basis Set	Ref.
1996	OSO		99.8	B3LYP/ cc-pVTZ	111
	OSO		98.2	BP86/ cc-pVTZ	
	OSO	SOO	107.3	B3LYP/ cc-pVTZ	
	OSO	SOO	99.7	BP86/ cc-pVTZ	
1995	OSO		104.3	CCSD(T)/ TZ2P(f)	114
	OSO	SOO	110.8	CCSD(T)/ TZ2P(f)	

^a Energies in kilocalories per mole.

4.1.5. Cyclic Selenium Dioxide, SeO₂

A number of studies have been carried out on selenium oxide [SeO_x (x = 1, 2, 3)], but no experimental evidence exists for the cyclic SeO₂ intermediate. However, in 1996, a study of the reaction of selenium and O₂ provided evidence for various acyclic Se_xO_y molecules, such as SeO, OSeO, SeOO, SeOOO, and OSeOO.^{131,132} Complex infrared absorptions in solid argon identified the selenium oxide species. The observed frequencies were corroborated with B3LYP/LANL1DZ calculations, from which frequency, intensity, and isotopic-shift data for the absorptions of Se_xO₂ molecules were obtained. It was proposed that the formation of OSeO in the reactions of Se with O₂ and photolysis of SeOO may go through a cyclic intermediate (cyclic SeO₂) (Scheme 23). The open isomer OSeO product is considerably lower in energy than the acyclic SeOO or cyclic SeO₂ intermediates.

Scheme 23. Reaction of Selenium with O₂

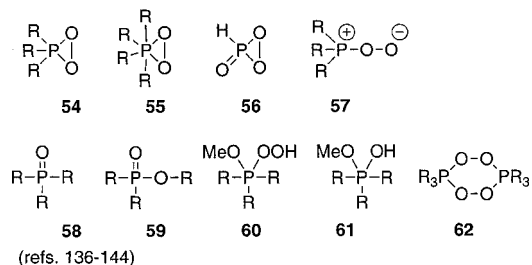
4.2. Trigonal Bipyramidal Dioxiranes

Trigonal bipyramidal (TBP) XO₂ dioxiranes are hypervalent peroxides of the form R₃PO₂, R₂SO₂, R₂SeO₂, and R₂TeO₂. Peroxide structures bearing two or more oxygen bonds to hypervalent phosphorus, sulfur, selenium, or tellurium centers are uncommon, although molecules such as phosphine and phosphite ozonides R₃PO₃ are known.^{133–135} Spectroscopic evidence exists for the R₃PO₂ dioxirane, but not for R₂SO₂, R₂SeO₂, and R₂TeO₂. Computational studies have focused on the R₃PO₂ and R₂SO₂ dioxiranes, but not on R₂SeO₂ and R₂TeO₂.

4.2.1. Dioxaphosphirane, R₃PO₂

4.2.1.1. Background Information. A phosphoranide ion,¹³⁶ a sterically hindered aryl phosphine,¹³⁷ a 1,1'-binaphthyl phosphine,¹³⁸ and a PH₃-ozone complex¹³⁹ served as precursors to dioxaphosphiranes (**54–56**), for which direct spectroscopic evidence was obtained (Chart 1 and Table 25).

Chart 1. Phosphorus- and Oxygen-Containing Compounds

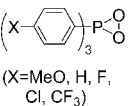
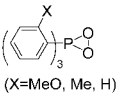
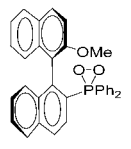
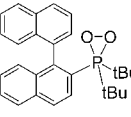
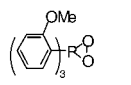
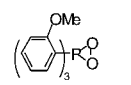
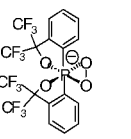
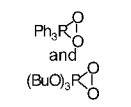
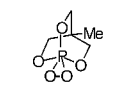
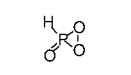
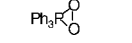


Dioxaphosphirane **55** is a hexacoordinated species. A number of other studies have provided indirect experimental evidence for the formation of dioxaphosphiranes. Various oxidants have been used in the generation of dioxaphosphiranes, such as ¹O₂, ³O₂, O₃, and hydrogen peroxide.^{136–144} A previous review has summarized recent work on phosphine-¹O₂ reactions.⁴ Early work on phosphine autoxidation reactions dates from 1962 to 1984,^{145–147} although dioxaphosphiranes were not proposed as intermediates.

There is yet no evidence for the formation of peroxyphosphine oxide **57**, although it was proposed in a ring-closure phosphoranide-O₂ reaction.¹³⁶ Dioxaphosphirane **54** readily reacts with the substrate (PR₃) to form two equivalents of phosphine oxide **58**, but **54** also rearranges to the phosphonate **59** or is converted to hydroperoxyphosphine **60** and hydroxyphosphorane **61** in methanol. There is no experimental evidence that dioxaphosphirane dimerizes to a six-membered-ring diperoxide tetradiphosphinane (**62**).

4.2.1.2. Low Temperature. NMR Spectroscopy. In 2003, the synthesis of tris(*o*-methoxyphenyl)dioxaphosphirane was reported in CH₂Cl₂ and CH₂Cl₂/toluene solutions at 193 K and was followed by ³¹P and ¹⁷O NMR spectroscopy (Scheme 24 and Table 26).^{137a} The reaction of singlet oxygen from irradiated air-saturated solutions containing tetraphenylporphyrin sensitizer in the presence of tris(*o*-methoxyphenyl

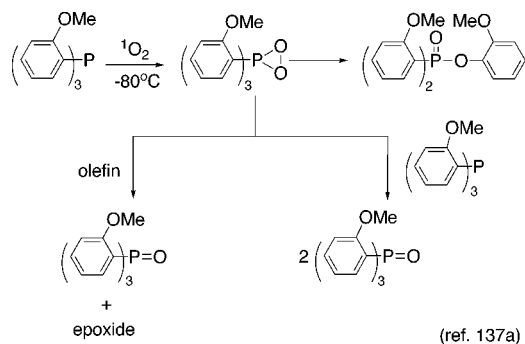
Table 25. Generation of Dioxaphosphiranes (R_3PO_2 Dioxiranes)^a

Year	Structure	Evidence of Formation	T (K)	Method of Preparation	Ref.	Comments
2006		Trapping and rate constant study	298	A	137b	Phosphine oxide products formed
	(X=MeO, H, F, Cl, CF ₃)					
		Trapping and rate constant study	298	A	137b	Phosphinate and phosphine oxide formed
	(X=MeO, Me, H)					
		Intramolecular trapping	298	A	138	
		NMR spectroscopy and trapping	218-258	A	138	³¹ P NMR spectroscopy was conducted in addition to trapping with cyclohexene
2003		NMR spectroscopy	193	A	137a	³¹ P and ¹⁷ O NMR spectroscopy was conducted along with olefin trapping studies
2001		Kinetic analysis	298	A	140	meta- and para-methoxyphenylphosphine reaction with singlet oxygen also conducted
1999		NMR and X-ray crystallography	273	B	136	Potassium 18-crown-6 was the counter ion
1993		Trapping and ¹⁸ O labelling	298	A	143a	Peroxyphosphine oxide and [1,2,4,5,3,6]tetradiphosphinane are not formed
1993		Trapping and product study	293	A	154	Oxidation of olefins and thianthrene-5-oxide provide tentative evidence for the dioxaphosphirane
1987		IR spectroscopy	12-18	C	139	Other species formed such as HPO, HOPO, and HOPO ₂
1983		Product study	237	D	144	

^a A, solution-phase phosphine or phosphite photooxidation; B, reaction between triplet oxygen and the phosphoramidate ion; C, Ar-matrix irradiation of a PH_3-O_3 complex; D, reaction between Ph_3P , H_2O_2 , and diethyl azocarboxylate.

yl)phosphine produced the dioxaphosphirane. Chemical quenching of 1O_2 by the phosphine was very efficient and led to phosphine oxide (*o*-MeOC₆H₄)₃P=O. The ability of phosphine to convert 1O_2 to 3O_2 (physical quenching) has not been observed in these reactions. The *ortho*, *meta*, and *para* isomers of (MeOC₆H₄)₃P also show no physical quenching of 1O_2 regardless of the solvent.^{137,143} With enriched $^{17}O_2$ gas used in the photooxidation, ^{17}O NMR data showed a broad peak at 740 ppm, which along with the ^{31}P NMR peak at -48.3 ppm was assigned to the three-membered ring system (*o*-MeOC₆H₄)₃PO₂. The *o*-methoxyphenyl groups exerted steric interactions that slowed the bimolecular reaction of the dioxaphosphirane with the

substrate (*o*-MeOC₆H₄)₃P. For phosphines that possess small cone angles, as described for metal complexes,^{148,149} the dioxaphosphirane has a longer lifetime by slowing bimolecular reactions. Alkene-trapping experiments showed that (*o*-MeOC₆H₄)₃PO₂ dioxaphosphirane transfers an oxygen atom to alkenes to yield epoxides, analogous to R₂CO₂ dioxiranes such as dimethyldioxirane (Table 27). As yet, no information is available whether the apical or the equatorial dioxaphosphirane oxygen is donated, although the equatorial oxygen should be the more electrophilic.¹⁵⁰⁻¹⁵² There is a reduced computed charge on O_{eq} compared to the O_{ax} atom. In the absence of an external trap, the intramolecular rearrangement of dioxaphosphirane afforded the phosphonate

Scheme 24. Reaction of Tris(*o*-methoxyphenyl)phosphine with Singlet Oxygen


59. In the presence of methanol as solvent, its addition leads to hydroperoxyphosphine and subsequently to hydroxyphosphorane and tris(*o*-methoxyphenyl)phosphine oxide, after reaction with the substrate.

In 2006, a dioxaphosphirane intermediate **63** was observed in the reaction of 1,1'-binaphthyl-di-*tert*-butyl-2-phosphine with $^1\text{O}_2$ in toluene at temperatures ranging from -40 to -80 °C (Scheme 25 and Table 26).¹³⁸ Evidence for the existence of the dioxaphosphirane came from an assignment of the ^{31}P NMR signal at -18.6 ppm and the subsequent decomposition of this intermediate upon warming to give the corresponding phosphine oxide. Warming of the mixture in the presence of cyclohexene afforded its epoxide. The intramolecular oxidation of dioxaphosphirane **63** gave naphthalene epoxide and subsequently a hydroxylated naphthalene product via an NIH-shift mechanism. A similar rearrangement was observed in the reaction of *R*-(+)-2-(diphenylphosphino)-2'-methoxy-1,1'-binaphthyl (**63'**) with $^1\text{O}_2$ according to ^{31}P NMR spectroscopy.¹³⁸

X-ray Crystallography. In 1999, the synthesis of a hexacoordinate 12-P-6 dioxaphosphirane **68** was accomplished in a reaction of $^3\text{O}_2$ with 3,3,3',3'-tetrakis(trifluoromethyl)-1,1'-spirobi[3H,2,1λ⁵-benzoxaphosphoranide ion] (**65**), generated from a P-H phosphorane **64** at 273 K (Scheme 26).¹³⁶ Exposure of the 10-P-4 phosphoranide to O_2 in a thermal process involved electron transfer (phosphoranyl radical/superoxide radical pair, **66**) to give the corresponding dioxaphosphirane **68**. A cyclization of peroxyphosphine oxide **67** was proposed with pseudorotation to place the oxygen atom equatorial and the aryl carbons axial. On the basis of ^{31}P and ^{19}F NMR spectroscopy, the dioxaphosphirane structure was assigned (Table 26). The dioxaphosphirane crystallized with potassium 18-crown-6 as the salt and was found to be stable in the solid state at room temperature. With Ph_3P it rapidly deoxygenated in solution to give oxidophosphorane **69** and $\text{Ph}_3\text{P}=\text{O}$. Except for Ph_3P , oxygen-transfer reactions to alkenes or other trapping agents were not explored. The synthesis of diastereomeric analogues was conducted, in which one of the CF_3 groups was replaced by CH_3 . A slow interconversion of the *endo* and *exo* forms of the R side groups implies rigid three-membered peroxide rings in **68a'** and **68a''** and, thus, inefficient pseudorotation.

IR Spectroscopy. In 1987, the generation of a dioxaphosphirane [$\text{HP}(\text{=O})\text{O}_2$] in the visible-light photolysis of a phosphine(PH_3)-ozone complex in solid argon (12–18 K) was reported (Scheme 27 and Table 26).¹³⁹ The infrared study in an argon matrix of the reaction of $^{16,18}\text{O}_3$ with $\text{PH}_x\text{D}_{3-x}$ ($x = 0, 1, 2, 3$) and subsequent decomposition of the phosphine- O_3 complex showed the presence of a number of compounds, which included phosphine oxide $\text{H}_3\text{P}=\text{O}$, phos-

phinic acid H_2POH , phosphonic acid $(\text{HO})_2\text{HP}=\text{O}$, and metaphosphoric acid HOPO_2 . The reaction is thought to produce the $\text{HP}=\text{O}$ intermediate, which adds O_2 to give acyclic $\text{HOOP}=\text{O}$ and the $\text{HP}(\text{=O})\text{O}_2$ dioxaphosphirane upon further irradiation. The results do not support the interconversion between the acyclic $\text{HOOP}=\text{O}$ and the dioxaphosphirane $\text{HP}(\text{=O})\text{O}_2$. On the basis of the observed fundamental vibrational frequencies, $\text{HP}(\text{=O})\text{O}_2$ and $\text{DP}(\text{=O})\text{O}_2$ structures were assigned, which are given in Table 26. Rotationally, vibrationally, and electronically excited intermediates were suggested.

4.2.1.3. Room Temperature. Trapping, intramolecular rearrangement, and ^{18}O -tracer experiments provided indirect evidence for the dioxaphosphirane intermediates in reactions of $^1\text{O}_2$ with phosphites and phosphines. Phosphites are less reactive and may be used as trapping agents in the $^1\text{O}_2$ reactions.¹⁵³ For example, trimethylphosphite traps the anethole-singlet oxygen intermediate(s) because it reacts slowly with $^1\text{O}_2$.¹⁵⁰

In 1993, the photooxidation of tributylphosphite and triphenylphosphine was conducted with sulfoxides [$(p\text{-YC}_6\text{H}_4)_2\text{SO}$; $\text{Y} = \text{MeO}, \text{Me}, \text{H}, \text{and Cl}$] and sulfides [$(p\text{-YC}_6\text{H}_4)_2\text{S}$; $\text{Y} = \text{Me}$ and H] as trapping agents (Scheme 28 and Table 28).¹⁴³

Singlet oxygen was generated by irradiation ($\lambda > 400$ nm) in air-saturated acetonitrile solutions with methylene blue as sensitizer. The reactivity of the intermediate in the reaction with these trapping agents correlated well with electrophilic dioxaphosphirane. A negative ρ value of -0.63 for trapping by diaryl sulfide was obtained. Oxygen transfers to Ph_2S and to Ph_2SO were inefficient compared to the more oxophilic $(\text{BuO})_3\text{P}$ molecule. The relative reactivity was 300:4:1 for $(\text{BuO})_3\text{P}/\text{Ph}_2\text{S}/\text{Ph}_2\text{SO}$. An ^{18}O -tracer experiment indicated retention of the two ^{18}O atoms, which suggests a unimolecular rearrangement of dioxaphosphirane ($\text{Ph}_3\text{P}^{18}\text{O}_2$) to phenyl diphenylphosphinate $\text{Ph}^{18}\text{OP}(\text{O}^{18})\text{Ph}_2$. Retention indicates that the two oxygen atoms in the phosphinate product are derived from one O_2 molecule. Scrambling implies that the oxygen atoms come from different O_2 molecules. The labeling data do not rule out unimolecular rearrangement of an acyclic peroxyphosphine oxide (Scheme 29).

The reaction of $^1\text{O}_2$ with *para*-substituted arylphosphines was investigated in detail (Scheme 30).^{137b} Formation of the corresponding phosphine oxides took place efficiently (no physical quenching of $^1\text{O}_2$), which showed a correlation with the Hammett σ parameter ($\rho = -1.53$ in CDCl_3) and with the Tolman electronic parameter.^{148,149} The phosphine oxide products were proposed to arise from the reaction of phosphine with dioxaphosphirane intermediates.


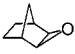
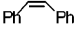
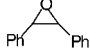

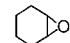
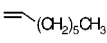
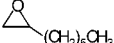
In 1993 and 1994, indirect evidence for the existence of a dioxaphosphirane came from the reaction of $^1\text{O}_2$ with a bicyclic phosphite (1-methyl-4-phospha-3,5,8-trioxabicyclo-[2.2.2]octane) in the presence of norbornene (Scheme 31).^{154,155} The data point to a dioxaphosphirane intermediate in view of the epoxidation of norbornene. The bicyclic dioxaphosphirane would have no possibility for pseudorotation. The reaction was followed by GLC analysis, and the corresponding phosphate was formed as the product. Addition of the radical trap triphenylmethane did not influence the epoxidation reaction, which is similar to work on $(o\text{-MeOC}_6\text{H}_4)_3\text{P}$ in 2003.^{137a} Less nucleophilic olefins such as stilbene and styrene are oxidized less efficiently. Analysis with the thianthrene 5-oxide probe also confirmed electrophilic oxidation behavior.^{154,155,168–170}

Table 26. Spectral Properties of Dioxaphosphiranes^a

Year	Structure	³¹ P NMR (ppm)	¹⁷ O NMR (ppm)	Coupling Constants	X-ray structure	IR data (cm ⁻¹)			Ref.	Comments
						mode	observed	calculated		
2006		-18.6							138	
2003		-48.3	740						137a	Also detected as the hydroperoxyphosphine and hydroxyphosphorane in MeOH
1999		-121.0		$\delta = -74.73$ (q, $J_{\text{PF}} = 8.8$ Hz), -75.36 (q, $J_{\text{PF}} = 8.8$ Hz)	$a = 10.446(5) \text{ \AA}$ $b = 12.265(6) \text{ \AA}$ $c = 15.206(6) \text{ \AA}$ $\alpha = 70.088(3)^\circ$ $\beta = 80.669(4)^\circ$ $\gamma = 69.164(3)^\circ$ ($R = 0.047$)				136	¹ H and ¹³ C NMR data are also reported
1987						$\tilde{\nu}(\text{P-H})$	2490.1 2489.4	2489.8 2489.7	139	
							1370.3 1362.4, 1372.0	1370.1 1366.8		
						$\tilde{\nu}(\text{P=O})$	1331.6 1368.1 1329.3 1326.9	1330.4 1368.4 1328.1 1326.0		
						$\tilde{\nu}_s(-\text{PO}_2)$	974.1 939.4 965.9 959.0 950.8 931.8	977.3 943.5 963.1 961.5 948.0 932.4		
						$\delta(\text{HPO})$		935.3 927.6		
						$\tilde{\nu}_{\text{as}}(-\text{PO}_2)$	833.2 833.2	853.6 833.3 833.1 813.8		
						$\tilde{\nu}_s(-\text{PO}_2)$	587.3 560.0	586.8 559.4		
						$\omega(\text{OPO}_2)$	436.7	436.5 423.2		

^a Temperatures of the experiments range from 12 to 298 K.

Table 27. Oxidation of Alkenes by in-Situ Generated Tris(*o*-methoxyphenyl)dioxaphosphirane^a

Alkene	Epoxide	Yield (%)
		60
		65
		80
		75

^a Reference 137b.

In 1974, the formation of trialkyl phosphates was reported in the dye-sensitized photooxidation reactions of phosphites [(MeO)₃P, (EtO)₃P, (*i*-PrO)₃P, (*n*-BuO)₃P, (cyclic-C₆H₁₁O)₃P, and (CH₂=CHCH₂O)₃P].¹⁵⁶ Singlet oxygen was generated in benzene–methanol mixtures (4:1) with methylene blue or in acetone with Rose Bengal as sensitizer at 298 K. The transient formation of a phosphite–O₂ intermediate was implicated, but its structure was not suggested at that time.

4.2.1.4. Miscellaneous. Diethyl Azodicarboxylate–H₂O₂ Reaction. In one paper, the use of hydrogen peroxide was suggested to generate triphenyldioxaphosphirane.¹⁰⁸ In 1983, a betaine(**70**)–H₂O₂ reaction was reported (Scheme 32).¹⁴⁴ Migration of the phenyl group to give **73** was taken as evidence for the presence of the dioxaphosphirane or tetradiphosphinane intermediate (Scheme 33). Further experiments to probe the nature of the intermediate(s) in the reaction have not been conducted.

Arylphosphines Used as Jet-Fuel Stabilizers. Over the past decade, arylphosphines have been examined as possible stabilizers of jet fuels.^{158–163} The thermal oxidative and pyrolytic stability of the jet fuel was enhanced with additions of triphenylphosphine or dicyclohexylphenylphosphine over a temperature range of 190–250 °C. Oxophilic stabilizers such as phosphines are selectively oxidized rather than the jet fuel. Autoxidation of the phosphines has been suggested to take place by an electron-transfer and/or a charge-transfer process (Scheme 34). High temperatures were necessary to initiate a reaction between Ar₃P and ³O₂ in view of the large activation energy (*E*_a < 30 kcal/mol). Thus, decomposition of a possible dioxaphosphirane intermediate is expected to take place rapidly under the high-temperature conditions.

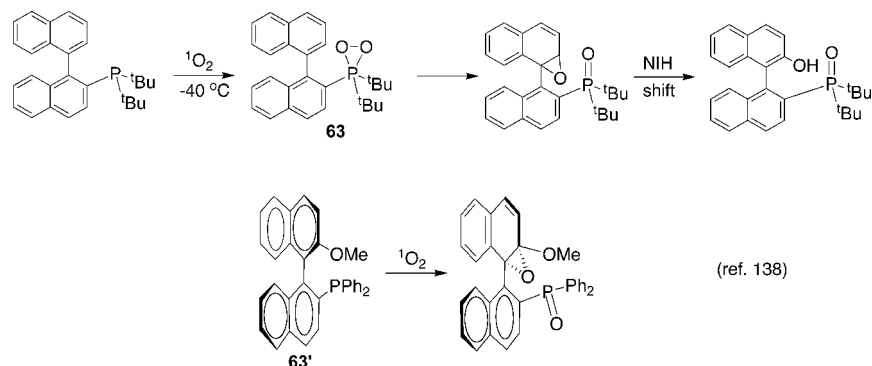
Thermolysis of a Bis(diphenyl)phosphinic Peroxide. In 1965, a reaction was reported which involved the thermal decomposition of a bis(diphenyl)phosphinic peroxide **74** (Scheme

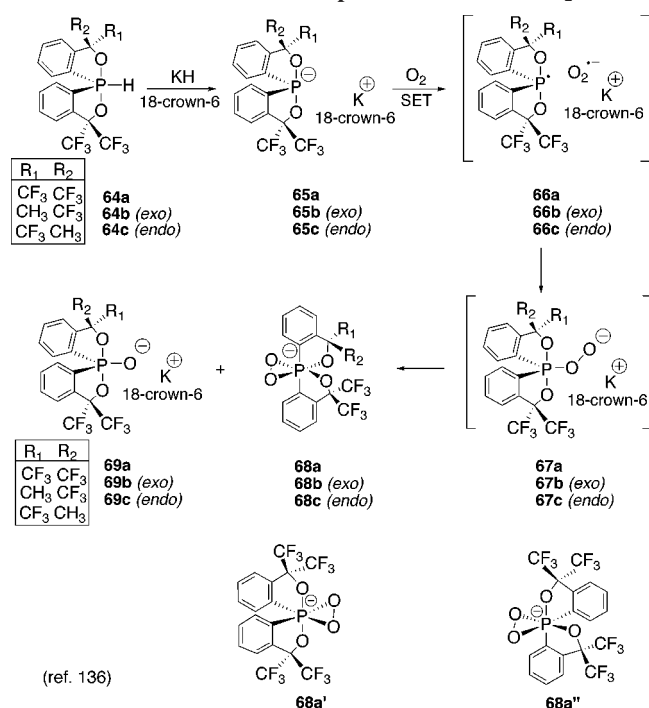
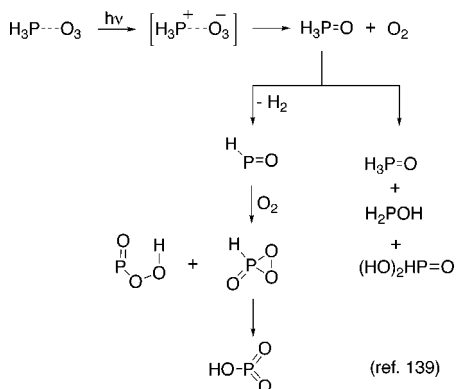
35).¹⁵⁷ Decomposition of bis(diphenyl)phosphinic peroxide with phenyl migration occurred in chloroform, tetrachloroethane, DMF, and acetic acid, but not in alcohol solvents, in which an anhydride is formed. The result was interpreted tentatively in terms of a heterolytic cleavage reaction and production of transient peroxidic intermediates, such as the acyclic Ph₂(RO)POO (**76**) and dioxaphosphirane Ph₂(RO)-PO₂ (**77**), prior to formation of the anhydride product. It is uncertain whether a dioxaphosphirane is formed in the reaction. Further experiments and computations are needed to validate the mechanistic suggestion.

4.2.1.5. Calculations. Structure. Dioxaphosphiranes H₃PO₂, Me₃PO₂, and (HO)₃PO₂ optimize to minima at various levels of theory and basis set extension, including HF/STO-3G(d), HF/3-21G(d), HF/6-31G(d), MP2/6-31G(d), and CASSCF/6-31G(d).^{143,164} Calculated bond distances and bond angles are shown in Table 29. The parent dioxaphosphirane HPO₂ has also been studied and optimizes to a minimum at the SCF and SCF/CEPA-1 levels.¹⁶⁵ Calculations predict that peroxyphosphine oxide does not form in phosphine–¹O₂ reactions.¹⁶⁴ The acyclic peroxyphosphine oxides (HO)₃POO, H₃POO, and Me₃POO are not found as minima at any level of theory.^{143,164,165} Dioxaphosphirane H₃PO₂, (HO)₃PO₂, and Me₃PO₂ bond distances for the O₁–O₂ bond range from 1.599 to 1.560 Å. The dioxaphosphirane structure is calculated with one of the peroxide oxygens in an equatorial position and the other in an apical position. The apical P–O₁ bond is 0.059–0.202 Å longer than the equatorial P–O₂ bond, as would be expected for a TBP structure (Table 29). A sample computed structure for the unsubstituted dioxaphosphirane is given in Figure 3. The sensitivity of the dioxaphosphirane geometry to the R substituent has not been examined in detail.

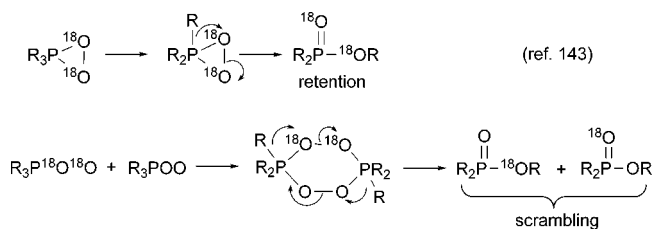
Wilke and Weinhold have recently calculated resonance bonding patterns in H₃PO₃ dioxaphosphirane (Scheme 36).¹⁴¹ The use of Natural Resonance Theory (NRT) and Natural Bond Orbitals (NBOs)¹⁶⁶ predicted that the nonhypervalent ionic resonance forms II and III are more important than the valence-shell expanded¹⁶⁷ (octet-violating hypervalent structures) I, ionic IV, and π-complex V forms. The hypervalent form I, with participation of d orbitals in the hybridized structure, is a minor contributor in the structures I–V according to the NRT/NBO analysis.

Energetics. A computational investigation of the phosphine–singlet oxygen reaction appeared in 1993 (Table 30).¹⁶⁴ The barrier connecting PH₃ and ¹O₂ with dioxaphosphirane H₃PO₂ is 24.8 kcal/mol at the MP2/6-31G(d) level. The conversion of PH₃ and ¹O₂ to dioxaphosphirane H₃PO₂ is calculated to be –32.0 kcal/mol exothermic at the MP2/6-31G(d) level. The formation of dioxaphosphirane Me₃PO₂

Scheme 25. Reaction of Binaphthyl-Containing Phosphines with Singlet Oxygen

Scheme 26. Reaction of a Phosphoranide Ion with O₂Scheme 27. Photolysis of a Phosphine–Ozone Complex^a

^a Participation of intermediates that are rotationally excited, vibrationally excited, or electronically excited is not noted here.

Scheme 28. ¹⁸O-Labeling Study of a Dioxaphosphirane Rearrangement

from PMe_3 and $^{18}\text{O}_2$ is calculated to be exothermic by -52.5 kcal/mol at the MP2/6-31G(d)//HF/6-31G(d) level, whereas the cyclization of the acyclic $\text{HP}(=\text{O})_2$ to dioxaphosphirane HPO_2 is endothermic by 85.0 kcal/mol at the SCF level.

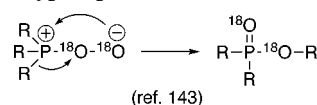
In conclusion, the spectroscopic evidence for dioxaphosphiranes **54–56** is now in hand. Dioxaphosphirane **54** arises from the reaction of phosphine or phosphite with $^{18}\text{O}_2$, but not from the primary formation of peroxyphosphine oxide. The singlet oxygen attaches in a side-on manner to the trivalent phosphorus center. Dioxaphosphiranes derived from

Table 28. ¹⁸O-Tracer Study of the Formation of Phenyl Diphenylphosphinate [$\text{Ph}_2\text{P}(=\text{O})\text{Ph}$] from Ph_3P and $^{18}\text{O}_2$ ^a

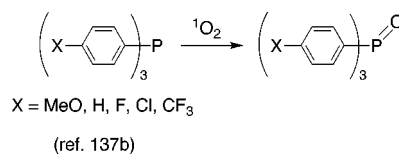
entry	conditions ^b	product	masses ^b		
			M	M + 2	M + 4
Observed					
1	20 mM $\text{Ph}_3\text{P}/^{18}\text{O}_2$ ^c	$\text{Ph}_2\text{P}(=\text{O})\text{Ph}$	100	11.8	5.9
2	20 mM $\text{Ph}_3\text{P}/^{18}\text{O}_2$ ^d	$\text{Ph}_2\text{P}(=\text{O})\text{Ph}$	100	10.5	0.3
			100	1.3	5.6
(difference between entries 1 and 2 ^e)					
Calculated					
3			100	0.5	6.2
4			100	3.6	0.0
(retention)					
(scramble)					

^a Reference 143a. ^b Mass spectral data for $\text{Ph}_2\text{P}(=\text{O})\text{Ph}$, $M = 294$. The observed values are the mean of two determinations. ^c Oxygen gas: $^{32}\text{O}_2/^{34}\text{O}_2/^{36}\text{O}_2 = 100:0.5:6.2$. ^d Control experiment with natural oxygen gas under the same conditions. ^e Net values for ^{18}O contents.

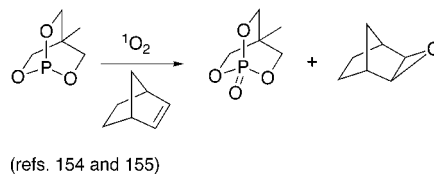
Scheme 29. Peroxyphosphine Oxide Rearrangement



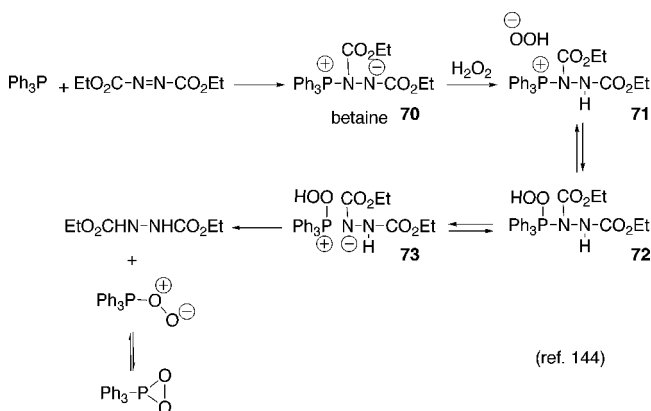
Scheme 30. Reaction of Aryl Phosphines with Singlet Oxygen



Scheme 31. Reaction of a Bicyclic Phosphite with Singlet Oxygen



Scheme 32. Reaction of a Betaine with Hydrogen Peroxide

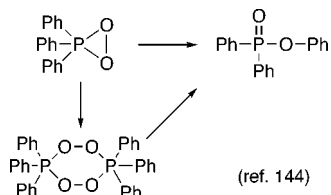
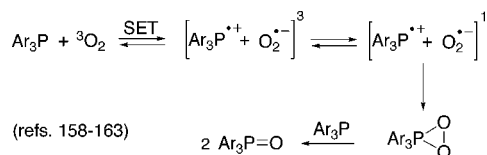


sterically bulky phosphine ligands have synthetic versatility that should be further investigated.

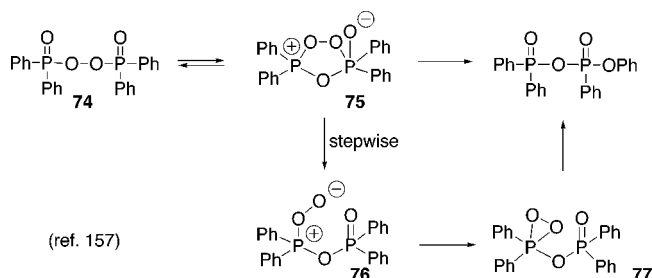
4.2.2. Dioxathiirane, R_2SO_2

4.2.2.1. Background Information. Dioxathiirane (thia-dioxirane, **79**) has been suggested as an intermediate in sulfur oxidation reactions. Since seven previous reviews have focused on organic sulfide or metal thiolate–ligand photo-

Scheme 33. Phenyl Migration in Triphenyldioxaphosphirane

Scheme 34. Reaction of Triarylphosphine with O₂

Scheme 35. Thermal Reaction of Bis(diphenylphosphinic) Peroxide



oxidations and the possible formation of R₂SO₂ dioxathiranes,^{2,4,171-176} we shall focus our discussion on the new findings.

No direct spectroscopic data exist yet for the dioxathirane R₂SO₂ intermediate. Routes that have been suggested to give

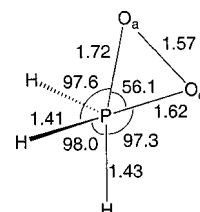
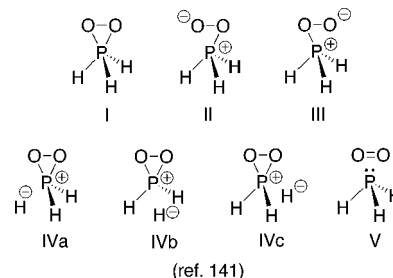


Figure 3. B3LYP/6-31+G(d) computed structure of the unsubstituted dioxaphosphirane from ref 141. Bond lengths in angstroms; bond angles in degrees.

Scheme 36. Resonance Forms of Dioxaphosphirane



dioxathirane include reagents such as ¹O₂, ³O₂, and superoxide.^{2,4,171-176} Dioxathirane **79** may arise from the reaction of the sulfide radical cation with superoxide ion. There is no evidence that dioxathirane is present in sulfide-¹O₂ reactions.

Experimental and computational data suggest that various species arise in sulfide oxidation chemistry, which include dioxathirane **79**, persulfide **80**, sulfide radical ion superoxide pair **81**, S-hydroperoxysulfonium ylide **82**, sulfoxide **83**, and sulfone **84** (Chart 2). Sulfide photooxidations can lead to hydroperoxysulfurane **85** or a hydrogen-bonded

Table 29. Calculated Energies and Geometries of Dioxaphosphiranes

Year	Structure	Energy ^a	Method of Basis Set	O ¹ -O ² ^b	P-O ¹ ^b	P-O ² ^b	P-O ¹ -O ² ^c	Ref.	Comments
2006			B3LYP/6-31+G(d)	1.570	1.720	1.620	58.6	141	Calculations were also performed with other methods [HF, MP2, QC1SD(T)] and basis sets (3-21G, ang-cc-pVOZ, ang-cc-pVTZ)
1993		-492.53079	MP2/6-31G(d)	1.599	1.697	1.630	63.4	164	
		-492.12798	CASSCF/6-31G(d)	1.630	1.681	1.622	62.3		Calculation on a 12-orbital system with 10 filled and 2 virtual orbitals
		-610.05313	MP2(FC)/6-31G(d)	1.560	1.782	1.580	69.2		
1993		-713.10466	HF/3-21G(d)	1.572	1.654	1.568	--	143a	HF/STO-3G(d) calculations have also been reported

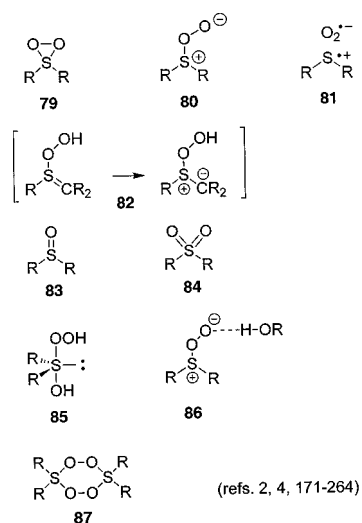
^a Calculated for the S₀ state. ^b Bond distances in angstroms. ^c Bond angles in degrees.

Table 30. Calculated Energies^a for the Intramolecular and Intermolecular Reactions of Dioxaphosphiranes

Year	A	B	$\Delta E_{A \rightarrow B}$	Method and Basis Set	Ref.	Comments
1993	$\text{PH}_3 + {}^1\text{O}_2$		-32.0	MP2/6-31G(d)	164	An energy minimum was not found for acyclic H_3POO nor Me_3POO at any theoretical level
	$\text{PH}_3 + {}^1\text{O}_2$		24.8			
	$2\text{PH}_3 + {}^1\text{O}_2$	$2\text{H}_3\text{PO}$	-111.2			
	$\text{Me}_3\text{P} + {}^1\text{O}_2$		-52.5	MP2/6-31G(d)//HF/6-31G(d)		
	$\text{Me}_3\text{P} + {}^1\text{O}_2$		20.7	HF/3-21G(d)		
	$2\text{Me}_3\text{P} + {}^1\text{O}_2$	$2\text{Me}_3\text{PO}$	-163.0	MP2/6-31G(d)//HF/6-31G(d)		
1992			85.0	SCF	165	Electron correlation was conducted with the CEPA-1 method by using SCF geometries
			79.6	SCF/CEPA-1	165	

^a Energies in kilocalories per mole.

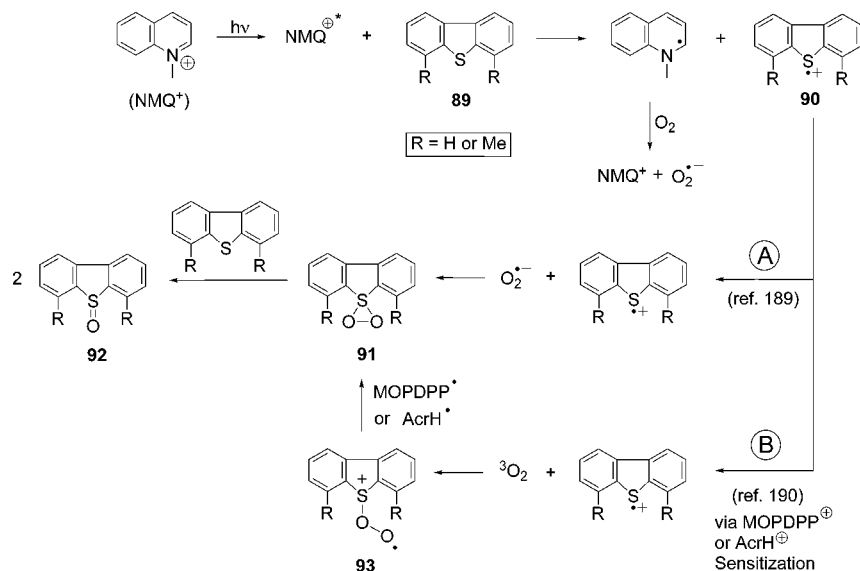
Chart 2. Sulfur- and Oxygen-Containing Compounds

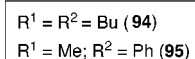
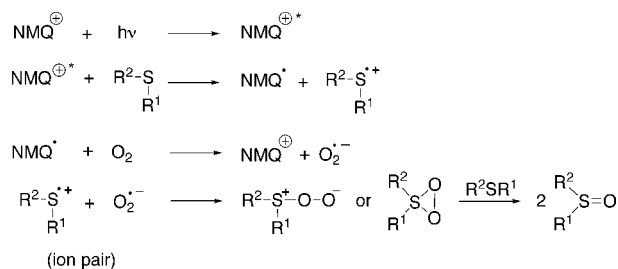


persulfide **86** in alcohol solvents.^{4,171-187} The acidity of the medium and dependence on the trapping efficiency suggest the presence of **86**.¹⁷¹ ^{17}O -labeled substrates implied the participation of **85**. Alcohol adducts and nucleophilic oxygen-transfer chemistry suggest a dipolar form of the persulfide ($\text{R}_2\text{S}^+\text{OO}^-$) rather than a diradical form ($\text{R}_2\text{S}^-\text{OO}^*$) in solution.¹⁸⁸ There is no evidence that $\text{R}_2\text{S}^+\text{OO}^-$ persulfide or R_2SO_2 dioxathirane dimerize to a six-membered-ring diperoxide **87**. Quantum calculations have been used to predict the structures and energetics of intermediates generated in the oxidation of sulfur compounds.^{164,176,184,188}

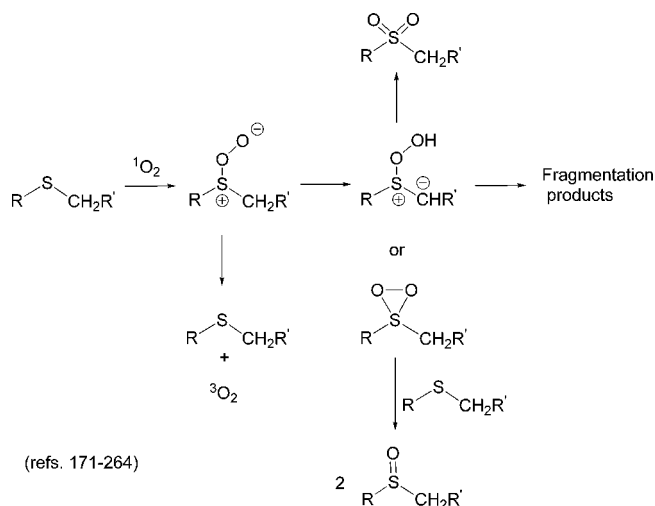
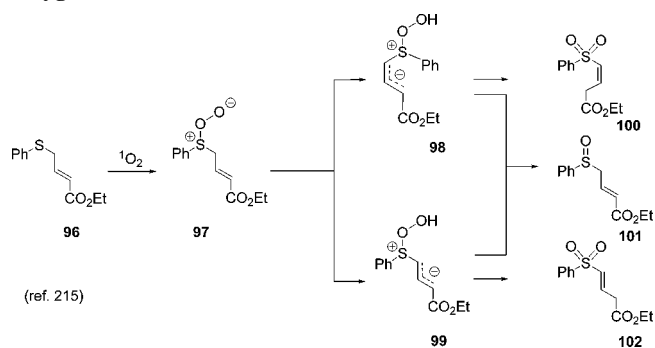
4.2.2.2. Room Temperature. Electron-Transfer Photooxidation. Dioxathiranes may arise from electron-transfer photooxidations with the use of electron-deficient sensitizers.^{184,185,189,190} In 2005 and 2006, experiments conducted in O_2 -saturated acetonitrile implied that the sulfide radical ion **90** ($\text{R} = \text{H}$ or Me), dioxathirane **91** ($\text{R} = \text{H}$ or Me), and sulfoxide **92** ($\text{R} = \text{H}$ or Me) are generated in the photooxidation of dibenzothiophene **89** ($\text{R} = \text{H}$) and 4,6-dimeth-

Scheme 37. Electron-Transfer Photooxidation of Dibenzothiophenes

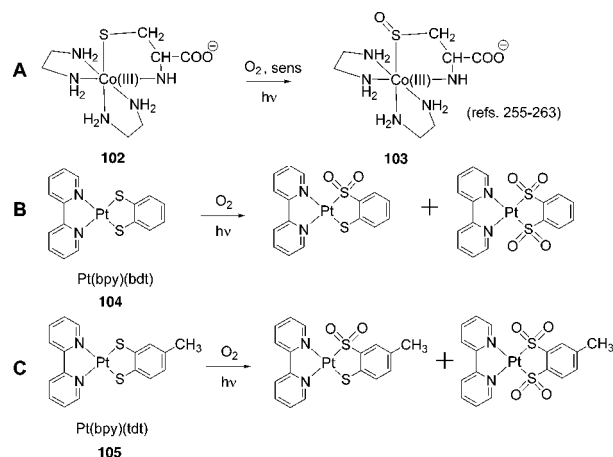
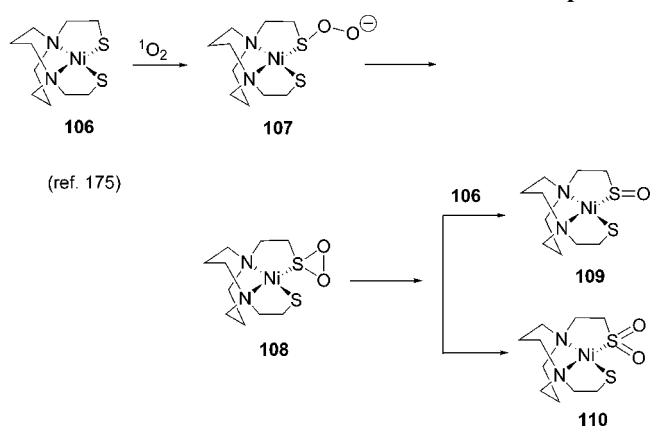


Scheme 38. Electron-Transfer Photooxidation of Dibutylsulfide and Thioanisole


(ref. 184)

Scheme 39. Reaction of Sulfides with Singlet Oxygen

Scheme 40. Reaction of γ -Phenylthiocrotonate with Singlet Oxygen


ylidibenzothiophene **89** ($\text{R} = \text{Me}$), sensitized by *N*-methylquinolinium tetrafluoroborate ($\text{NMQ}^+\text{BF}_4^-$), 10-methylacridine hexafluorophosphate ($\text{AcrH}^+\text{PF}_6^-$), or 2-(4-methoxyphenyl)-4,6-diphenylpyrylium ($\text{MOPDPP}^+\text{BF}_4^-$) in Scheme 37.^{189,190} Laser photolysis, ESR, and fluorescence-quenching data were collected, and the formation of dioxathirane **91** was proposed. It was speculated that the superoxide ion¹⁸⁹ added to the sulfide radical ion in one step (Scheme 37A). It was also suggested that ground state $^3\text{O}_2$ ¹⁹⁰ reacted with the sulfide radical ion in a stepwise manner (via **93** followed by back-electron transfer to MOPDPP^* or AcrH^* , Scheme 37B). EPR data indicated that the superoxide ion is formed by electron transfer from the sensitizer radical (e.g., NMQ^{\bullet}). Sulfoxide production is reduced in the presence of the electron trap 1,4-benzoquinone, which reacts with NMQ^{\bullet} and superoxide to give NMQ^+ and O_2 . Compound **89** does not form the

Scheme 41. Photooxidation of Cobalt- and Platinum-Thiolate Complexes

Scheme 42. Photooxidation of a Nickel-Thiolate Complex


S-hydroperoxysulfonium ylide **82** due to the absence of α protons.

In 2003, the photooxidation of dibutylsulfide (**94**) and thioanisole (**95**) in O_2 -saturated acetonitrile, sensitized by NMQ^+ and 9,10-dicyanoanthracene (DCA), was conducted at 298 K (Scheme 38).¹⁸⁴ Time-resolved laser flash photolysis of NMQ^+ revealed the formation of sulfide radical cations [dimeric $(\text{Bu}_2\text{S})_2^{\bullet+}$, $\text{PhSMe}^{\bullet+}$, and dimeric $(\text{PhSMe})_2^{\bullet+}$]. DCA photolysis also led to the production of radical ions for PhSMe , but not Bu_2S . The persulfoxide exists as a primary intermediate in sulfide- $^1\text{O}_2$ reactions,¹⁸⁸ but in the NMQ^+ and DCA systems, dioxathirane was suggested to arise from a direct reaction between sulfide radical ion and the superoxide ion. The evidence for dioxathirane derives from the electrophilic character of the intermediate in bimolecular trapping experiments, as confirmed by data from computations. The computations predict an energetically facile conversion of $\text{R}_2\text{S}^{\bullet+}$ (from **94** and **95**) with the superoxide ion to give the corresponding dioxathiranes.¹⁸⁴

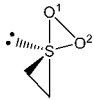
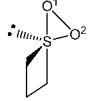
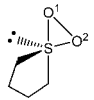
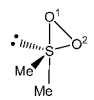
Other work has also focused on generation of sulfide radical ions, some via electron-transfer photosensitizers [DCA (free or covalently bound to silica), triphenylpyrylium tetrafluoroborate, 2,3,5,6-tetrachloro-1,4-benzoquinone, $\text{Ru}(2,2'\text{-bipyrazine})_3^{2+}$, TiO_2 , CdS, and acetone], although the intermediacy of dioxathiranes is not suggested in these cases.¹⁹¹⁻²⁰³

*Singlet Oxygen Reactions.*¹⁷¹⁻²⁶⁴ Early sulfide photooxidation work of Schenck (from 1962 to about 1970) suggested

Table 31. Calculated Geometries of Dioxathiiranes

Year	Structure	Method of Basis Set	O ¹ -O ^{2a}	S-O ^{1a}	S-O ^{2a}	S-O ¹ -O ^{2b}	Ref.		
1998		B3LYP/6-31+G(d)	1.535	2.077	1.597		212		
1998, 1996		MP2/6-31G(d)	1.556	1.811	1.651		243, 244		
		MP2/6-311+G(2df)	1.531	1.817	1.609				
1998		MP2/6-311+G(3df,2p)	1.542	1.755	1.607	67.7	176		
		QCISD/6-31+G(d)	1.562	1.982	1.597	77.7			
		MP2/6-311+G(3df,2p)	1.527	1.809	1.601	70.6			
		MP2/6-311+G(3df,2p)	1.53	1.798	1.603	70			
1997		MP2/6-31G(d)	1.556	1.811	1.652		213		
			1.547	1.797	1.666				
			1.555	1.747	1.634				
			1.555	1.753	1.639				
			1.549	1.771	1.650				
			1.551	1.786	1.649				
			1.546	1.803	1.649				
			1.546	1.800	1.659				
			1.549	1.773	1.642				
			1.552	1.780	1.643				
	1996			RHF-PM3	1.580	1.790	1.710		242

Table 31 (Continued)

Year	Structure	Method of Basis Set	O ¹ -O ^{2a}	S-O ^{1a}	S-O ^{2a}	S-O ¹ -O ^{2b}	Ref.
1996			1.564	1.793	1.648		243
			1.555	1.812	1.646		
			1.553	1.825	1.647		
1992		MP2/6-31G(d)	1.555	1.809	1.648		231

^a Bond distances in angstroms. ^b Bond angles in degrees.

a sensitizer–oxygen complex (moloxide) rather than a diffusible ¹O₂ species.^{204,205} In the 1980s and 1990s, efforts were increased to understand the intermediates generated in the sulfide–¹O₂ chemistry. In these studies, the production of dioxathiranes was searched for by using flash photolysis and competitive kinetic techniques. The reaction mechanism in Scheme 39 proposes the persulfoxide **80** as the first intermediate. The high-energy barrier computed for the formation of the dioxathirane from the persulfoxide suggests that the *S*-hydroxysulfonium ylide is a key reaction intermediate. The *S*-hydroxysulfonium ylide is most likely an additional intermediate in the photosensitized oxidations of sulfides in aprotic solvents. The formation of a *S*-hydroperoxysulfonium ylide explains the experimental results in many cases.^{207–216} For example, in 2002, the reaction of ¹O₂ with ethyl γ -phenylthiocrotonate (**96**) was conducted in C₆D₆ at 298 K (Scheme 40).²¹⁵ From the observation of the sulfoxide **101** and sulfone **100** and **102** products by ¹H NMR spectroscopy, the intermediacy of the *S*-hydroperoxysulfonium ylides **98** and **99** was implied. In this study, the source of ¹O₂ was 1,4-dimethylnaphthalene endoperoxide.

Despite all the work conducted on the reactions of ¹O₂ with nickel-, platinum-, and cobalt-thiolate complexes, little is known about the formation of the corresponding dioxathiranes in these systems (Scheme 41 and 42).^{255–263} The nickel- and platinum-thiolate ligand photooxidations were conducted in aprotic solvents (*N,N*-dimethylformamide, acetonitrile, and DMSO), which paralleled the organic sulfide–¹O₂ reactions observed in aprotic solvents.¹⁷⁵ Kinetic data and trapping experiments suggest a mechanism analogous to the photooxidation of organic sulfides. The singlet oxygen oxidizes the thiolato group of the complex [Co(III)-(en)₂(S-cys)]⁺(BF₄)[−] (**103**) in water to give the corresponding sulfenato complex (Scheme 41A). The Pt(bpy)(bdt) [bpy = 2,2′-bipyridine (**104**); bdt = 1,2-benzenedithiolate (**105**)] is oxidized by the ¹O₂ to form the sulfinate [Pt(bpy)(bdtO₂)] and disulfinate [Pt(bpy)(bdtO₄)] products (Scheme 41B,C). Nickel dithiolate complexes react with ³O₂ or ¹O₂ to generate the corresponding sulfenato and sulfonate products through the persulfoxide **107** and dioxathirane **108** intermediates (Scheme 42).

4.2.2.3. Calculations. Structure. A number of computational papers have focused on the reaction of ¹O₂ with

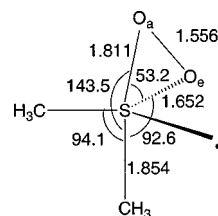


Figure 4. MP2/6-31G(d) computed structure of the dimethyldioxathirane from ref 213. Bond lengths in angstroms; bond angles in degrees.

sulfides. Theory suggests that the dioxathirane is a minimum on the potential energy surface. The calculated O–O and S–O bond distances are shown in Table 31. The dioxathirane structures resemble each other in many of the basic geometric trends. Dioxathirane O–O bond distances range from 1.562 to 1.527 Å, which depends on the structure and the level of theory; the dioxathirane ring is unsymmetric, with two nonequivalent S–O bonds. The oxygen atoms occupy apical and equatorial positions, with the apical bonds longer than the equatorial ones by ca. 0.08–0.48 Å. A sample computed structure for dimethyldioxathirane is given in Figure 4.

Dioxathiranes have negative charges on the oxygen atoms. The atomic charges as predicted by the NBO method for a series of dioxathiranes MeS(O₂)X (where X = Me, NMe₂, F, OMe, SMe, NH₂, NHMe, OH, and SH) indicate a greater negative charge at the apical oxygens (O₁) compared to the equatorial ones (O₂); see Table 32. MP2/6-31G(d) computed vibrational frequencies, IR intensities, and isotropic shifts of dioxathirane Me₂SO₂ are shown in Tables 33 and 34.

Energetics. The transition state that connects the persulfoxide and the dioxathirane is high in energy with a barrier of ~20 kcal/mol; thus, the dioxathirane is not expected to form as a reaction intermediate along this route. Once formed, the persulfoxide converts to the *S*-hydroperoxysulfonium ylide by a lower barrier process (~10 kcal/mol). The strongest experimental evidence for the formation of dioxathiranes comes from the use of electron-poor sensitizers in the photooxidation of sulfides. In contrast, the *S*-hydroperoxysulfonium ylide is in most cases the second intermediate formed in sulfide–¹O₂ reactions (Table 35).

Table 32. Calculated Charges of the Sulfur and Oxygen Atoms in Dioxathiiranes^a

Year	Structure	Natural Bond Order Charges			Method
		S	O ¹	O ²	
1997		1.32	-0.55	-0.46	MP2/6-31G(d)
		1.45	-0.55	-0.46	
		1.59	-0.51	-0.41	
		1.34	-0.47	-0.39	
		1.52	-0.52	-0.44	
		1.20	-0.52	-0.42	
		1.45	-0.55	-0.46	
		1.45	-0.55	-0.46	
		1.52	-0.52	-0.43	
		1.22	-0.51	-0.41	

^a Reference 213.

4.2.3. Dioxaselenirane and Dioxatellurirane

In 1994, the reaction of singlet oxygen with diaryl selenides and benzyl-substituted selenides was reported.²⁶⁵ Surprisingly, the identities of the R groups of the starting selenides **111** were not explicitly stated in the publication.²⁶⁵ The diaryl selenides yielded the corresponding selenoxides Ar₂Se=O, while the benzyl-substituted selenides afforded benzaldehyde and diselenide ArSeSeAr. Initial formation of a peroxy-selenoxide **112** was proposed; however, the mechanism is not well understood. No mention was made of R₂SeO₂ dioxaselenirane **113** as a possible reaction intermediate (Scheme 43).

In 1976, a selenide photooxidation reaction was conducted in anhydrous methanol at room temperature.²⁶⁶ Unfiltered light from an iodine lamp was employed, and Rose Bengal served as the sensitizer; the selenoxide yields are given in Table 36. No trapping reactions were conducted, although aryl selenides and selenoxides have been used as trapping agents²⁶⁷ in other photooxidation processes.^{268–270}

Table 33. Calculated Vibrational Frequencies ($\bar{\nu}$) and IR Intensities of Dimethyldioxathiirane^{a,b}

$\bar{\nu}$, cm ⁻¹	I ^c	$\bar{\nu}$, cm ⁻¹	I ^c
156	3.4	1083	39.0
235	0.1	1389	9.3
270	0.9	1422	8.1
326	5.5	1509	7.8
359	6.8	1517	2.0
366	6.5	1526	2.4
450	66.4	1536	19.5
649	54.8	3107	2.4
740	30.5	3123	3.7
807	56.9	3217	4.4
945	8.2	3226	3.0
963	9.2	3229	3.1
966	34.2	3258	0.8
1045	25.5		

^a Reference 231. ^b Calculated at the MP2/6-31G(d) level. ^c IR intensities.**Table 34. Calculated Isotopic Shifts (cm⁻¹) of Selected Vibrations of Dimethyldioxathiirane^{a,b}**

$\bar{\nu}$	$\Delta\bar{\nu}$	$\Delta\bar{\nu}$	$\Delta\bar{\nu}$	$\Delta\bar{\nu}$
156	-4	-2	-6	0
326	-3	-2	-5	-1
359	-3	-3	-6	-3
366	-1	-3	-4	-1
450	-7	-15	-21	-1
649	-2	0	-2	-5
740	-6	-2	-8	-7
807	-15	-4	-18	-8
945	-4	-8	-28	-1
963	-14	-17	-18	-4
966	-3	-4	-4	-1
1045	-2	-1	-3	-4

^a Reference 231. ^b Calculated at the MP2/6-31G(d) level.

Little data exists on the dioxatellurirane, R₂TeO₂. Near-IR-absorbing tellurapyrylium dyes **114–118** have been suggested to form either R₂Te⁺OO⁻ pertelluroxide or R₂TeO₂ dioxatellurirane intermediates upon photooxidation with singlet oxygen,^{271,272} but no distinction between the two intermediates was made (Scheme 44). The irradiation of the tellurapyrylium dyes was conducted in air-saturated aqueous solutions with unfiltered light from a tungsten bulb in the absence of trapping agents. A reaction between pertelluroxide or dioxatellurirane and substrate R₂Te may take place, to account for the formation of the R₂Te=O product, which is readily hydrated to the diol R₂Te(OH)₂. The tellurium-containing dyes **114–116** reacted with singlet oxygen 20–80 times faster than the corresponding selenium and oxygen derivatives **117** and **118**. The tellurium-containing dye **114** reacted two times faster with singlet oxygen than **116**. The impetus to study the photooxidation of the tellurapyrylium dyes was their potential use in photodynamic therapy (PDT). Theoretical studies on the photooxygenation of selenides and tellurides should be informative. The possible formation of R₂SeO₂ and R₂TeO₂ heterodioxiranes, their cleavage products, and Se-hydroperoxyselenium and Te-hydroperoxytellurium ylides should be of interest.

4.3. Cyclic and Ring-Opened Species

To assess the difference in stability between the various XO₂ heterodioxiranes, the computed energies between ring-

Table 35. Calculated Energies for Intramolecular and Intermolecular Reactions of Dioxathiiranes^a

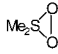
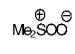
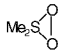
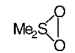
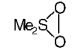
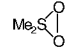
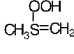
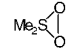
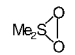
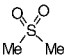
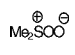
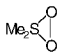
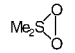
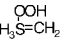
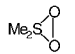
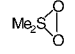
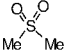

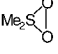
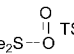
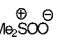
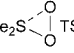
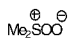
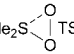
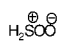
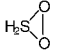
Year	A	B	$\Delta E_{A \rightarrow B}$	Method and Basis Set	Ref.	Comments
2003	$\text{Me}_2\text{S}^{+} + \text{O}_2^{-}$		-158.6	MP2/6-31+G(2d,p)	184	
			-151.2	QCISD/6-31+G(2d,p)		
			-1.7	MP2/6-31+G(2d,p)		
			2.3	QCISD/6-31+G(2d,p)		
		$\text{Me}_2\text{S} + {}^1\text{O}_2$	-11.1	MP2/6-31+G(2d,p)		
			-15.1	QCISD/6-31+G(2d,p)		
	$\text{Me}_2\text{S} + {}^1\text{O}_2$ TS	9.9 ^b	MP2/6-31+G(2d,p)			
		6.2	QCISD/6-31+G(2d,p)			
1998			-12.2	B3LYP/6-31+G(d)	212	
			-7.4	QCISD(T)/6-31+G(d)		
			-5.9	QCISD(T)/6-311+G(3df,2p)		
		$\text{Me}_2\text{S} + {}^1\text{O}_2$	-22.2	B3LYP/6-31+G(d)	22 kcal/mol experimental value added to ${}^3\text{O}_2$	
			-13.9	QCISD(T)/6-31+G(d)		
			-3.5	QCISD(T)/6-311+G(3df,2p)		
			-87.6	B3LYP/6-31+G(d)		
			-85.9	QCISD(T)/6-31+G(d)		
			-101.8	QCISD(T)/6-311+G(3df,2p)		
			3.0	B3LYP/6-31+G(d)		
			0.9	QCISD(T)/6-311+G(3df,2p)		
			-6.7	MP2/6-31G(d)	176	
			-7.2	CCSD(T)/6-311+G(2df) ^b		
		$\text{Me}_2\text{S} + {}^1\text{O}_2$	-19.4	MP2/6-31G(d)		
			-3.2	CCSD(T)/6-311+G(2df) ^b		
			-94.5	MP2/6-31G(d)		
			-3.0	MP2/6-31G(d)		
			1.4	CCSD(T)/6-311+G(2df) ^b		
	$\text{Me}_2\text{S} + {}^1\text{O}_2$		32.8 ^b	MP2/6-31G(d)		
11.2			CCSD(T)/6-311+G(2df) ^b			
		19.0 ^b	MP2/6-31G(d)			
		(Ring closure)	20.6		CCSD(T)/6-311+G(2df) ^b	
		13.2 ^b	MP2/6-31G(d)	TS' represents a second pathway found to the dioxathiirane		
		(Ring closure)	11.1		CCSD(T)/6-311+G(2df) ^b	
1998			-6.3	MP2/6-31+G(d)	176	
			-0.1	CCSD(T)/6-31+G(d)//MP2/6-31+G(d)		
			1.5	QCISD/6-31+G(d)		
			-7.9	MP2/6-31++G(2d,p)		

Table 35 (Continued)

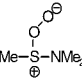
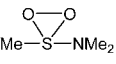
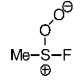
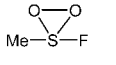
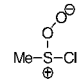
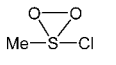
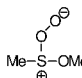
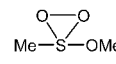
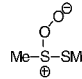
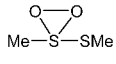
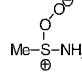
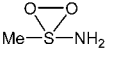
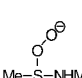
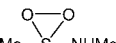
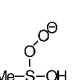
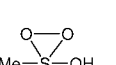
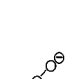
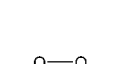
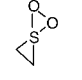
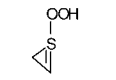
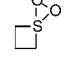
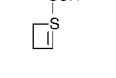
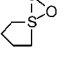
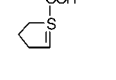
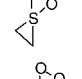
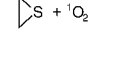
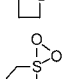
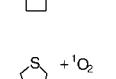
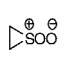
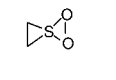


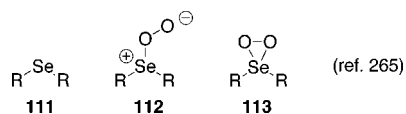
Year	A	B	$\Delta E_{A \rightarrow B}$	Method and Basis Set	Ref.	Comments
			-10.7	MP2/6-31+G(2df,p)		
			-10.6	MP2/6-31+G(2df,p)		
1997, 1998			-9.3	MP2/6-31G(d)	213, 214	
			-31.1	MP2/6-31G(d)		
			-24.3	CCSD(T)/6-31G(d)		
			-30.1	MP2/6-311G(2d)		
			-13.6	MP2/6-31G(d)		
			-15.9	CCSD(T)/6-31G(d)		
			-14.4	MP2/6-311G(2d)		
			-19.7	MP2/6-31G(d)		
			-25.6	MP2/6-31G(d)		
			-12.2	MP2/6-31G(d)		
			-7.2	CCSD(T)/6-31G(d)		
			-10.8	MP2/6-311G(2d)		
			-11.8	MP2/6-31G(d)		
			-22.9	MP2/6-31G(d)		
			-16.7	CCSD(T)/6-31G(d)		
			-21.6	MP2/6-311G(2d)		
			-18.0	MP2/6-31G(d)		
			-10.9	CCSD(T)/6-31G(d)		
			-16.5	MP2/6-311G(2d)		
1996			11.5	MP2/6-31G(d)	243	
			1.7			
			-7.8			
			-24.1			
			-11.9			
			-19.0			
			-4.4			

Table 35 (Continued)

Year	A	B	$\Delta E_{A \rightarrow B}$	Method and Basis Set	Ref.	Comments
			-8.0			
			-2.3			
			TS			
			TS			
			TS'		176	TS' represents a second pathway found to the dioxathiirane
1996			-2.6	PM3	242	
			17.6			

^a Energies in kilocalories per mole. ^b Transition state energies.

Scheme 43. Selenide, Peroxyselenoxide, and Dioxaselenirane

Table 36. Selenoxide Yields in the Reaction of Singlet Oxygen with Selenides (R^1SeR^2)^a

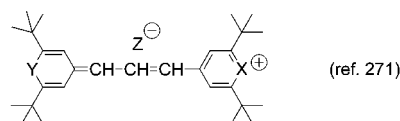
R ¹	R ²	Yield (%)
Ph	Me	95
Ph		70
Me		85
Me		70

^a Reference 266.

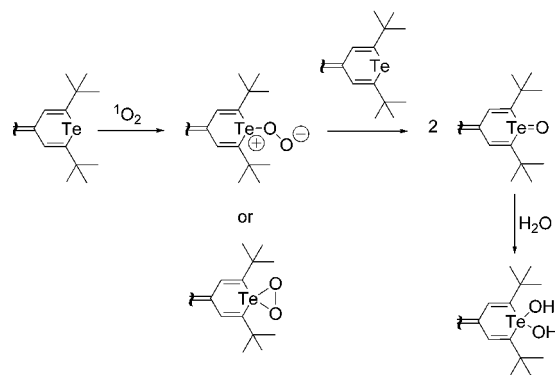
closed and ring-opened structures shall be compared. With the exception of Sawaki's review,³ no comparison of this sort exists for the XO₂ dioxiranes. The relative energetics of the XO₂ dioxiranes compared to O–X–O acyclic compounds are summarized in Table 37. Breaking of the O–O bond in XO₂ dioxiranes may lead, for example, to a nitro compound in the case of dioxaziridine (cf. entries 1–5, Table 37). In contrast, a Baeyer–Villiger reaction for some of the XO₂ dioxiranes may afford heteroatom-substituted esters or acids (cf. entries 6–11, Table 37). The above reactions are highly exothermic, favoring the acyclic structures rather than the corresponding XO₂ dioxiranes. We see that the energy difference is the greatest in the SO₂ system. Schaefer et al. have noted a decrease in this energy change for the heavier XO₂ dioxiranes (H₂C > H₂Si > H₂Ge > H₂Sn ~ H₂Pb).⁹⁰ More systematic computational data is needed to recognize the factors that determine dioxirane stability. The data on the transition states for unimolecular O–O bond breaking processes in XO₂ dioxiranes are scarce.

The calculated cyclization barriers for X–O–O into XO₂ dioxirane (X = RN, R₂Si, R₂S, and S) can be compared with the ~19 kcal/mol cyclization barrier for carbonyl oxides to dioxiranes (Table 38).²⁷³ Computational data is not available

Scheme 44. Photooxidation of Tellurium-, Selenium-, and Oxygen-Containing Dyes



Structure	X	Y	Z
114	Te	Te	BF ₄ [−]
115	Te	Se	ClO ₄ [−]
116	Te	O	ClO ₄ [−]
117	Se	O	ClO ₄ [−]
118	O	O	ClO ₄ [−]



for the acyclic X–O–O to cyclic XO₂ conversion (where X = R₃P, R₂Se, R₂Ge, R₂Sn, R₂Pb, R₂Te, and Se). Not for all XO₂ dioxiranes has an acyclic XOO counterpart been computationally found. For example, R₃P appears to be such a case, for which many theoretical methods conclude that the acyclic R₃POO species does not intervene in reactions of R₃P with ¹O₂. Sawaki has conducted B3LYP/6-31G(d) calculations of the reaction enthalpies and activation energies for the cyclization of X–O–O to cyclic XO₂ (where X = O, HN, H₂C, S, HP, H₂Si, Se, HAS, and H₂Ge).³ A lower

Table 37. Relative Energetics of the Heteroatom Dioxiranes Compared to Their Corresponding O–X–O Acyclic Counterparts^a

entry	XO ₂ cyclic structure	O–X–O acyclic structure	method and basis set	ΔE_{A-B}	ref
1	PhNO ₂ dioxaziridine	PhNO ₂ nitrobenzene	B3LYP/6-31G(d)	–80.7	7
2	HNO ₂ dioxaziridine	HNO ₂ nitro compound	B3LYP/6-31G(d)	–74.0	7
3	SO ₂ cyclic	O=S=O	B3LYP/cc-pVTZ	–99.8	111
4	HPO ₂ dioxaphosphirane	HP(=O) ₂	SCF-CEPA-1	–79.6	165
5	Me ₂ SO ₂ dioxathiirane	Me ₂ S(=O) ₂ sulfone	B3LYP/6-31+G(d)	–87.6	212
6	MeSi(O) ₂ Ph dioxasilirane	MeSi(=O)OPh ester	B3LYP/6-311++G(d,p)	–61.7	51
7	H ₂ SiO ₂ dioxasilirane	HSi(=O)OH acid	B3LYP/TZ2P-ECP	–81.0	90
8	H ₂ GeO ₂ dioxagermirane	HGe(=O)OH acid	B3LYP/TZ2P-ECP	–74.9	90
9	H ₂ SnO ₂ dioxastannirane	HSn(=O)OH acid	B3LYP/TZ2P-ECP	–70.6	90
10	H ₂ PbO ₂ dioxastilbirane	HPb(=O)OH acid	B3LYP/TZ2P-ECP	–71.8	90
11	H ₂ CO ₂ dioxirane	HC(=O)OH acid	B3LYP/TZ2P	–94.6	90

^a Energies in kilocalories per mole.

Table 38. Calculated Cyclization Barriers for the Reaction of Acyclic X–O–O to the Corresponding XO₂ Dioxiranes^a

X–O–O acyclic structure	XO ₂ cyclic structure	method and basis set	ΔE_{A-B}	TS barrier	ref
trans HNOO nitroso oxide	HNO ₂ dioxaziridine	SFC/6-31G+p	4.2	43.8	44
MeSi(OO)Ph silanone <i>O</i> -oxide	MeSi(O) ₂ H dioxasilirane	B3LYP/6-311++G(d,p)	–49.6	0.8	51
SOO acyclic	SO ₂ cyclic	B3LYP/cc-pVTZ	–7.5		111
Me ₂ SOO peroxy sulfoxide	Me ₂ SO ₂ dioxathiirane	MP2/6-31G(d)	–3.0	19.0	176
H ₂ COO carbonyl oxide	H ₂ CO ₂ dioxirane	MP2/6-31G(d)	–28.6	19.1	273a

^a Energies in kilocalories per mole.

activation energy was predicted for the cyclization of X–O–O in higher-row elements, for example, H₂Si < H₂Ge < HP < H₂C ~ H₂S < HN < O. The second-row elements have more prominent 1,3-dipoles and enhanced double bond character in the X–O bond, whereas the higher-row elements have less double bond character.³ It has also been suggested that a larger difference in the electronegativity between the X and O atoms results in a lower rotation barrier of X–O–O, which facilitates cyclization to the dioxirane.^{143b}

4.4. Intermolecular Reactions

Carbon-based dioxiranes may donate an oxygen atom to acceptor molecules, such as alkenes, phosphines, sulfides, and in some cases even saturated hydrocarbons.^{4,6,274–276} Since R₂CO₂ dioxiranes have low strain energies (~11 kcal/mol for R = Me; ~16 kcal/mol for R = H), their enhanced oxidative reactivity²⁷⁷ does not derive from the strain release in the oxygen-transfer process.^{89,278–280} Instead, it is a result of the weak peroxide bond.^{89,278–280} Some heteroatom-substituted XO₂ dioxiranes are able to transfer an oxygen atom to acceptor molecules (Table 39), but the literature is limited in comparison to R₂CO₂ dioxiranes.^{4,6} An oxygen-transfer reaction of dioxaziridine RNO₂ or dioxasiliranes R₂SiO₂ has not yet been established. Oxygen-transfer studies of other XO₂ dioxiranes (X = R₂Se, R₂Ge, R₂Sn, R₂Pb, R₂Te, S, and Se) have also not been done.

Alkenes. Dioxaphosphirane (*o*-MeOC₆H₄)₃PO₂ has been used to convert alkenes to epoxides.⁹⁹ This alkene epoxidation appears to be a nonradical process. The mechanism of deoxygenation of (*o*-MeOC₆H₄)₃PO₂ does not involve a unimolecular fragmentation of an oxygen atom.¹³⁷ A dioxaphosphirane derived from 1-methyl-4-phospha-3,5,8-trioxabicyclo[2.2.2]octane reacts supposedly with norbornene to give norbornene oxide.^{154,155a} There are no data available that demonstrates an intermolecular oxygen transfer from an intermediary dioxaziridine to an alkene. A problem is that the alkene, e.g., 2,3-dimethyl-2-butene reacts with the ground state triplet nitrene to form an aziridine instead of a reaction with dioxaziridine to give the epoxide. An oxygen-substituted

nitrene reaction exemplifies this, in which the triplet nitrene CH₃ON (**119**) reacts with 2,3-dimethyl-2-butene to produce the aziridine **120** (Scheme 45).^{10,23f} Acyclic nitroso oxides have been proposed to convert alkenes to epoxides **121**.³ Nitroso oxide (e.g., PhNOO) and dioxaziridine (e.g., PhNO₂) will also rapidly oxidize additional triplet nitrene, since the reaction of nitrene with ³O₂ is slower.^{39b} The highly reactive PhN[•]OO[•] transfers an oxygen atom to toluene and anisole. At present, there is not sufficient data available for comparing possible oxygen-transfer reactions of dioxaziridines and nitroso oxides.

Phosphorus- and Sulfur-Containing Reactants. Dioxaphosphiranes are capable of delivering an oxygen atom to phosphines, sulfides, and sulfoxides.^{136–140,142,143,154,155} Also, dioxathiiranes, e.g., PhMeSO₂ and Bu₂SO₂ (generated from sulfide radical cation–superoxide reactions), react presumably with phenyl sulfide to give phenyl sulfoxide.^{184,185}

4.5. Synthetic Prospectives

Disappointingly, heteroatom-containing dioxiranes have not yet been found useful as oxidant alternatives for the popularly used carbon-based dioxiranes. Except for dioxaphosphirane, the XO₂ dioxiranes have only been of mechanistic interest, but their synthetic versatility remains still to be established; whereas the mechanistic aspects of XO₂ dioxiranes (X = R₃P, RN, R₂Si, and R₂S) are becoming better understood, little or no experimental evidence confirms the existence of the remaining XO₂ dioxiranes (X = R₂Se, R₂Ge, R₂Sn, R₂Pb, R₂Te, S, and Se).

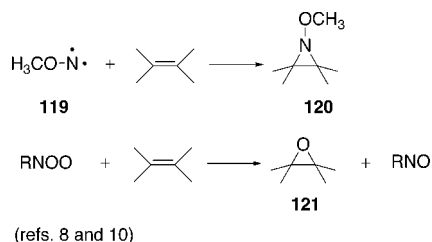
Early research on R₂CO₂ dioxiranes showed that they were formed in carbene–O₂ reactions under conditions (e.g., low-temperature matrix, combustion, etc.) that proved of little use in synthetic applications. The versatility of R₂CO₂ dioxiranes in synthetic organic chemistry emerged after the discovery of their generation from aqueous oxone–ketone reactions.^{4,6} The use of oxone to generate dioxiranes from ketones was an important discovery. R₂CO₂ dioxiranes are generated from ketones in other ways, including the reaction with arenesulfonic peracids [generated from (arenesulfonyl)-imidazole/H₂O₂/NaOH],²⁷² peroxyimidic acid MeC(=NH)-

Table 39. Bimolecular Reaction of XO₂ Dioxiranes

Year	Structure	Trap	Product	Ref.	Comments
2006, 2003		alkenes	epoxides ^a	137	
2004		CH ₂ =CH ₂		63-73	Tentative assignment of a silica gel-attached dioxasilirane
2003		Ph ₂ S	Ph ₂ SO	184	
2001		Ar ₃ P	Ar ₃ PO	140	
1999		Ph ₃ P	Ph ₃ PO	136	
1993		Ph ₂ SO	Ph ₂ SO ₂ (sulfone)	143a	
1993		Ar ₂ S	Ar ₂ SO	143a	
1993		Ar ₂ SO	Ar ₂ SO ₂ (sulfone)	143a	
1993		norbornene	norbornene oxide	154	
				154	(major product)
		Ph ₂ S	Ph ₂ SO		
		Ph ₂ S	Ph ₂ SO		

^a Corresponding epoxides from norbornene, *cis*-stilbene, cyclohexene, and 1-octene.

Scheme 45. Reaction of a Nitrene or Nitroso Oxide with an Alkene



OOH (thought to be generated from MeCN/H₂O₂),²⁷⁴ and possibly peroxyxynitrite.^{275,276} Overcoming obstacles in generating experimentally useful concentrations of R₂CO₂ dioxiranes and in developing catalytic processes for their production was essential for synthetic applications to be realized.

No XO₂ dioxiranes have yet been generated from their corresponding X=O precursors, analogous to the preparation of R₂CO₂ dioxiranes from ketones. Attempts in this regard have been sparsely reported. For example, generating dioxaphosphirane Ph₃PO₂ by the oxidation of Ph₃P=O with MCPBA or H₂O₂-trifluoroacetic acid-trifluoroacetic an-

hydride was unsuccessful.² A reaction of ¹⁸O-labeled dimethylsulfoxide with oxone failed to generate the Me₂SO₂ dioxathiirane.¹ In view of their considerable instability and tendency to form polymers, the reaction of oxone with R₂Si=O silanones has not been explored, in an attempt to generate dioxasilirane.

5. Summary

Progress has been made in regard to the direct experimental evidence for the generation of R₃PO₂, RNO₂, and R₂SiO₂ dioxiranes. The R₂SO₂ and R₂TeO₂ dioxiranes are tentatively assigned based on indirect experimental methods; however, experimental evidence is lacking for the homologue dioxiranes R₂SeO₂, R₂GeO₂, R₂SnO₂, R₂PbO₂, SO₂, and SeO₂. Theoretical calculations predict that the XO₂ dioxiranes should persist under a variety of reaction conditions, but no computations have as yet been reported on the cyclic SeO₂.

The chemistry of XO₂ dioxiranes is still not well understood, and it is far less developed compared to that of R₂CO₂ dioxiranes,^{4,6} a serious shortcoming for the effective use of XO₂ dioxiranes in synthetic chemistry. In this regard, the dioxaphosphiranes are the only XO₂ dioxiranes that

display synthetic utility in intermolecular (oxygen-transfer) reactions.

Challenging problems that await exploration include the following: (i) the discovery of methods to generate XO₂ dioxiranes from their corresponding X=O (monoxide) precursors, (ii) the development of asymmetric XO₂ oxygen-transfer reactions (precursors or catalysts bearing chiral substituents on X), (iii) the discovery of a possible synthetic advantage of XO₂ over R₂CO₂ in cases where X itself is a chiral center, (iv) the design of heterogeneous reactions to tether XO₂ dioxiranes onto solid surfaces to minimize unwanted bimolecular reactions, (v) the creation of "persistent" or at least sufficiently long-lived XO₂ dioxiranes to enable their isolation under the more common laboratory conditions by stabilizing the dioxiranes kinetically (e.g., utilizing sterically bulky substituents to shield the peroxide center or by caging dioxiranes in host molecules such as carcerands or dendrimers) or thermodynamically (e.g., electronic substituent effects to reduce the energy difference between reactants and intermediate), and (vi) assessment of the nucleophilic or ambiphilic oxidation character of the XO₂ dioxirane oxygen atoms.

6. Acknowledgments

A.G. wishes to thank his group members who have inspired the research endeavors on this topic: Adebogun Adenike, David Aebisher, Nikolay Azar, Gina Bolnet, Edyta M. Brzostowska, Genrong Cao, Alvaro Castillo, Kevin Chan, Wang Chan, Nicola S. Farina, Richard Foucault, Aaron T. Frank, Onica Le Gendre, Magdalena Kiprowska, Edlaine Lucien, Adaickapillai Mahendran, Jesse Medina, Martine Paulynice, Roman Reznik, Sharmila Shakya, Michael Skowronski, Keith B. Thomas, Tanya Voloshchuk, Orrette R. Wauchope, Simon Wu, and Matibur Zamadar. This work was supported by research grants from the National Institutes of Health (S06 GM076168-01) and PSC-CUNY (67341-0036). We also wish to thank the reviewers and Edward L. Clennan, Raymond C. Fort, Paul Haberfield, Roald Hoffmann, Joel F. Liebman, and John P. Toscano for careful reading of the document and suggestions.

7. References

- Clennan, E. L. *Trends Org. Chem.* **1995**, *5*, 231.
- Clennan, E. L. *Sulfur Rep.* **1996**, *19*, 171.
- Ishiguro, K.; Sawaki, Y. *Bull. Chem. Soc. Jpn.* **2000**, *73*, 535.
- Clennan, E. L.; Pace, A. *Tetrahedron* **2005**, *61*, 6665.
- A small sample of references on metalloxidoxiranes, MO₂, includes: (a) Ho, R. Y. N.; Liebman, J. F.; Valentine, J. S. *Biological Reactions of Dioxygen: An Introduction*. In *Active Oxygen in Biochemistry*; Valentine, J. S., Foote, C. S., Greenberg, A., Liebman, J. F., Eds.; Blackie Academic & Professional: New York, NY, 1995; pp 1. (b) Vaska, L. *Acc. Chem. Res.* **1976**, *9*, 175. (c) MoO(O₂)₂(OPR₃) Mimoun-type complexes and ReO(O₂)₂Me Herrmann-type complexes: Deubel, D. V.; Frenking, G.; Gisdakis, P.; Herrmann, W. A.; Rosch, N.; Sundermeyer, J. *Acc. Chem. Res.* **2004**, *37*, 645. Abu-Omar, M. M.; Hansen, P. J.; Espenson, J. H. *J. Am. Chem. Soc.* **1996**, *118*, 4966. (d) Copper dioxygen complexes: Mirica, L. M.; Ottenwaelder, X.; Stack, T. D. P. *Chem. Rev.* **2004**, *104*, 1013. Zhang, C. X.; Liang, H.-C.; Humphreys, K. J.; Karlin, K. D. *Catal. Met. Complexes* **2003**, *26* (Advances in Catalytic Activation of Dioxygen by Metal Complexes), 79. Fox, S.; Karlin, K. D. *Dioxygen Reactivity in Copper Proteins and Complexes*. In *Active Oxygen in Biochemistry*; Valentine, J. S., Foote, C. S., Greenberg, A., Liebman, J. F., Eds.; Blackie Academic & Professional: New York, NY, 1995; pp 188. Mattar, S. M.; Ozin, G. A. *J. Phys. Chem.* **1988**, *92*, 3511. (e) Cobalt dioxygen complexes: Basolo, F.; Hoffman, B. M.; Ibers, J. A. *Acc. Chem. Res.* **1975**, *8*, 384. McLendon, G.; Martell, A. E. *Coord. Chem. Rev.* **1976**, *19*, 1. Tovrog, B. S.; Kitko, D. J.; Drago, R. S. *J. Am. Chem. Soc.* **1976**, *98*, 5144. Dedieu, A.; Rohrer, M. M.; Veillard, A. *J. Am. Chem. Soc.* **1976**, *98*, 5789. (f) Dioxygen complexes of manganese porphyrins: Hanson, L. K.; Hoffman, B. M. *J. Am. Chem. Soc.* **1980**, *102*, 4602. (g) Dioxygen complex of a titanium porphyrin: Guillard, R.; Fontesse, M.; Fournari, P. *Chem. Commun.* **1976**, 161. (h) Heme and non-heme dioxygen complexes: Mumentau, M.; Reed, C. A. *Chem. Rev.* **1994**, *94*, 659. Feig, A. L.; Lippard, S. J. *Chem. Rev.* **1994**, *94*, 759. Roelfes, G.; Vrajmasu, V.; Chen, K.; Ho, R. Y. N.; Rohde, J.-U.; Zondervan, C.; Ja Crois, R. M.; Schudde, E. P.; Lutz, M.; Spek, A. L.; Hage, R.; Feringa, B. L.; Muenck, E.; Que, L., Jr. *Inorg. Chem.* **2003**, *42*, 2639. (i) Vanadium dioxygen complexes: Sam, M.; Hwang, J. H.; Chanfreau, G.; Abu-Omar, M. M. *Inorg. Chem.* **2004**, *43*, 8447. (j) Ir(CO)Cl(PPh₃)₂O₂ complex: Selke, M.; Foote, C. S. *J. Am. Chem. Soc.* **1993**, *115*, 1166. (k) Rh(CO)Cl(PPh₃)₂O₂ complex: Selke, M.; Foote, C. S.; Karney, W. L. *Inorg. Chem.* **1993**, *32*, 5425. (l) Other examples exist for symmetrical dioxygen complexes with Nb, Cr, W, U, and Pt. (m) For a comparison between metal-peroxo species and dioxiranes, see: Adam, W.; Mitchell, C. M.; Saha-Moller, C. R.; Weichold, O. *Struct. Bonding* **2000**, *97*, 237. Adam, W.; Mitchell, C. M.; Saha-Moeller, C. R. *J. Org. Chem.* **1999**, *64*, 3699.
- (a) Bach, R. D. In *Chemistry of Peroxides*; Rappoport, Z., Ed.; Wiley & Sons Ltd.: Chichester, U.K., 2006; Vol. 2, Part 1, pp 1. (b) Adam, W.; Zhao, C. G. In *Chemistry of Peroxides*; Rappoport, Z., Ed.; Wiley & Sons Ltd.: Chichester, U.K., 2006; Vol. 2, Part 1, pp 1129. (c) Curci, R.; D'Accolti, L.; Fusco, C. *Acc. Chem. Res.* **2006**, *39*, 1. (d) Yang, D. *Acc. Chem. Res.* **2004**, *37*, 497. (e) Levai, A. *ARKIVOC* **2003**, *14*, 14. (f) Adam, W.; Saha-Moeller, C. R.; Zhao, C.-G. *Org. React.* **2002**, *61*, 219. (g) Shi, Y. *Yuki Gosei Kagaku Kyokaiishi* **2002**, *60*, 342. (h) Adam, W.; Saha-Moller, C. R.; Ganeshpure, P. A. *Chem. Rev.* **2001**, *101*, 3499. (i) Adam, W.; Degen, H.-G.; Pastor, A.; Saha-Moller, C. R.; Schambony, S. B.; Zhao, C.-G. *Peroxide Chem.* **2000**, *78*. (j) Frohn, M.; Shi, Y. *Synthesis* **2000**, *14*, 1979. (k) Bach, R. D. *Peroxide Chem.* **2000**, 569. (l) Kazakov, V. P.; Voloshin, A. I.; Kazakov, D. V. *Russ. Chem. Rev.* **1999**, *68*, 253. (m) Denmark, S. E.; Wu, Z. *Synlett* **1999**, 847. (n) Dryuk, V. G.; Kartsev, V. G. *Russ. Chem. Rev.* **1999**, *68*, 183. (o) Kabal'nova, N. N.; Khursan, S. L.; Shereshovets, V. V.; Tolstikov, G. A. *Reactions of dioxiranes*. *Kinet. Catal.* **1999**, *40*, 207. (p) Murphree, S. S.; Padwa, A. *Prog. Heterocycl. Chem.* **1998**, *10*, 49. (q) Adam, W.; Smerz, A. K. *Bull. Soc. Chim. Belg.* **1996**, *105*, 581. (r) Curci, R.; Dinioi, A.; Rubino, M. F. *Pure Appl. Chem.* **1995**, *67*, 811. (s) Sauter, M.; Adam, W. *Acc. Chem. Res.* **1995**, *28*, 289. (t) Adam, W.; Hadjarapoglou, L. *Top. Curr. Chem.* **1993**, *164*, 45. (u) Padwa, A. *Prog. Heterocycl. Chem.* **1993**, *5*, 54. (v) Adam, W.; Hadjarapoglou, L. P.; Curci, R.; Mello, R. *Org. Peroxides* **1992**, 195. (w) Bunnelle, W. H. *Chem. Rev.* **1991**, *91*, 335. (x) Curci, R. *Adv. Oxygenated Proc.* **1990**, *2*, 1. (y) Murray, R. W. *Chem. Rev.* **1989**, *89*, 1187. (z) Adam, W.; Curci, R.; Edwards, J. O. *Acc. Chem. Res.* **1989**, *22*, 205. (aa) Murray, R. W. *Mol. Struct. Energ.* **1988**, *6*, 311. (bb) Kafafi, S. A.; Martinez, R. I.; Herron, J. T. *Mol. Struct. Energ.* **1988**, *6*, 283. (cc) Adam, W.; Curci, R. *Chim. Ind. (Milan, Italy)* **1981**, *63*, 20.
- Harder, T.; Wessig, P.; Bendig, J.; Stösser, R. *J. Am. Chem. Soc.* **1999**, *121*, 6580.
- Ishikawa, S.; Nojima, T.; Sawaki, Y. *J. Chem. Soc., Perkin Trans. 2* **1996**, *1*, 127.
- Brinen, J. S.; Singh, B. *J. Am. Chem. Soc.* **1971**, *93*, 6623.
- Srinivasan, A.; Kebede, N.; Saavedra, J. E.; Nikolaitchik, A. V.; Brady, D. A.; Yourd, E.; Davies, K. M.; Keefer, L. K.; Toscano, J. P. *J. Am. Chem. Soc.* **2001**, *123*, 5465.
- Ishikawa, S.; Tsuji, S.; Sawaki, Y. *J. Am. Chem. Soc.* **1991**, *113*, 4282.
- Sawaki, Y.; Ishikawa, S. *J. Am. Chem. Soc.* **1987**, *109*, 584.
- Zelentsov, S. V.; Zelentsova, N. V.; Shchepalov, A. A. *High Energy Chem.* **2002**, *36*, 326.
- Zelentsov, S. V.; Zelentsova, N. V. In *Peroxides at the Beginning of the Third Millennium*; Antonovsky, V. L., Kasaikina, O. T., Zaikov, G. E., Eds.; Nova Sciences Publishers, Inc.: New York, 2004; pp 239.
- Safiullin, R. L.; Khursan, S. L.; Chainikova, E. M.; Danilov, V. T. *Russ. Kinet. Catal.* **2004**, *45*, 640.
- Makareeva, E. N.; Lozovskaya, E. L.; Zelentsov, S. V. *High Energy Chem.* **2001**, *35*, 177.
- Liang, T. Y.; Schuster, G. B. *J. Am. Chem. Soc.* **1987**, *109*, 7803.
- Schuster, G. B.; Platz, M. S. *Adv. Photochem.* **1992**, *17*, 69.
- Zelentsov, S. V.; Zelentsova, N. V.; Zhezlov, A. B.; Oleinik, A. V. *High Energy Chem.* **2000**, *34*, 164.
- Zhezlov, A. B.; Zelentsov, S. V.; Oleinik, A. V. *High Energy Chem.* **1999**, *33*, 87.
- Zelentsov, S. V.; Bykova, E. A.; Ezhevskii, A. A.; Oleinik, A. V. *High Energy Chem.* **1997**, *31*, 397.
- Treushnikov, V. M.; Pomerantseva, L. L.; Frolova, N. V.; Zelentsov, S. V.; Oleinik, A. V. *Zh. Prikl. Spektrosk.* **1978**, *28*, 484.

- (23) (a) Betterton, E. A.; Craig, D. *J. Air Waste Manage. Assoc.* **1999**, *49*, 1347. (b) Uppu, R. M.; Squadrito, G. L.; Cueto, R.; Pryor, W. A. *Methods Enzymol.* **1996**, *269B*, 311. (c) Janowicz, K.; Kurzawa, J. *Chem. Anal. (Warsaw)* **1996**, *41*, 77. (d) Neumann, D. K.; Coombe, R. D.; Ongstad, A. P.; Stech, D. J. *Proc SPIE Int. Soc. Opt. Eng.* **1988**, *875*, 142. (e) Manuszak, M.; Koppenol, W. H. *Thermochim. Acta* **1996**, *273*, 11. (f) Carey, F. A.; Hayes, L. J. *J. Org. Chem.* **1973**, *38*, 3107.
- (24) Harder, J.; Bendig, J.; Scholz, G.; Stösser, R. *J. Inf. Rec.* **1996**, *23*, 147.
- (25) (a) Harder, T.; Bendig, J.; Scholz, G.; Stösser, R. *J. Am. Chem. Soc.* **1996**, *118*, 2497. (b) Harder, T.; Stösser, R.; Wessig, P.; Bendig, J. *J. Photochem. Photobiol., A.* **1997**, *103*, 105.
- (26) Wasserman, E. *Prog. Phys. Org. Chem.* **1971**, *8*, 319.
- (27) (a) Platz, M. S. In *Azides and Nitrenes: Reactivity and Utility*; Scriven, E. F. V., Ed.; Academic Press: New York, 1984; pp 359–393. (b) For a recent example that uses femtosecond UV–visible spectroscopy, see: Burdzinski, G.; Hackett, J. C.; Wang, J.; Gustafson, T. L.; Hadad, C. M.; Platz, M. S. *J. Am. Chem. Soc.* **2006**, *128*, 13402.
- (28) Singh, B.; Brinen, J. S. *J. Am. Chem. Soc.* **1971**, *93*, 540.
- (29) Trozzolo, A. M.; Murray, R. W.; Smolinsky, G.; Yager, W. A.; Wasserman, E. *J. Am. Chem. Soc.* **1963**, *85*, 2526.
- (30) D'Sa, R. A.; Wang, Y.; Ruane, P. H.; Showalter, B. M.; Saavedra, J. E.; Davies, K. M.; Citro, M. L.; Booth, M. N.; Keefer, L. K.; Toscano, J. P. *J. Org. Chem.* **2003**, *68*, 656.
- (31) (a) Bushan, K. M.; Xu, H.; Ruane, P. H.; D'Sa, R. A.; Pavlos, C. M.; Smith, J. A.; Celius, T. C.; Toscano, J. P. *J. Am. Chem. Soc.* **2002**, *124*, 12640. (b) Wasylenko, W. A.; Kebede, N.; Showalter, B. M.; Matsunaga, N.; Miceli, A. P.; Liu, Y.; Ryzhkov, L. R.; Hadad, C. M.; Toscano, J. P. *J. Am. Chem. Soc.* **2006**, *128*, 13142. (c) Celius, T. C.; Toscano, J. P. *CRC Handbook of Organic Photochemistry and Photobiology*, 2nd ed.; CRC Press: Boca Raton, FL, 2004; pp 92/1–92/10. (d) Ruane, P. H.; Bushan, K. M.; Pavlos, C. M.; D'Sa, R. A.; Toscano, J. P. *J. Am. Chem. Soc.* **2002**, *124*, 9806. (e) Pavlos, C. M.; Xu, H.; Toscano, J. P. *Free Radical Biol. Med.* **2004**, *37*, 745.
- (32) Pavlos, C. M.; Cohen, A. D.; D'Sa, R. A.; Sunoj, R. B.; Wasylenko, W. A.; Kapur, P.; Relyea, H. A.; Kumar, N. A.; Hadad, C. M.; Toscano, J. P. *J. Am. Chem. Soc.* **2003**, *125*, 14934.
- (33) (a) Go, C. L.; Waddell, W. H. *J. Org. Chem.* **1983**, *48*, 2897. (b) Waddell, W. H.; Go, C. L. *J. Am. Chem. Soc.* **1982**, *104*, 5804.
- (34) Leyva, E.; Platz, M. S.; Persy, G.; Wirz, J. *J. Am. Chem. Soc.* **1986**, *108*, 3783.
- (35) Liang, T. Y.; Schuster, G. B. *J. Am. Chem. Soc.* **1986**, *108*, 546.
- (36) Liang, T. Y.; Schuster, G. B. *Tetrahedron Lett.* **1986**, *27*, 3328.
- (37) Abramovitch, R. A.; Challand, S. R. *J. Chem. Soc., Chem. Commun.* **1972**, *16*, 964.
- (38) Nay, B.; Scriven, E. F. V.; Suschitzky, H.; Thomas, D. R.; Carroll, S. E. *Tetrahedron Lett.* **1977**, *21*, 1811.
- (39) (a) Platz, M. S. In *Reactive Intermediate Chemistry*; Moss, R. A., Platz, M. S., Jones, M., Jr., Eds.; Wiley: New York, 2004; pp 501–559. (b) Liu, J.; Hadad, C. M.; Platz, M. S. *Org. Lett.* **2005**, *7*, 549. (c) Borden, W. T.; Gritsan, N. P.; Hadad, C. M.; Karney, W. L.; Kemnitz, C. R.; Platz, M. S. *Acc. Chem. Res.* **2000**, *33*, 765.
- (40) Abramovitch, R. A.; Davis, B. A. *Chem. Rev.* **1964**, *64*, 149.
- (41) Atkinson, R. S. In *Azides and Nitrenes: Reactivity and Utility*; Scriven, E. F. V., Ed.; Academic Press: New York, 1984; pp 290.
- (42) Shchepalov, A. A.; Zelentsov, S. V.; Razuvaev, A. G. *Russ. Chem. Bull.* **2001**, *50*, 2346.
- (43) Fueno, K.; Yokoyama, K.; Takane, S.-Y. *Theor. Chim. Acta* **1992**, *82*, 299.
- (44) Alcamí, M.; de Paz, J. L. G.; Yanez, M. *J. Comput. Chem.* **1989**, *10*, 468.
- (45) Li, Y.; Iwata, S. *Bull. Chem. Soc. Jpn.* **1997**, *70*, 79.
- (46) Alcamí, M.; Mo, O.; Yanez, M. *J. Comput. Chem.* **1998**, *19*, 1072.
- (47) Nakamura, S.; Takahashi, M.; Okazaki, R.; Morokuma, K. *J. Am. Chem. Soc.* **1987**, *109*, 4142.
- (48) (a) Yamaguchi, K.; Yabushita, S.; Fueno, T. *J. Chem. Phys.* **1979**, *71*, 2321. (b) Jones, W. H. *J. Phys. Chem.* **1992**, *96*, 594.
- (49) Melius, C. F.; Binkley, J. S. In *ACS Symposium Series; The Chemistry of Combustion Processes*; Sloane, T. M., Ed.; American Chemical Society: Washington, DC, 1984; Vol. 249, pp 103.
- (50) Takane, S.-Y.; Fueno, K. *Theor. Chim. Acta.* **1994**, *87*, 431.
- (51) Bornemann, H.; Sander, W. *J. Am. Chem. Soc.* **2000**, *122*, 6727.
- (52) Patyk, A.; Sander, W.; Gauss, J.; Cremer, D. *Chem. Ber.* **1990**, *123*, 89.
- (53) Patyk, A.; Sander, W.; Gauss, J.; Cremer, D. *Angew. Chem.* **1989**, *101*, 920.
- (54) Patyk, A.; Sander, W.; Gauss, J.; Cremer, D. *Angew. Chem., Int. Ed. Engl.* **1989**, *28*, 898.
- (55) Sander, W.; Kirschfeld, A. In *Matrix-Isolation of Strained Three-Membered Ring Systems*; Halton, B., Ed.; JAI Press: London, U.K., 1995; Vol. 4, Chapter 2, pp 1–80.
- (56) Sander, W.; Trommer, M.; Patyk, A. In *Organosilicon Chemistry III: From Molecules to Materials*; Auner, N., Weis, J., Eds.; Wiley-VCH Verlag GmbH: Weinheim, Germany, 1996; p 86.
- (57) Becerra, R.; Bowes, S.-J.; Ogden, J. S.; Cannady, J. P.; Adamovic, I.; Gordon, M. S.; Almond, M. J.; Walsh, R. *Phys. Chem. Chem. Phys.* **2005**, *7*, 2900.
- (58) Uchino, T.; Kurumoto, N.; Sagawa, N. *Phys. Rev. B* **2006**, *73*, 2031.
- (59) (a) Gaspar, P. P.; Boo, B.-H.; Chari, S.; Ghosh, A. K.; Holten, D.; Kirmaier, C.; Konieczny, S. *Chem. Phys. Lett.* **1984**, *105*, 153. (b) Gaspar, P. P.; Holten, D.; Konieczny, S.; Corey, J. Y. *Acc. Chem. Res.* **1987**, *20*, 329.
- (60) Sabdhu, V.; Jodhan, A.; Safarik, I.; Strausz, O. P. *Chem. Phys. Lett.* **1987**, *135*, 260.
- (61) Hartman, J. R.; Famil-Ghirriha, J.; O'Neal, H. E. *Combust. Flame* **1987**, *68*, 43.
- (62) Inoue, G.; Suzuki, M. *Chem. Phys. Lett.* **1985**, *122*, 361.
- (63) Permenov, D. G.; Radzigi, V. A. *Kinet. Catal.* **2004**, *45*, 273.
- (64) Radzigi, V. A. *Kinet. Catal.* **1996**, *37*, 302.
- (65) Radzigi, V. A.; Baskir, E. G.; Korolev, V. A. *Kinet. Catal.* **1995**, *36*, 568.
- (66) Radzigi, V. A. *Khim. Fiz.* **1995**, *14*, 125.
- (67) Radzigi, V. A. *Sov. J. Chem. Phys.* **1993**, *10*, 1958.
- (68) Bobyshev, A. A.; Radzigi, V. A. *Sov. J. Chem. Phys.* **1991**, *7*, 1641.
- (69) Radzigi, V. A. *Khim. Fiz.* **1991**, *10*, 1262.
- (70) Bobyshev, A. A.; Radzigi, V. A. *Kinet. Catal.* **1990**, *31*, 925.
- (71) Radzigi, V. A.; Senchenya, I. N.; Bobyshev, A. A.; Kazanskii, V. B. *Kinet. Catal.* **1989**, *30*, 1334.
- (72) Bobyshev, A. A.; Radzigi, V. A. *Khim. Fiz.* **1988**, *7*, 950.
- (73) Bobyshev, A. A.; Radzigi, V. A. *Kinet. Catal.* **1988**, *29*, 638.
- (74) Murakami, Y.; Koshi, M.; Matsui, H.; Kamiya, K.; Umeyama, H. *J. Phys. Chem.* **1996**, *100*, 17501.
- (75) Conlin, R. T.; Gaspar, P. P. *J. Am. Chem. Soc.* **1976**, *98*, 868.
- (76) Drahnak, T. J.; Michl, J.; West, R. *J. Am. Chem. Soc.* **1981**, *103*, 1845.
- (77) Arrington, C. A.; West, R.; Michl, J. *J. Am. Chem. Soc.* **1983**, *105*, 6176.
- (78) Maier, G.; Mihm, G.; Reisenauer, H. P.; Littmann, D. *Chem. Ber.* **1984**, *117*, 2369.
- (79) Arrington, C. A.; Klingensmith, K. A.; West, R.; Michl, J. *J. Am. Chem. Soc.* **1984**, *106*, 525.
- (80) (a) Raabe, G.; Michl, J. *Chem. Rev.* **1985**, *85*, 419. (b) Raabe, G.; Vancik, H.; West, R.; Michl, J. *J. Am. Chem. Soc.* **1986**, *108*, 671.
- (81) Trommer, M.; Sander, W.; Patyk, A. *J. Am. Chem. Soc.* **1993**, *115*, 11775.
- (82) (a) Akasaka, T.; Nagase, S.; Yabe, A.; Ando, W. *J. Am. Chem. Soc.* **1988**, *110*, 6270. (b) Akasaka, T.; Yabe, A.; Nagase, S.; Ando, W. *Nippon Kagaku Kaishi* **1989**, *8*, 1440.
- (83) West, R.; Fink, M. J.; Michl, J. *Science* **1981**, *214*, 1343.
- (84) Gaspar, P. P. *Reactive Intermediates*; John Wiley: New York, 1978; Vol. 1, pp 229; 1981, Vol. 2, 335; 1985, Vol. 3, 333.
- (85) Morterra, C.; Low, M. J. D. *Ann. N. Y. Acad. Sci.* **1973**, *220*, 133.
- (86) Morterra, C.; Low, M. J. D. *J. Phys. Chem.* **1969**, *73*, 327.
- (87) Morterra, C.; Low, M. J. D. *J. Phys. Chem.* **1969**, *73*, 321.
- (88) Morterra, C.; Low, M. J. D. *Chem. Commun.* **1968**, *72*, 203.
- (89) Bach, R. D.; Dmitrenko, O. *J. Am. Chem. Soc.* **2006**, *128*, 4598.
- (90) Richardson, N. A.; Rienstra-Kiracofe, J. C.; Schaefer, H. F. *Inorg. Chem.* **1999**, *38*, 6271.
- (91) Liebman, J. F.; Skancke, P. N. *Int. J. Quantum Chem.* **1996**, *58*, 707.
- (92) Nagase, S.; Kudo, T.; Akasaka, T.; Ando, W. *Chem. Phys. Lett.* **1989**, *163*, 23.
- (93) Darling, C. L.; Schlegel, H. B. *J. Phys. Chem.* **1993**, *97*, 8207.
- (94) Darling, C. L.; Schlegel, H. B. *J. Phys. Chem.* **1994**, *98*, 8910.
- (95) Zachariah, M. R.; Tsang, W. **1995**, *99*, 5308.
- (96) Harshavardhan, K.; Solomon, A.; Hegde, M. S. *Solid State Commun.* **1989**, *69*, 117.
- (97) Neumann, W. P. *Chem. Rev.* **1991**, *91*, 311.
- (98) Becerra, R.; Walsh, R. *Spectrum* **2004**, *17*, 16.
- (99) Jasinski, J. M.; Becerra, R.; Walsh, R. *Chem. Rev.* **1995**, *95*, 1203.
- (100) Becerra, R.; Walsh, R. Kinetics & mechanisms of silylene reactions: A prototype for gas-phase acid/base chemistry. In *Research in Chemical Kinetics*; Compton, R. G., Hancock, G., Eds.; Elsevier: Amsterdam, 1995; Vol. 3, pp 263.
- (101) Driess, M.; Grützmacher, H. *Angew. Chem., Int. Ed. Engl.* **1996**, *35*, 828.
- (102) Richardson, N. A.; Rienstra-Kiracofe, J. C.; Schaefer, H. F. *J. Am. Chem. Soc.* **1999**, *121*, 10813.
- (103) Myerson, A. L.; Taylor, F. R.; Hanst, P. L. *J. Chem. Phys.* **1957**, *26*, 1309.

- (104) Norrish, R. G. W.; Zeelenberg, A. P. *Proc. R. Soc. London, Ser. A* **1957**, *240*.
- (105) Norrish, R. G. W.; Oldershaw, G. A. *Proc. R. Soc. London, Ser. A* **1957**, *249*, 498.
- (106) Meyer, B.; Philips, L. F.; Smith, J. J. *Proc. Natl. Acad. Sci.* **1968**, *61*, 7.
- (107) Deveze, D.; Rumpf, P. C. *R. Acad. Sci., Ser. C* **1968**, *266*, 1001.
- (108) Brown, J.; Burns, G. *Can. J. Chem.* **1969**, *47*, 4291.
- (109) Plach, H. J.; Troe, J. *Int. J. Chem. Kinet.* **1984**, *16*, 1531.
- (110) Zen, C. C.; Chen, I. C.; Lee, Y. P. *J. Phys. Chem. A* **2000**, *104*, 771.
- (111) Chen, L.-S.; Lee, C.-I.; Lee, Y.-P. *J. Chem. Phys.* **1996**, *105*, 9454.
- (112) Kaupp, G. *J. Mol. Struct.* **2006**, *786*, 140.
- (113) Kellogg, C. B.; Schaefer, H. F. *Theor. Chem. Acc.* **1997**, *96*, 7.
- (114) Kellogg, C. B.; Schaefer, H. F. *J. Chem. Phys.* **1995**, *102*, 4177.
- (115) Dunning, T. H., Jr.; Raffanetti, R. C. *J. Phys. Chem.* **1981**, *85*, 1350.
- (116) Hayes, E. F.; Pfeiffer, G. V. *J. Am. Chem. Soc.* **1968**, *90*, 4773.
- (117) Ivanić, J.; Atchity, G. J.; Ruedenberg, K. *J. Chem. Phys.* **1997**, *107*, 4307.
- (118) Elliott, R.; Compton, R.; Levis, R.; Matsika, S. *J. Chem. Phys. A* **2005**, *109*, 11304.
- (119) Martinez, R. I.; Herron, J. T. *Chem. Phys. Lett.* **1980**, *72*, 77.
- (120) Groves, C.; Lewars, E. *THEOCHEM* **2000**, *530*, 265.
- (121) Studies have also been conducted on oligomers of NO₂: Liebman, J. F. *J. Chem. Phys.* **1974**, *60*, 2944.
- (122) Hoffmann, R. *Am. Sci.* **2004**, *92*, 23.
- (123) Sung, S.; Hoffmann, R. *J. Mol. Sci.* **1983**, *1*, 1.
- (124) Plass, R.; Egan, K.; Collazo-Davila, C.; Grozea, D.; Landree, E.; Marks, L. D.; Gajdardziska-Josifovska, M. *Phys. Rev. Lett.* **1998**, *81*, 4891.
- (125) Xie, D. Q.; Guo, H.; Bludsky, O.; Nachtigall, P. *Chem. Phys. Lett.* **2000**, *329*, 503.
- (126) Zuniga, J.; Bastida, A.; Requena, A. *J. Chem. Phys.* **2001**, *115*, 139.
- (127) Rodrigues, S. P. J.; Sabin, J. A.; Varandas, A. J. C. *J. Phys. Chem. A* **2002**, *106*, 556.
- (128) Ma, G. B.; Chen, R. Q.; Guo, H. *J. Chem. Phys.* **1999**, *110*, 8408.
- (129) Kamiya, K.; Matsui, H. *Bull. Chem. Soc. Jpn.* **1991**, *64*, 2792.
- (130) Flemmig, B.; Wolczanski, P. T.; Hoffmann, R. *J. Am. Chem. Soc.* **2005**, *127*, 1278.
- (131) Brabson, G.; Andrews, L. *J. Phys. Chem.* **1996**, *100*, 16487.
- (132) Brabson, G.; Citra, A.; Andrews, L.; Davy, R. D.; Neurock, M. *J. Am. Chem. Soc.* **1996**, *118*, 5469.
- (133) Bartlett, P. D.; Mendenhall, G. D. *J. Am. Chem. Soc.* **1970**, *92*, 210.
- (134) Schaap, A. P.; Bartlett, P. D. *J. Am. Chem. Soc.* **1970**, *92*, 6055.
- (135) Stephenson, L. M.; McClure, D. E. *J. Am. Chem. Soc.* **1973**, *95*, 3074.
- (136) Nakamoto, M.; Akiba, K.-Y. *J. Am. Chem. Soc.* **1999**, *121*, 6958.
- (137) (a) Ho, D. G.; Gao, R.; Celaje, J.; Chung, H.-Y.; Selke, M. *Science* **2003**, *302*, 259. (b) Zhang, D.; Ye, B.; Ho, D. G.; Gao, R.; Selke, M. *Tetrahedron* **2006**, *62*, 10729.
- (138) Zhang, D.; Gao, R.; Afzal, S.; Vargas, M.; Sharma, S.; McCurdy, A.; Yousuffuddin, M.; Stewart, T.; Bau, R.; Selke, M. *Org. Lett.* **2006**, *8*, 5125.
- (139) Withnall, R.; Andrews, L. *J. Phys. Chem.* **1987**, *91*, 784.
- (140) Gao, R.; Ho, D. G.; Dong, T.; Khuu, D.; Franco, N.; Sezer, O.; Selke, M. *Org. Lett.* **2001**, *3*, 3719.
- (141) Wilke, J. J.; Weinhold, F. *J. Am. Chem. Soc.* **2006**, *128*, 11850.
- (142) Armstrong, A.; Knight, J. D. *Ann. Rep. Prog. Chem.: Org. Chem.* **2004**, *100*, 51.
- (143) (a) Tsuji, S.; Kondo, M.; Ishiguro, K.; Sawaki, Y. *J. Org. Chem.* **1993**, *58*, 5055. (b) Bennett, G. D.; Paquette, L. A. *Chemtracts: Org. Chem.* **1994**, *7*, 21.
- (144) Itzstein, M. V.; Jenkins, I. D. *J. Chem. Soc., Chem. Commun.* **1983**, *4*, 165.
- (145) Buckler, S. A. *J. Am. Chem. Soc.* **1962**, *84*, 3093.
- (146) Burkett, H. D.; Hill, W. E.; Worley, S. D. *Phosphorus Sulfur* **1984**, *20*, 169.
- (147) (a) Howard, J. A.; Tait, J. C. *Can. J. Chem.* **1978**, *56*, 2163. (b) Phosphines have been suggested to reduce hydroperoxides by nonradical paths: Hiatt, R.; McColeman, C. *Can. J. Chem.* **1971**, *49*, 1709. (c) A radiolysis study was published recently: Alfassi, Z. B.; Neta, P.; Beaver, B. *J. Phys. Chem. A* **1997**, *101*, 2153.
- (148) Tolman, C. A. *Chem. Rev.* **1977**, *77*, 313.
- (149) Crabtree, R. H. *The Organometallic Chemistry of the Transition Metals*; John Wiley & Sons: New York, 1988; pp 72.
- (150) Greer, A.; Vassilikogiannakis, G.; Lee, K.-C.; Koffas, T. S.; Nahm, K.; Foote, C. S. *J. Org. Chem.* **2000**, *65*, 6876.
- (151) Hayes, R. A.; Martin, J. C. *Organic Sulfur Chemistry. Theoretical and Experimental Advances*; Elsevier: Amsterdam, 1985; Vol. 19, pp 408.
- (152) Kuczman, A.; Kapovits, I. *Organic Sulfur Chemistry. Theoretical and Experimental Advances*; Elsevier: Amsterdam, 1985; Vol. 19, pp 191.
- (153) Nahm, K.; Foote, C. S. *J. Am. Chem. Soc.* **1989**, *111*, 909.
- (154) Akasaka, T.; Kita, I.; Haranaka, M.; Ando, W. *Quim. Nova* **1993**, *16*, 325.
- (155) (a) Akasaka, T.; Ando, W. *Phosphorus, Sulfur Silicon Relat. Elem. Jpn.* **1982**, *55*, 3037. (b) Tamagaki, S.; Akatsuka, R. *Bull. Chem. Soc.* **1994**, *95*–69, 437.
- (156) Bolduc, P. R.; Goe, G. L. *J. Org. Chem.* **1974**, *39*, 3178.
- (157) Dannley, R.; Kabre, L. K. R. *J. Am. Chem. Soc.* **1965**, *87*, 4805.
- (158) Sobkowiak, M.; Clifford, C. E. B.; Beaver, B. *Prepr.—Am. Chem. Soc., Div. Pet. Chem.* **2004**, *49*, 450.
- (159) Beaver, B.; Gao, L.; Fedak, M. *Prepr.—Am. Chem. Soc., Div. Pet. Chem.* **2004**, *49*, 448.
- (160) Beaver, B. D.; Burgess Clifford, C.; Fedak, M. G.; Gao, L.; Iyer, P. S.; Sobkowiak, M. *Energy Fuels* **2006**, *20*, 1639.
- (161) Beaver, B. D.; Gao, L.; Fedak, M. G.; Coleman, M. M.; Sobkowiak, M. *Energy Fuels* **2002**, *16*, 1134.
- (162) Beaver, B.; DeMunshi, R.; Heneghan, S. P.; Whitacre, S. D.; Neta, P. *Energy Fuels* **1997**, *11*, 396.
- (163) Beaver, B.; Rawlings, D.; Neta, P.; Alfassi, Z. B.; Das, T. N. *Heteroat. Chem.* **1998**, *9*, 133.
- (164) Nahm, K.; Li, Y.; Evanseck, J. D.; Houk, K. N.; Foote, C. S. *J. Am. Chem. Soc.* **1993**, *115*, 4879.
- (165) Schoeller, W. W.; Busch, T. *Chem. Ber.* **1992**, *125*, 1319.
- (166) Weinhold, F.; Landis, C. R. *Valency and Bonding: A Natural Bond Orbital Donor–Acceptor Perspective*; Cambridge University Press: Cambridge, U.K., 2005; pp 275.
- (167) Trippett, S. *Phosphorus Sulfur* **1976**, *73*, 1.
- (168) Adam, W.; Haas, W.; Sieker, G. *J. Am. Chem. Soc.* **1984**, *106*, 5020.
- (169) Adam, W.; Golsch, D. *J. Org. Chem.* **1997**, *62*, 115.
- (170) Adam, W.; Blancafort, L. *J. Org. Chem.* **1997**, *62*, 1623.
- (171) Clennan, E. L. Sulfide Photooxidation: A Question Of Mechanism. In *Advances in Oxygenated Processes*; JAI Press, Inc.: New York, 1995; Vol. 4, pp 49–80.
- (172) Clennan, E. L. *ACS Symp. Ser. (Petroleum Chemistry)* **1992**, *377*.
- (173) Ando, W. *Sulfur Rep.* **1981**, *1*, 147.
- (174) Ando, W.; Takata, T. In *Singlet O₂ Reaction Modes and Products. Part 2*; Frimer, A. A., Ed.; CRC Press: Boca Raton, FL, 1985; Vol. III; pp 1.
- (175) Grapperhaus, C. A.; Darensbourg, M. Y. *Acc. Chem. Res.* **1998**, *31*, 451.
- (176) Jensen, F.; Greer, A.; Clennan, E. L. *J. Am. Chem. Soc.* **1998**, *120*, 4339.
- (177) Liang, J.-J.; Gu, C.-L.; Kacher, M. L.; Foote, C. S. *J. Am. Chem. Soc.* **1983**, *105*, 4717.
- (178) Bonesi, S. M.; Fagnoni, M.; Albini, A. *J. Org. Chem.* **2004**, *69*, 928.
- (179) Clennan, E. L.; Greer, A. *J. Org. Chem.* **1996**, *61*, 4793.
- (180) Sysak, P. K.; Foote, C. S.; Ching, T.-Y. *Photochem. Photobiol.* **1977**, *27*, 19.
- (181) Miskoski, S.; Garcia, N. A. *Photochem. Photobiol.* **1993**, *57*, 447.
- (182) Bonesi, S. M.; Albini, A. *J. Org. Chem.* **2000**, *65*, 4532.
- (183) Bonesi, S. M.; Mella, M.; d'Alessandro, N.; Aloisi, G. G.; Vanossi, M.; Albini, A. *J. Org. Chem.* **1998**, *63*, 9946.
- (184) Baciocchi, E.; Giacco, T. D.; Eliesi, F.; Gerini, M. F.; Guerra, M.; Lapi, A.; Liberali, P. *J. Am. Chem. Soc.* **2003**, *125*, 16444.
- (185) Baciocchi, E.; Del Giacco, T.; Ferrero, M. I.; Rol, C.; Sebastiani, G. V. *J. Org. Chem.* **1997**, *62*, 4015.
- (186) Baciocchi, E.; Del Giacco, T.; Gerini, M. F.; Lanzalunga, O. *Org. Lett.* **2006**, *8*, 641.
- (187) Baciocchi, E.; Del Giacco, T.; Gerini, M. F.; Lanzalunga, O. *Tetrahedron* **2006**, *62*, 6566.
- (188) Clennan, E. L. *Acc. Chem. Res.* **2001**, *34*, 875.
- (189) Che, Y.; Ma, W.; Ren, Y.; Chen, C.; Zhang, X.; Zhao, J.; Zang, L. *J. Phys. Chem. B* **2005**, *109*, 8270.
- (190) Che, Y.; Ma, W.; Ji, H.; Zhao, J.; Ling, Z. *J. Phys. Chem. B* **2006**, *110*, 2942.
- (191) Latour, V.; Pigot, T.; Simon, M.; Cardy, H.; Lacombe, S. *Photochem. Photobiol. Sci.* **2005**, *4*, 221.
- (192) Lacombe, S.; Cardy, H.; Simon, M.; Khoukh, A.; Soumillion, J. Ph.; Ayadim, M. *Photochem. Photobiol. Sci.* **2002**, *1*, 347.
- (193) Soggiu, N.; Cardy, H.; Habib Jiwan, J. L.; Leray, I.; Soumillion, J. Ph.; Lacombe, S. *J. Photochem. Photobiol., A* **1999**, *124* (1–2), 1.
- (194) Clennan, E. L.; Zhou, W.; Chan, J. *J. Org. Chem.* **2002**, *67*, 9368.
- (195) Thanasekaran, P.; Rajagopal, S.; Ramaraj, R.; Srinivasan, C. *Radiat. Phys. Chem. (Symp.)* **1996**, *49*, 103.
- (196) Gu, K.; Cao, Y.; Zhang, B. *Huaxue Xuebao* **1989**, *47*, 668.
- (197) Miller, B. L.; Kuczera, K.; Schoenich, C. *J. Am. Chem. Soc.* **1998**, *120*, 3345.
- (198) Baciocchi, E.; Del Giacco, T.; Gerini, M. F.; Lanzalunga, O. *Org. Lett.* **2006**, *8*, 641.
- (199) Rehorek, D. *Z. Chem.* **1990**, *30*, 447.
- (200) Fox, M. A.; Miller, P. K.; Reiner, M. D. *J. Org. Chem.* **1979**, *44*, 1103.
- (201) Inoue, K.; Matsuura, T.; Saito, I. *Tetrahedron* **1985**, *41*, 2177.

- (202) Ando, W.; Nagashima, T.; Saito, K.; Kohmoto, S. *J. Chem. Soc., Chem. Commun.* **1979**, 154.
- (203) Eriksen, J.; Foote, C. S.; Parker, T. L. *J. Am. Chem. Soc.* **1977**, *99*, 6455.
- (204) Schenck, G. O.; Krauch, C. H. *Angew. Chem.* **1962**, *74*, 510.
- (205) Schenck, G. O. *Ann. N. Y. Acad. Sci.* **1970**, *171*, 67.
- (206) Corey, E. J.; Ouannes, C. *Tetrahedron Lett.* **1976**, *47*, 4263.SA33.
- (207) Ando, W.; Kabe, Y.; Miyazaki, H. *Photochem. Photobiol.* **1979**, *31*, 191.
- (208) Jori, G.; Cauzzo, G. *Photochem. Photobiol.* **1970**, *12*, 231.
- (209) Casagrande, M.; Gennari, G.; Cauzzo, G. *Gazz. Chim. Ital.* **1979**, *104*, 1251.
- (210) Takata, T.; Hoshino, K.; Takeuchi, E.; Tamura, Y.; Ando, W. *Tetrahedron Lett.* **1984**, *25*, 4767.
- (211) Ando, W.; Sonobe, H.; Akasaka, T. *Tetrahedron Lett.* **1986**, *27*, 4473.
- (212) McKee, M. L. *J. Am. Chem. Soc.* **1998**, *120*, 3963.
- (213) Greer, A.; Chen, M.-F.; Jensen, F.; Clennan, E. L. *J. Am. Chem. Soc.* **1997**, *119*, 4380.
- (214) Clennan, E. L.; Chen, M.-F.; Greer, A.; Jensen, F. *J. Org. Chem.* **1998**, *63*, 3397.
- (215) Clennan, E. L.; Aebischer, D. *J. Org. Chem.* **2002**, *67*, 1036.
- (216) Foote, C. S.; Peters, J. W. *J. Am. Chem. Soc.* **1971**, *93*, 3795.
- (217) Gu, C.-L.; Foote, C. S.; Kacher, M. L. *J. Am. Chem. Soc.* **1981**, *103*, 5949.
- (218) Sawaki, Y.; Ogata, Y. *J. Am. Chem. Soc.* **1981**, *103*, 5947.
- (219) Gu, C.-L.; Foote, C. S. *J. Am. Chem. Soc.* **1982**, *104*, 6060.
- (220) Kacher, M. L.; Foote, C. S. *Photochem. Photobiol.* **1978**, *29*, 765.
- (221) Jensen, F.; Foote, C. S. *J. Am. Chem. Soc.* **1987**, *109*, 1478.
- (222) Bhardwaj, R. K.; Davidson, S. *Tetrahedron* **1987**, *43*, 4473.
- (223) Jensen, F.; Foote, C. S. *J. Am. Chem. Soc.* **1988**, *110*, 2368.
- (224) Ando, W.; Akasaka, T. The Role of Oxygen in Chemistry and Biochemistry, Proceeding of an International Symposium on Activation of Dioxxygen and Homogeneous Catalytic Oxidation. In *Studies of Organic Chemistry*; Vol. 33, Tsukoba, Japan, 1988; pp 99.
- (225) Nahm, K.; Foote, C. S. *J. Am. Chem. Soc.* **1989**, *111*, 1909.
- (226) Clennan, E. L.; Chen, X. *J. Am. Chem. Soc.* **1989**, *111*, 5787.
- (227) Clennan, E. L.; Yang, K. *J. Am. Chem. Soc.* **1990**, *112*, 4044.
- (228) Akasaka, T.; Sakurai, A.; Ando, W. *J. Am. Chem. Soc.* **1991**, *113*, 2696.
- (229) Akasaka, T.; Haranaka, M.; Ando, W. *J. Am. Chem. Soc.* **1991**, *113*, 9898.
- (230) Watanabe, Y.; Kuriki, N.; Ishiguro, K.; Sawaki, Y. *J. Am. Chem. Soc.* **1991**, *113*, 2677.
- (231) Jensen, F. *J. Org. Chem.* **1992**, *57*, 6478.
- (232) Clennan, E. L.; Wang, D. X.; Yang, K.; Hodgson, D. J.; Oki, A. R. *J. Am. Chem. Soc.* **1992**, *114*, 3021.
- (233) Laakso, D.; Marshall, P. *J. Phys. Chem.* **1992**, *96*, 2471.
- (234) Clennan, E. L.; Yang, K. *Tetrahedron Lett.* **1993**, *34*, 1697.
- (235) Clennan, E. L.; Zhang, H. *J. Org. Chem.* **1994**, *59*, 7952.
- (236) Pasto, D. J.; Cottard, F. *J. Am. Chem. Soc.* **1994**, *116*, 8973.
- (237) Clennan, E. L.; Wang, D.; Zhang, H.; Clifton, C. H. *Tetrahedron Lett.* **1994**, 4723.
- (238) Clennan, E. L.; Zhang, H. *J. Am. Chem. Soc.* **1994**, *116*, 809.
- (239) Clennan, E. L.; Chen, M.-F. *J. Org. Chem.* **1995**, *60*, 6444.
- (240) Clennan, E. L.; Dobrowolski, P.; Greer, A. *J. Am. Chem. Soc.* **1995**, *117*, 9800.
- (241) Clennan, E. L.; Greer, A. *Tetrahedron Lett.* **1996**, *37*, 6093.
- (242) Ishiguro, K.; Hayashi, M.; Sawaki, Y. *J. Am. Chem. Soc.* **1996**, *118*, 7265.
- (243) Greer, A.; Jensen, F.; Clennan, E. L. *J. Org. Chem.* **1996**, *61*, 4107.
- (244) Shanguan, C.; McAllister, M. A. *THEOCHEM* **1998**, 422, 123.
- (245) Touthkine, A.; Clennan, E. L. *J. Org. Chem.* **1999**, *64*, 5620.
- (246) Touthkine, A.; Clennan, E. L. *J. Am. Chem. Soc.* **2000**, *122*, 1834.
- (247) Madhavan, D.; Pitchumani, K. *Tetrahedron* **2001**, *57*, 8391.
- (248) Touthkine, A.; Aebischer, D.; Clennan, E. L. *J. Am. Chem. Soc.* **2001**, *123*, 4966.
- (249) Sofikiti, N.; Rabalakos, C.; Stratakis, M. *Tetrahedron Lett.* **2004**, *45*, 1335.
- (250) Bonesi, S. M.; Fagnoni, M.; Albini, A. *J. Org. Chem.* **2004**, *69*, 928.
- (251) Clennan, E. L.; Hightower, S. E.; Greer, A. *J. Am. Chem. Soc.* **2005**, *127*, 11819.
- (252) Shiraishi, Y.; Koizumi, H.; Hirai, T. *J. Phys. Chem. B* **2005**, *109*, 8580.
- (253) Clennan, E. L.; Hightower, S. E. *J. Org. Chem.* **2006**, *71*, 1247.
- (254) Akasaka, T.; Yabe, A.; Ando, W. *J. Am. Chem. Soc.* **1987**, *109*, 8085.
- (255) Grapperhaus, C. A.; Maguire, M. J.; Tuntulani, T.; Darensbourg, M. Y. *Inorg. Chem.* **1997**, *36*, 1860.
- (256) Farmer, P. J.; Solouki, T.; Mills, D. K.; Soma, T.; Russell, D. H.; Reibenspies, J. H.; Darensbourg, M. Y. *J. Am. Chem. Soc.* **1992**, *114*, 4601.
- (257) Darensbourg, M. Y.; Tuntulani, T.; Reibenspies, J. H. *Inorg. Chem.* **1995**, *34*, 6287.
- (258) Farmer, P. J.; Solouki, T.; Soma, T.; Russell, D. H.; Darensbourg, M. Y. *Inorg. Chem.* **1993**, *32*, 4171.
- (259) Buonomo, R. M.; Font, I.; Maguire, M. J.; Reibenspies, J. H.; Tuntulani, T.; Darensbourg, M. Y. *J. Am. Chem. Soc.* **1995**, *117*, 963.
- (260) Buonomo, R. M.; Font, I.; Maguire, M. J.; Reibenspies, J. H.; Tuntulani, T.; Darensbourg, M. Y. *J. Am. Chem. Soc.* **1995**, *117*, 5427.
- (261) Grapperhaus, C. A.; Darensbourg, M. Y.; Sumner, L. W.; Russell, D. H. *J. Am. Chem. Soc.* **1996**, *118*, 1791.
- (262) Galvez, C.; Ho, D. G.; Azod, A.; Selke, M. *J. Am. Chem. Soc.* **2001**, *123*, 3381.
- (263) Connick, W. B.; Gray, H. B. *J. Am. Chem. Soc.* **1997**, *119*, 11620.
- (264) Zhang, Y.; Ley, K. D.; Schanze, K. S. *Inorg. Chem.* **1996**, *35*, 7102.
- (265) Akasaka, T.; Ando, W. *Phosphorus, Sulfur Silicon Relat. Elem.* **1994**, *95-69*, 437.
- (266) Hevesi, L.; Krief, A. *Angew. Chem., Int. Ed. Engl.* **1976**, *15*, 381.
- (267) Sofikiti, N.; Rabalakos, C.; Stratakis, M. *Tetrahedron Lett.* **2004**, *45*, 1335.
- (268) Wasserman, H. H.; Lu, T. *J. Recl. Trav. Chim. Pays-Bas* **1986**, *105*, 345.
- (269) Tamagaki, S.; Akatsuka, R. *Bull. Chem. Soc. Jpn.* **1982**, *55*, 3037.
- (270) Kojima, N.; Yamada, A.; Takahashi, K.; Okamoto, T.; Konagai, M.; Saito, K. *Jpn. J. Appl. Phys. Lett.* **1993**, *32*, L887.
- (271) Detty, M. D.; Merkel, P. B.; Powers, S. K. *J. Am. Chem. Soc.* **1988**, *110*, 5920.
- (272) Schultz, M.; Liebsch, S.; Kluge, R.; Adam, W. *J. Org. Chem.* **1997**, *62*, 188.
- (273) (a) Bach, R. D.; Andres, J. L.; Owensby, A. L.; Schlegel, H. B.; McDouall, J. J. W. *J. Am. Chem. Soc.* **1992**, *114*, 7207. (b) Warner, P. M. *J. Org. Chem.* **1996**, *61*, 7192.
- (274) Shu, L.; Shi, Y. *Tetrahedron Lett.* **1999**, *40*, 8721.
- (275) Yang, D.; Tang, Y. C.; Chen, J.; Wang, X. C.; Bartberger, M. D.; Houk, K. N.; Olson, L. *J. Am. Chem. Soc.* **1999**, *121*, 11976.
- (276) Merenyi, G.; Lind, J.; Goldstein, S. *J. Am. Chem. Soc.* **2002**, *124*, 40.
- (277) Liebman, J. F.; Greenberg, A. *Chem. Rev.* **1989**, *89*, 1225.
- (278) Bach, R. D.; Dmitrenko, O. *J. Am. Chem. Soc.* **2004**, *126*, 4444.
- (279) Bach, R. D.; Dmitrenko, O. *J. Org. Chem.* **2002**, *67*, 2588.
- (280) Bach, R. D.; Dmitrenko, O. *J. Org. Chem.* **2002**, *67*, 3884.

CR0400717